EPIGENETIC REGULATION OF NEUROINFLAMMATION IN THE AGED MOUSE BRAIN

BY

STEPHANIE MARIE MATT

DISSERTATION

Submitted in partial fulfillment of the requirements
for the degree of Doctor of Philosophy in Neuroscience
in the Graduate College of the
University of Illinois at Urbana-Champaign, 2018

Urbana, Illinois

Doctoral Committee:

Professor Rodney W. Johnson, Chair
Assistant Professor Andrew J. Steelman
Associate Professor Monica Uddin
Associate Professor Stephanie Ceman

ABSTRACT

As the average lifespan continues to rise, there is a significant increase in the number of people suffering from age-related chronic inflammatory diseases such as autoimmune disorders, cancer, and neurodegenerative diseases. Therefore, there is a greater need to understand the factors that contribute to quality of life in the elderly. Growing evidence indicates that the immune system plays a critical role in regulating the progression of brain aging. However, an important question remains of whether inflammatory pathways become hyperactivated with age, or whether deficient immune responses, which fail to cope with age-related deterioration, may contribute to disease.

Microglia, the resident immune cells of the brain, are key players in regulating neuroinflammation. They function as the primary immune surveillance, provide the first host defense by secreting factors such as cytokines and chemokines, and carry out specific central nervous system functions such as synaptic pruning and secretion of neurotrophic factors. Of note, microglia are also long-lived within the brain and have a limited turnover, suggesting that they are a likely target for epigenetic regulation.

In order to determine possible causes and targets for interventions to promote healthy aging, the current dissertation explored the role of epigenetic regulation in microglia as well as potential pharmacological and dietary interventions that could be beneficial for chronic age-related neuroinflammation. This dissertation was divided into three major sections. In Chapter 2, we determined that aged mice had decreased methylation of the *Il1b* gene promoter in primary microglia basally or following systemic lipopolysaccharide (LPS) that is associated with increased *Il1b* mRNA, intracellular IL-1β production, as well as prolonged sickness behavior. We also determined changes in epigenetic regulator gene expression with both age and LPS.

Furthermore, we found that inhibiting DNA methylation increased *Il1b* gene expression and decreased DNA methylation of BV2 and primary microglial cells similar to microglia from aged mice. In Chapter 3, we investigated whether inhibiting DNA methylation in the brain of adult mice would alter sickness behavior, DNA methylation of the *Il1b* promoter and expression of inflammatory genes in microglia similar to aged mice. However, we found that inhibiting DNA methylation and injecting LPS in the brain of adult mice produced faster recovery of burrowing behavior compared to mice treated only with LPS. Genes of inflammatory markers, epigenetic regulators, and the microglial sensory apparatus (i.e. the sensome) were also differentially expressed by inhibiting DNA methylation alone or in combination with LPS. Lastly, DNA methylation of *Il1b* proximal promoter was changed by inhibiting DNA methylation alone or in combination with LPS, and these changes persisted 48 hours after LPS treatment. In Chapter 4, we investigated whether injections of butyrate or increases in butyrate through a highly fermentable diet could affect microglial activation, and specifically microglial activation in aging. We determined that gene expression of inflammatory markers, epigenetic regulators, and the microglial sensome were altered by both diet and age, in that aged animals had a more anti-inflammatory profile on the high fiber diet.

In summary, the studies outlined in this dissertation comprise evidence that epigenetic changes are present in aging microglia, and that pharmacological agents and nutrients that act as epigenetic modifiers can alter microglial phenotypes. This could lead to the development of therapeutic interventions aimed at specifically promoting beneficial microglia reactivity associated with infection, which may be important for fostering better recovery from sickness and reducing cognitive deficits and age-associated disease in the elderly.

ACKNOWLEDGEMENTS

First and foremost, I want to thank Dr. Rodney Johnson for giving me the opportunity to pursue a Ph.D. in his lab. He taught me to be independent and I developed a number of skills and techniques that I will be able to use for the rest of my career. I would also like to thank my committee members for their guidance and encouragement. Furthermore, I want to thank my past and current lab mates and undergraduates of the Johnson Lab, as I could not have completed this work without their continual help with studies and intellectual input. I would also like to thank my family and my friends who have supported me, especially all of my friends in Urbana-Champaign and my amazing boyfriend Dan. We have made this place a wonderful home in the past five years and I never would have been as successful as a scientist without all of your help. I will miss everyone greatly, but I look forward to the adventures to come. Thank you!!!

TABLE OF CONTENTS

CHAPTER 1: INTRODUCTION

1.1 Aging and Neuroinflammation

Most research focuses on the diseases of aging, yet the healthy aging brain undergoes a number of changes in the absence of disease. Structural and functional changes include decreases in brain mass, altered hippocampal and neocortical circuits, and increased permeability of the blood-brain barrier (BBB) (Montagne et al., 2015; Morrison & Hof, 2002; Peters, 2006). Moreover, cellular changes include telomere shortening, improper maintenance of metabolic homeostasis, increases in oxidative stress and DNA damage, as well as an increase in inflammatory activity (Chung et al., 2009; Ivanisevic et al., 2016; Pal & Tyler, 2016; Sparkman & Johnson, 2008). This can confer risk to age-associated pathologies such as cancer, autoimmunity, and neurodegenerative diseases.

Generally, neuroinflammation is beneficial as an acute, transient response to injurious conditions such as tissue damage or infection, the primary goal being to remove harmful agents and facilitate recovery through activation of receptors and production of cytokines and proteins. However, mechanisms responsible for limiting inflammation become altered during aging, leading to low-grade and persistent neuroinflammation, even in the absence of a pathologic stimulus (Pizza, Agresta, D'Acunto, Festa, & Capasso, 2011; von Bernhardi, Eugenín-von Bernhardi, & Eugenín, 2015).

It was once thought that the brain was an "immune-privileged" organ due to its seclusion by the BBB, but there are now many recognized routes of communication between the immune system and brain (Quan & Banks, 2007). The signals required to convey the information between these two systems are inflammatory mediators that predominantly consist of cytokines. The major pathways of communication include passive diffusion of cytokines from the blood to the

brain via regions of the brain that lack a BBB (circumventricular organs), passage of cytokines through energy-dependent, saturable transport systems on brain endothelium, activation of cytokine receptors on endothelial cells that form the BBB that subsequently release cytokines or second messengers, and transmission of cytokine signals via afferent nerve fibers, such as the vagus nerve. Further, with the recent discovery of functional lymphatic vessels lining the dural sinuses, there is an additional way in which brain-resident immune cells communicate with peripheral immune cells (Aspelund et al., 2015; Louveau et al., 2015).

Chronic neuroinflammation attributed to dysregulation of the brain-immune pathways mentioned above is an important factor contributing to age-related cognitive decline (Simen, Bordner, Martin, Moy, & Barry, 2011). Animal studies show that increased levels of inflammatory molecules in the brain impair behavioral and cognitive performance. Mice or rats injected intraperitoneally with lipopolysaccharide (LPS), a cell wall component of gram-negative bacteria, have increased interleukin (IL)-1β in the brain, which is associated with impairments in spatial working memory, contextual fear conditioning, and classic signs of sickness behavior including loss of appetite, sleep, and anhedonia (Dantzer, 2009; Dantzer, O'Connor, Freund, Johnson, & Kelley, 2008). All of these behaviors can be recapitulated by injecting recombinant IL-1β directly into the brain (Dantzer, 2001). Furthermore, injecting IL-1 receptor antagonist (IL-1RA) into the brain can prevent many age-associated deficits caused by immune stimuli in the periphery, including dysfunction of hippocampal long-term potentiation and exaggerated LPS-induced sickness behaviors (Abraham & Johnson, 2009; Chapman, Barrientos, Ahrendsen, Maier, & Patterson, 2010).

In human studies, increases in the cytokines IL-6 and tumor necrosis factor (TNF)-α as well as the acute-phase protein C-reactive protein have been found in serum in elderly men and

women, and this increase is inversely related to performance on attention/working memory and executive function tasks (Simen et al., 2011). Furthermore, aged individuals are increasingly sensitive to insults such as infections, stress, or recent surgical procedures, and often experience cognitive and behavioral consequences that are more intense and prolonged than in adults. It is still unclear whether peripherally or centrally derived cytokines play a larger role in eliciting central responses, but regardless, the immune cells of the brain, microglia, and the cytokines they produce, are key components of both the central and overall immune response. Mounting evidence suggests that age-related dysregulation of microglial cell activity may be responsible for a discordant central response to peripheral immune signals (Dilger & Johnson, 2008).

1.2 Microglia

Microglia account for around 10% of all cells within the brain, and show relatively limited turnover (L. J. Lawson, Perry, Dri, & Gordon, 1990; Mittelbronn, Dietz, Schluesener, & Meyermann, 2001; R. M. Ransohoff & Perry, 2009; Tay et al., 2017). They develop early in embryogenesis in the embryonic yolk sac and migrate to the central nervous system (CNS) where they remain and are rarely replaced (Ginhoux et al., 2010). Once thought of as "resting" or "quiescent" cells in the healthy brain, it is now known that microglia are far from inactive and many recent *in vivo* observations have shown that microglia extend their processes to actively scan the microenvironment (Nimmerjahn, Kirchhoff, & Helmchen, 2005; Wake, Moorhouse, Jinno, Kohsaka, & Nabekura, 2009). When sensing a danger associated molecular pattern (e.g., ATP or heat shock proteins), or a pathogen associated molecular pattern (e.g., LPS), microglia enlarge their cell body and become activated. Depending on the stimuli, microglia exhibit different activation patterns. Quiescent surveying microglia (M0) can become M1, or "classically" activated cells, as defined by the release of cytokines and chemokines that promote

inflammation, including IL-1β, TNF-α, IL-6, and IL-18. A second type of microglia known as M2, or "alternatively" activated cells, produce anti-inflammatory cytokines and neurotrophic factors that facilitate healing such as IL-4, IL-10, IL-1RA, and brain-derived neurotrophic factor. (Cherry, Olschowka, & O'Banion, 2014). Activated microglia are generally categorized as M1 or M2, but given the complexity of their behavior, this classification may be over-simplistic and, in actuality, microglia may show a continuous spectrum of activation patterns depending on the nature of stimulation (Richard M. Ransohoff, 2016). An increasing number of transcriptomic studies using primary microglia have revealed gene signatures extending far beyond "M1" and "M2" genes (Orre et al., 2014; Wes, Holtman, Boddeke, Möller, & Eggen, 2016). Notably, Hickman et al. identified 100 genes specifically enriched in microglia that were collectively named the microglial sensome, thus creating a new way to discriminate between other CNS cells and immune cells (Hickman et al., 2013).

Despite the dynamic role of microglia in maintaining homeostasis, their long-lived nature and general inability to be replaced by circulating peripheral cells makes them particularly sensitive to oxidative stress, DNA damage, and a lifetime of inflammatory insults. Aged microglia display a deramified morphology, with fewer and shorter processes and increased soma volume. They lose their homogeneous tissue distribution, and are less efficient at clearing damaged neurons due to ineffective phagocytosis (Damani et al., 2011).

Over time, these cells may also become hypersensitive or primed. With normal aging, microglia are characterized by up-regulation of glial activation markers including major histocompatibility complex II (MHC II), cluster of differentiation molecule 11b (CD11b), and CD68, a finding that is consistent in several species including human post-mortem tissue, rodents, and non-human primates (Conde & Streit, 2006; Perry, Matyszak, & Fearn, 1993;

Sheffield & Berman, 1998; Sobel & Ames, 1988). For example, approximately 25% of microglia isolated from aged mice stain positive for major histocompatibility complex class II compared to less than 3% of microglia isolated from young adults (Henry, Huang, Wynne, & Godbout, 2009). Microglia from aged brains also show increased basal production of the pro-inflammatory cytokines IL-1β, IL-6 and TNF-α and decreased production of the anti-inflammatory cytokines IL-10 and IL-4. Accordingly, when the immune system is challenged by a pro-inflammatory agent such as LPS, microglial activation is amplified and prolonged in the aged brain compared with adults, leading to exaggerated neuroinflammation, sickness behavior and cognitive deficits (Godbout et al., 2005; Henry et al., 2009). It has even been recently found that exaggerated microglial responses to systemic inflammation are evident as early as middle age (9-10 month-old mice), which may have more profound consequences for age-related diseases than previously thought (M. Nikodemova, Small, Kimyon, & Watters, 2016). In order to validate the link between microglial phenotypes and age-related neuroinflammation, pharmacological and dietary manipulations that control microglial activation states have been explored, but very little has been documented on their epigenetic regulation. It has recently been proposed that microglial priming should be viewed as a type of trained immunity in the brain, which refers to the ability of mainly peripheral cells to display a 'memory' to inflammation through epigenetic reprogramming (Haley, Brough, Quintin, & Allan, 2017; Netea et al., 2016). As the immune system needs to respond to rapidly changing environmental cues to ensure an appropriate host response to pathogens, the molecular regulation of inflammatory responses is a likely target for epigenetic regulation.

1.3 Epigenetics

Epigenetics refers to changes in gene expression that are not dependent on DNA sequence, and is thought of as a mediator between gene-environment interactions (Bird, 2002). The concept of DNA as a static, fixed entity has been replaced by a new vision where DNA is highly dynamic, capable of large fluctuations, and able to interact actively with the environment (M. Szyf, McGowan, & Meaney, 2008). Epigenetic mechanisms are mediated by post-translational modifications of histones such as acetylation and methylation, non-coding RNA, and by methylation and more recently hydroxymethylation of DNA.

DNA methylation is the most well-studied epigenetic mechanism. When DNA is methylated, methyl groups from S-adenosyl-L-methionine are covalently transferred to cytosines in cytosine-guanine (CpG) dinucleotides (Jin, Li, & Robertson, 2011). These sequences can be found primarily within the promoter region of a gene and thus are in a good place to control the level of expression of a gene. DNA methylation is catalyzed by a family of DNA methyltransferases (DNMTs) that includes DNMT1, DNMT3a, and DNMT3b (Moore, Le, & Fan, 2013). DNMT1 is a maintenance methyltransferase that adds methyl groups to the complimentary strand of hemimethylated DNA, and maintains DNA methylation patterns during the DNA replication process. DNMT3a and DNMT3b are de novo methyltransferases, capable of catalyzing new methylation patterns of previously unmethylated sequences. Of note, the DNMT family also includes DNMT2, which acts as an RNA methyltransferase (Jurkowski et al., 2008), and DNMT3L, which exhibits no enzymatic activity, but plays a role in DNMT3a activity (Ooi et al., 2007). Methylated DNA can recruit methyl-CpG-binding domain (MBD) proteins such as Methyl-CpG Binding Protein-2 (MeCP2) and other corepressors like histone deacetylases

(HDACs), which recognize 5-methylcytosines (5-mC) and participate in chromatin silencing (McCabe, Brandes, & Vertino, 2009)

DNA demethylation can also occur, and is thought to be initiated by the oxidation of 5-mC into 5-hydroxymethylcytosine (5-hmC) by the ten-eleven translocation (TET) proteins (Kohli & Zhang, 2013). Additionally, Growth Arrest and DNA-Damage-Inducible (Gadd45) proteins assist in the localization of demethylation activity to specific gene promoters. It would be challenging to break the strong covalent bonds between methyl groups and cytosines, so instead Gadd45 functions through a DNA-repair-like mechanism, in which an unmethylated cytosine replaces the methylated cytosine following a sequence of molecular events (Ma, Guo, Ming, & Song, 2009).

Histone acetylation and methylation are the most studied modifications of histone proteins. The state of histone acetylation depends on histone acetyltransferases (HATs) and HDACs, enzymes responsible for acetylation and deacetylation, respectively (Bannister & Kouzarides, 2011). HATs, that transfer an acetyl group from acetyl-CoA on lysine histone tails, cause a loosening of the the chromatin structure by weakening electrostatic attraction between the histone proteins and DNA. This typically allows transcription factors to bind and increase transcription of a particular gene. HDACs act to remove acetyl groups from lysine histone tails, promoting chromatin condensation and not allowing transcription factors to bind, thus decreasing gene expression. In contrast, histone methylation may be linked to gene activation or repression, depending on the position where methylation is occurring, which is either at lysine or arginine residues of histones H3 or H4 (Kouzarides, 2007). Methylation is controlled by histone lysine methyltransferases (HKMTs) and protein arginine methyltransferase (PRMT), respectively,

whereas demethylation is controlled by histone lysine demethylases (HKDMs) and histone arginine demethylases (HRDMs).

It is well-documented that epigenetic changes contribute to aging and alter the lifespan (Hernandez et al., 2011; Zampieri et al., 2015). DNA methylation depends on a precise balance of methylation and demethylation reactions that are nicely balanced in mature cells, but with age this balance is strongly shifted to favor DNA hypomethylation (Pogribny & Vanyushin, 2010a). This could be due to passive age-dependent decline in DNA methylation, the increase of active DNA demethylation, or both. This could be linked to decreased methylation capacity of DNA methyltransferases caused by compromised genome integrity and/or the age-dependent decrease in the activity of DNA methyltransferases (Bollati et al., 2009; Lopatina et al., 2002). Histone modifications also undergo age-related alterations, including global loss of core histone proteins, and decreases in acetylation of histone 3 lysine 9 (H3K9Ac) and trimethylation of histone 3 lysine 27 (H3K27me3) (Bracken et al., 2007; Kawakami, Nakamura, Ishigami, Goto, & Takahashi, 2009). Not surprisingly, DNA methylation and histone modifications are dependent on one another to exert the changes observed during aging (Pal & Tyler, 2016). Therefore, it seems that age-associated alterations in epigenetic mechanisms like DNA methylation and histone modifications may lead to redistribution of heterochromatin, impair normal gene responsiveness to environmental signals, and increase genomic instability that could compromise cell function and contribute to a generalized functional decline. Aging could therefore be thought as a time-dependent, epigenetically mediated loss of phenotypic plasticity (Gravina & Vijg, 2010).

The cellular and physiological phenotype of aged microglial cells is likely related to epigenetic changes such as DNA methylation and histone modifications. To date, only a handful

of studies have used high-throughput sequencing to address the epigenetic landscape of primary microglia (Gosselin et al., 2014; Lavin et al., 2014), and there is yet to be a study comparing young to old. Fortunately, a number of recent studies have investigated specific epigenetic regulators in microglia. Sirtuin 1 (SIRT1) is a member of class III histone deacetylases and is known to play a role in longevity (Satoh et al., 2013). SIRT1 deficiency in aged microglia is related to increases of IL-1β transcription and decreased methylation of CpG sites within the IL-1β proximal promoter (Cho et al., 2015). As epigenetic regulation of other pro-inflammatory genes such as TNF- α and IL-6 has been demonstrated in other immune cell types (Eddy, Krukowski, Janusek, & Mathews, 2014; Sullivan et al., 2007), it will be pertinent to explore this possibility in microglia. It has also been observed that the suppressing histone H3K27me3 demethylase Jumonji domain containing 3 (Jmjd3) in the substantia nigra in vivo caused exaggerated microglial activation and provoked greater dopamine neuron death in a mouse model of Parkinson's disease (Tang et al., 2014). Moreover, the Jmjd3 level was lower in the midbrain of aged mice, which was accompanied by an elevated level of H3K27me3.

Since epigenetic modifications are controlled by reversible enzymatic reactions, they have the potential to be modulated by pharmacological agents (Moshe Szyf, 2017). Utilizing compounds that act as DNMT inhibitors (DNMTis) or HDAC inhibitors (HDACis) could reprogram pathological states and may identify new therapeutic targets for disease. Both DNMTis and HDACis have primarily been studied for cancer therapy, acting as tumor suppressors that increase the expression of tumor suppressor genes (Kristensen, Nielsen, & Hansen, 2009; Song, Han, & Bang, 2011), but they have also been recently shown as promising treatments for autoimmune, neurodegenerative, and psychiatric disorders (Heerboth et al., 2014; M. Szyf, 2009). Further, a handful of studies have demonstrated the effect of gene expression

regulation by DNMTis and HDACis in microglial behavior. For example, the DNMTi 5-aza-2'-deoxycytidine influences expression of several genes associated with the pathology of Alzheimer's disease in microglia-like BV-2 cells, (Byun et al., 2012). Butyrate, a short chain fatty acid that will be discussed in more detail in a later section (1.5), has also been shown to be anti-inflammatory in LPS treated microglial cell cultures and in microglia in rodent models of ischemic stroke (Durham, Grigg, & Wood, 2017; Huuskonen, Suuronen, Nuutinen, Kyrylenko, & Salminen, 2004; Patnala, Arumugam, Gupta, & Dheen, 2016). This leads to the hypothesis that these drugs have the ability to regulate age-related microglial activity.

1.4 Gut-Brain-Axis

The gastrointestinal (GI) tract is the most heavily colonized region of the human body, with bacterial concentrations ranging from 10^1–10^3 cells per gram in the upper intestine to 10^{11}–10^{12} per gram in the colon (Derrien & van Hylckama Vlieg, 2015; O'Hara & Shanahan, 2006). A recent sequencing study has also revealed that the microbiota in our gut comprise approximately 40,000 bacterial species (Frank & Pace, 2008). The intestinal barrier regulates the absorption of nutrients from the lumen into the circulation, but also acts as part of the host defense against microorganisms (Peterson & Artis, 2014). A mucus layer, composed of highly glycosylated proteins called mucins that are produced and maintained by goblet cells (Johansson, Larsson, & Hansson, 2011), contains secretory immunoglobulin (Ig) A and antimicrobial peptides that cover the epithelial cell lining. This functions to facilitate GI transport, and works as a protective layer against bacterial invasion. Additionally, to establish a barrier to paracellular transport, there is a monolayer of epithelial cells interconnected by tight junction proteins, including claudin, occludin, and tricullulin (Dorfel & Huber, 2012; Ivanov, Parkos, & Nusrat, 2010).

It is becoming increasingly clear that through bi-directional communication with the brain, the bacterial commensals help to maintain homeostasis of the CNS and influence neurotransmission and behavior. This is known as the microbiota–gut–brain axis. In the brain, endothelial cells separate the lumen of blood vessels from the CNS parenchyma, and are connected by the same tight junction proteins as intestinal epithelial cells (Doran, Banerjee, Disson, & Lecuit, 2013). Not surprisingly, there is evidence that the microbiota from the gut can modulate the BBB. Germ free mice have increased BBB permeability and decreased expression of tight junction proteins, and exposure of GF adult mice to the fecal microbiota from pathogen-free donors restores BBB permeability and tight junction protein expression (Braniste et al., 2014). The microbiota can signal to the brain through a variety of other mechanisms as well, including production of bacterial metabolites and immune mediators, such as cytokines, and signaling to the brain directly via the vagus nerve (Sherwin, Sandhu, Dinan, & Cryan, 2016).

Importantly for our research, the immune system acts as a key intermediary between the gut microbiota and the brain (El Aidy, Dinan, & Cryan, 2014). For instance, intestinal inflammation in mice was associated with increased neuronal activation, represented by c-Fos immunohistochemistry, in vagal sensory ganglia and in the nucleus of the solitary tract, which is the primary afferent of the vagus nerve (Goehler et al., 2005). In addition, the anxiety-like behavior in a mouse model of chronic colitis was attenuated following vagotomy, indicating that the vagus nerve is an intermediary in facilitating the detrimental behavioral effects of colonic inflammation (Bercik et al., 2011).

Recently, research has revealed that the microbiota can specifically regulate microglia function (Erny et al., 2015). Germ free mice were found to have an increased number of ionized calcium-binding adapter molecule 1 (Iba1) positive microglia in the cortex and hippocampus,

and these microglia displayed an immature phenotype, lacking the markers CD44, CD62L and MHC class II. They also failed to display an activated phenotype following LPS administration. Antibiotic treatment, which depletes microbiota, produces this same effect upon microglial morphology and activation as well (Erny et al., 2015). Further, new evidence suggests that the maternal microbiome can influence microglial properties during prenatal stages and that the depletion of the microbiome can impact microglia in a sex- and time-specific manner (Matcovitch-Natan et al., 2016; Thion et al., 2018).

Just as in the aging brain, there are changes with permeability and immune function as the gastrointestinal tract ages (Biagi et al., 2013). The impairment of the gut associated lymphoid tissue to efficiently synthesize secretory IgA, together with the reduced efficiency of the innate immune defenses, such as antimicrobial peptides and mucus secretion, can result in failure to control microbiota, possibly creating an excessive bacterial load. The fact that microbiota are key regulators of immune function and inflammatory responses, it is likely that a change in their composition as well as intestinal permeability during aging plays a role in the gradual activation of the immune system, which could then lead to inflammation of the brain (Guigoz, Dore, & Schiffrin, 2008; Kelly et al., 2015).

1.5 Fiber and Butyrate

A large body of literature has demonstrated the benefits of a high fermentable fiber diet in the colon, including reducing risk of type 2 diabetes, colon cancer, obesity, and cardiovascular disease (Slavin, 2013). Bacterial fermentation of fiber in the colon produces a class of molecules known as short-chain fatty acids (SCFAs), with acetic, propionic and butyric acids being the most studied. These metabolites are found in high concentrations in the intestinal tract, and are taken up by colonocytes as their predominant ATP source. In addition, SCFAs modulate

colonocyte and immune cell development and survival, as well as intestinal barrier function, through activation of G protein coupled receptors (FFAR2, FFAR3, GPR109a) and by histone modifications, predominantly HDAC inhibition (Corrêa-Oliveira, Fachi, Vieira, Sato, & Vinolo, 2016).

Many of the reported beneficial effects of fiber have been associated with the microbiome and its ability to produce the SCFA butyrate. Studies have demonstrated that butyrate is anti-inflammatory, modulating development, function, and activation of peripheral immune cells such as neutrophils, macrophages, and dendritic cells (Corrêa-Oliveira et al., 2016). Butyrate also exerts a protective role in the intestinal epithelium, stimulating the release of mucins, improving tight junction integrity, thus improving gastrointestinal homeostasis by reducing intestinal permeability (Bischoff et al., 2014). As there is a lower capacity to produce butyrate in the elderly gut microbiome, due to the findings of significantly fewer copies of the butyrilCoA:acetateCoA transferase gene compared to younger adults and lower amounts of bacterial groups which are known butyrate producers (Biagi, Candela, Franceschi, & Brigidi, 2011; Hippe et al., 2011), an increase in butyrate through a high fiber diet could counterbalance the age-related microbiota depletion. Of note, inulin has been shown to be a rich source of soluble dietary fiber that increases butyrate-producing bacteria (G. Schaafsma & Slavin, 2015). Inulin belongs to a group of non-digestible carbohydrates called fructans, and in food is considered a prebiotic (Roberfroid, 2007). Inulin has even been shown to be beneficial for age-related inflammation, as a nutritional supplement with inulin increased innate immunity and protection against infections in elderly people (Bunout et al., 2004).

Pharmacologically, there is substantial evidence that butyrate has a profoundly beneficial effect on brain disorders (Sherwin et al., 2016). Specifically, the HDACi properties of butyrate

have attractive therapeutic potential due to its ability to increase histone acetylation and promote the expression of neurotrophic genes. For example, sodium butyrate (NaB), the sodium salt of butyrate, can protect neurons from cell death in models of Parkinson's disease (Sharma & Taliyan, 2015). NaB also demonstrated a profound effect on improving learning and memory, as treatment in a mouse model of Alzheimer's disease restored histone acetylation, expression of learning-associated genes, and improvement in contextual memory (Govindarajan, Agis-Balboa, Walter, Sananbenesi, & Fischer, 2011; Kilgore et al., 2010). As mentioned previously, butyrate is also capable of regulating microglia (Huuskonen et al., 2004; Patnala et al., 2016). Moreover, long-term SCFA treatment has been reported to reverse microglial immaturity and malformation observed in germ-free mice, which was dependent upon activation of FFAR2 (Erny et al., 2015).

Evidence indicates that high fiber, butyrate-producing diets are capable of improving the health of our brains, although this is largely understudied (Bourassa, Alim, Bultman, & Ratan, 2016). One study found significant immune benefits in the brain of mice fed a high fermentable (soluble) fiber diet and found that they recovered faster from LPS-induced sickness (Sherry et al., 2010). After exposure to LPS, mice fed the soluble fiber diet showed an increase in IL-1RA and a decrease in IL-1β and TNF-α in the brain. Brain IL-4 mRNA was also increased, and as IL-4 expression is enhanced by increased histone acetylation, the authors hypothesized that the elevated butyrate from the dietary fiber fermentation may contribute to the immune response. It is still not fully understood however, if an increase in butyrate-producing bacteria in the gut as a consequence of soluble fiber diet, could affect microglial activation, and specifically microglial activation in aging.

1.6 Conclusion

As age-related microglial dysfunction could lead to pathologies such as autoimmune and neurodegenerative diseases, there is an urgent need to define the underlying mechanisms responsible for the contribution of microglia in chronic neuroinflammation. Although there is an increasing amount of data indicating that epigenetics play a role in aging, aging-related diseases, microglial phenotype, and pro-inflammatory cytokine regulation, to my knowledge these research areas have never been synthesized and looked at collectively. Thus, my dissertation research is focused on discovering relationships between epigenetic modifications and microglial activation, as well as using pharmacological agents and nutrients that act as epigenetic modifiers to alter microglial phenotypes. Understanding and manipulating the epigenome holds promise for preventing and treating age-related diseases, such as therapies targeted to restore the DNA methylation and histone modification profile of aging cells to that of young cells. Specifically, a better understanding of how epigenetic mechanisms become dysregulated with age in microglia is needed to improve our understanding of what triggers neuroinflammatory complications observed in age-related neurological disorders.

CHAPTER 2: AGING AND PERIPHERAL LIPOPOLYSACCHARIDE CAN MODULATE EPIGENETIC REGULATORS AND DECREASE IL-1β PROMOTER DNA METHYLATION IN MICROGLIA

Adapted from Neurobiology of Aging (renumbered figures and formatting). Matt, S. M., Lawson, M. A., & Johnson, R. W. (2016). Aging and peripheral lipopolysaccharide can modulate epigenetic regulators and decrease IL-1β promoter DNA methylation in microglia. *Neurobiol Aging, 47*, 1-9. doi:10.1016/j.neurobiolaging.2016.07.006, with permission from Elsevier.

2.1 Abstract

In aged mice, peripheral stimulation of the innate immune system with lipopolysaccharide (LPS) causes exaggerated neuroinflammation and prolonged sickness behavior due in part to microglial dysfunction. Epigenetic changes to DNA may play a role in microglial dysfunction; therefore, we sought to determine whether aged microglia displayed DNA hypomethylation of the interleukin-1 beta (IL-1β) promoter and altered expression of epigenetic regulators. We further examined whether the demethylating agent 5-azacytidine induced IL-1β expression in BV2 and primary microglia similar to microglia from aged mice. Novel findings indicated that aged mice had decreased methylation of the IL-1β gene promoter in primary microglia basally or following systemic LPS that is associated with increased IL-1β mRNA, intracellular IL-1β production, as well as prolonged sickness behavior. Last, 5-azacytidine increased IL-1β gene expression and decreased DNA methylation of BV2 and primary microglial cells similar to microglia from aged mice. Taken together, these data indicate that DNA methylation promotes heightened microglial activation in the aged brain.

2.2 Introduction

In the aged brain, it is common for microglia to have an inflammatory gene expression profile and a deramified morphology com- parable to the morphology of activated adult microglia (Damani et al., 2011; Sierra, Gottfried-Blackmore, McEwen, & Bulloch, 2007;

Tremblay, Zettel, Ison, Allen, & Majewska, 2012). What's more, microglia in the brain of aged animals are hypersensitive to signals emerging from the peripheral immune system during infection, resulting in an aberrant neuroinflammatory response that is more intense and longer lasting (Dilger & Johnson, 2008; Henry et al., 2009; Sierra et al., 2007). This exaggerated proinflammatory response can be neurotoxic, lead to behavioral pathology (e.g., anorexia, acute cognitive disorders, and delirium) and exacerbate neurodegenerative diseases (e.g., Alzheimer's disease), greatly enhancing morbidity and mortality in older adults (Franceschi & Campisi, 2014). Why microglia become proinflammatory during aging and why they are hypersensitive to signals from the peripheral immune system is not known.

One way that microglial dysfunction may occur is through epigenetic modifications. Epigenetics refers to changes in gene expression that are independent of changes in the DNA sequence; it is thought of as a mediator between gene environment interactions (Bird, 2007; Jaenisch & Bird, 2003). Epigenetics impact gene regulation though mechanisms such as DNA methylation and posttranslational modifications to histone tails, with DNA methylation being the most well-studied mechanism. DNA methylation is catalyzed by DNA methyltransferases (DNMTs) that includes DNMT1, DNMT3a, and DNMT3b (Moore et al., 2013). DNMT1 is a maintenance methyltransferase that maintains DNA methylation patterns during the DNA replication process, whereas DNMT3a and DNMT3b are de novo methyltransferases, capable of catalyzing new methylation patterns of previously unmethylated sequences. Another protein associated with DNA methylation is MeCP2, which binds to methylated cytosines and recruits histone deacetylases (HDACs) and other corepressors. This promotes higher-affinity interaction between DNA and histone core, condensing the chromatin, and typically suppresses transcription

factor binding and gene expression (Bird, 2002; Strahl & Allis, 2000). In addition, Gadd45b protein plays an important role in active DNA demethylation (Ma et al., 2009).

DNA methylation depends on a precise balance of methylation and demethylation reactions that are nicely balanced in mature cells, but with age, there is a strong shift to favor DNA hypomethylation (Pogribny & Vanyushin, 2010b). Age-related DNA hypomethylation may lead to redistribution of heterochromatin, impair normal gene responsiveness to environmental signals, and increase genomic instability that could compromise proper cell function. Aging could therefore be thought of as a time- dependent, epigenetically mediated loss of phenotypic plasticity (Gravina & Vijg, 2010), suggesting that aberrant DNA methylation patterns may be candidate mechanisms for explaining how microglia from aged mice seem to be "stuck" in a proinflammatory phenotype.

A handful of studies have demonstrated gene expression regulation by DNA methylation in microglia. One using BV2 cells, a murine microglial cell line, reported that DNA methylation influences the expression of several genes associated with the pathology of Alzheimer's disease (Byun et al., 2012), and another revealed that promoting increased maternal care alters the methylation pattern of the IL-10 gene, leading to increased IL-10 expression in the nucleus accumbens and a reduction in morphine-induced addiction behavior (Schwarz & Bilbo, 2013). Very recently, it has also been determined that SIRT1 deficiency in aging microglia is related to increased IL-1β transcription and decreased methylation of CpG sites within the IL-1β proximal promoter (Cho et al., 2015).

Although increasing evidence suggests microglial phenotype is regulated by epigenetic mechanisms, little is known about DNA methylation of proinflammatory cytokines of healthy microglia from aged animals and the contribution of enzymes that significantly impact the

epigenetic landscape. Because it is thought that microglia are the major producers of IL-1β in the brain and one of the most consistently upregulated cytokines with age (Burton, Rytych, Amin, & Johnson, 2016; Chen et al., 2008), the objectives of this study were to determine whether there are promoter IL-1β DNA methylation modifications as well as altered gene expression of epigenetic regulators present between brain immune cells of young and old mice exposed to an immune challenge. Using the demethylating drug 5-azacytidine (5-aza), we also tested whether and how IL-1β gene expression is regulated in BV2 and primary microglial cells. We hypothesized that aged mice and those stimulated with an immune challenge would have IL-1β promoter hypomethylation associated with increased IL-1β gene expression, decreased expression of epigenetic regulators that promote DNA methylation, and that BV2 and adult primary microglial cells would have IL-1β promoter hypomethylation similar to an "aging" phenotype with the treatment of 5-aza.

2.3 Methods

Animals

Adult (4- to 6-month old) C57BL/6 mice were either purchased from Charles River or reared in-house, and aged (24- to 26-month old) C57BL/6 mice were purchased from the National Institute on Aging. They were individually housed in a temperature-controlled environment with a reversed-phase light/dark cycle (lights on 9 PM). Mice that were purchased were allowed to acclimate to their environment for at least 4 weeks before experimentation. All studies were carried out in accordance with United States National Institutes of Health guidelines and were approved by the University of Illinois Institutional Animal Care and Use Committee.

Immune Challenge

Escherichia coli lipopolysaccharide (LPS; serotype 0127:B8, Sigma, St. Louis, MO, USA) was dissolved in sterile saline before experimentation. Mice from both age groups were given LPS (0.33 mg/kg body weight) or saline intraperitoneal. This dose of LPS was selected based on previous studies demonstrating that 0.33 mg/kg LPS produced prolonged sickness behavior in aged compared with young mice (Godbout et al., 2005). Treatments were administered at 9 AM for all cohorts.

Behavioral Testing

Sickness behavior was assessed by changes in body weight and locomotor activity. Body weight and locomotor behavior were measured at baseline and 4 or 24 hours after treatment. Mice were placed in clear plexiglass cages identical to their home cage but devoid of bedding or nesting material. Clear plexiglass lids were placed on top of test cages to prevent escape while facilitating video recording. Locomotor activity was evaluated by virtual division of the cage into 4 equal quadrants and then tallying the number of line crossings and rearings each mouse displayed during the 5-minute test period. Videos were scored by a trained experimenter blinded to treatment.

Microglia Isolation

Animals were euthanized via CO2 asphyxiation 4 or 24 hours after treatment, perfused with sterile ice-cold saline, and brain tissue was collected and used immediately for microglia isolation using a procedure adapted from Nikademova & Watters (Maria Nikodemova & Watters, 2012). To ensure a sufficient number of cells were recovered, tissue samples from 2 mice were pooled within a given experimental group. Brains were enzymatically digested using the Neural Tissue Dissociation Kit (Miltenyi Biotec, Germany) for 35 minutes at 37 C. Further

processing was per- formed at 4 C. Tissue debris was removed by passing the cell suspension through a 40-mm cell strainer. After myelin removal using 30% Percoll Plus (GE Healthcare, Princeton, NJ, USA), cells in phosphate-buffered saline supplemented with 0.5% bovine serum albumin (BSA) and 2-mM EDTA were incubated for 15 minutes with anti-fluorescein isothiocyanate (FITC) magnetic beads and anti- Cd11b-FITC antibody (BD Biosciences) for flow cytometry or anti- Cd11b magnetic beads (Miltenyi Biotec, Germany) for gene expression and DNA methylation arrays. $CD11b^+$ cells were extensively washed and separated in a magnetic field using MS columns (Miltenyi Biotec, Germany). Cell yields for isolated microglia were around 1×10^6 cells per 2 brains and were not different between treatments.

Extracellular and intracellular flow cytometric analysis

Flow cytometric analysis of $CD11b^+$ cell surface and intracellular markers was performed based on BD Cytofix/Cytoperm Plus fixation/permeabilization protocol (BD Biosciences, San Jose, CA, USA), as described previously, with a few modifications (Henry et al., 2009). Isolated cells were incubated in Dulbecco's Modified Eagle Medium (DMEM) (Bio-Whittaker, Cambrex, MD, USA) with 10% fetal bovine serum (FBS) (Hyclone, Logan, UT), 100 units/mL penicillin/streptomycin (Invitrogen, Carlsbad, CA, USA), and brefeldin A (BD Biosciences) at 37 C in a humidified incubator under 5% CO2 for 4 hours. After incubation cells were washed, resuspended in phosphate-buffered saline/0.5% BSA/0.01% sodium azide solution (flow buffer), and Fc receptors were blocked with anti-CD16/CD32 antibody (eBioscience, San Diego, CA, USA). Cells were then incubated with anti-CD45-allophycocyanin (APC), anti-MHC-II-R-Phycoerthrin (PE), and anti-Ly-6C-BV421 (BD Biosciences). Next, cells were fixed and permeabilized with BD Cytofix/CytoPerm solution, washed and resuspended in BD Perm/Wash buffer, and incubated with anti- IL-1β-PE (eBioscience) for 30 minutes. Cells were washed in

BD Perm/Wash buffer and resuspended in flow buffer. Expression of surface and intracellular antigens was deter- mined using a Becton-Dickinson LSR II Flow Cytometer (Red Oaks, CA, USA). Ten to twenty thousand events were collected, and gating was determined based on fluorescently labeled isotype antibodies for FITC, APC, PE, and BV421 (BD Biosciences) incubated for 15 minutes with compensation beads from the AbC Total Antibody Compensation Bead Kit (Thermo Fisher Scientific, Grand Island, NY, USA). Unstained samples were used as controls. Flow data were analyzed using FCS Express software (De Novo Software, Los Angeles, CA, USA).

BV2 and primary microglia cell culture and drug treatments

BV2 cells were maintained in 150-cm^2 tissue culture flasks (BD Falcon) in DMEM supplemented with 10% FBS and 100 units/mL penicillin/streptomycin at 37 C in a humidified incubator under 5% CO2. When cells reached confluence, they were passed by trypsinization, resuspended in serum-free DMEM, and seeded in 12-well plates (BD Falcon). Cells were treated one day later with 10 mM of 5-aza (Sigma, St. Louis, MO, USA) for 48 hours with daily media replacement and stimulated with 100 ng/mL LPS 4 or 24 hours later. Primary microglia from young adult mice were plated on poly-L-lysine (Sigma) coated 12-well plates in DMEM supplemented with 10% FBS, 100 units/mL penicillin/streptomycin, and 5 ng/mL GM-CSF and maintained at 37 C in a humidified incubator under 5% CO2. Cells were treated 7-8 days after culturing with 10-mM 5- aza for 24 hours and then 100 ng/mL LPS for 4 hours. Both media and cells were collected, and cells were put directly in Trizol reagent (Invitrogen) for all cell culture experiments. The viability of BV2 and primary-cultured microglia cells were evaluated using the Thermo Scientific Pierce Lactate Dehyrogenase Cytotoxicity Assay Kit (Thermo Scientific, Rockford, IL, USA) in accordance with the manufacturer's instructions and was <15%.

Gene Expression and DNA Methylation Assays

Total RNA and DNA from microglia were isolated using the Tri Reagent protocol (Invitrogen). Synthesis of complementary DNA was carried out using a high-capacity RT kit (Applied Biosystems, Grand Island, NY, USA) according to the manufacturer's instructions. Real-time quantitative reverse transcription polymerase chain reaction was performed on an ABI PRISM 7900HT- sequence detection system (Perkin Elmer, Forest City, CA, USA) to detect changes in messenger RNA (mRNA) expression of the epigenetic regulators DNMT1 (catalog no. Mm.PT.58.30881142), DNMT3a (Mm.PT.58.13545327), DNMT3b (Mm.PT.58.31955137), HDAC1 (Mm.PT.58.43356830.g), MeCP2 (Mm.PT.58.13934895.g), and Gadd45b (Mm.PT.58.10699383.g), the proinflammatory cytokine IL-1β (Mm00434228_m1), and regulators of IL-1β processing and signaling including IL-1RA (Mm00446186_m1), NLRP3 (Mm.PT.58.6779853.gs), and Casp1 (Mm.PT.58.8975671.gs). All genes were analyzed using PrimeTime real-time quantitative RT-PCR Assays (Integrated DNA Technologies, Coralville, IA, USA) and were compared with the housekeeping control gene GAPDH (Mm99999915_g1) using the 2 DDCt calculation method as previously described (Livak & Schmittgen, 2001). Data are expressed as fold change versus controls. To minimize unequal variances, gene expression for BV2 and primary cultured cells were log10 transformed for statistical analyses only. Methylation status was assessed via methylation-specific real-time PCR (MSP) on bisulfite-modified DNA (Zymo Research, Irvine, CA, USA). MSP primers were designed using Methprimer software (http://www. urogene.org/methprimer/): (Li & Dahiya, 2002). Primer sets targeted a methylated and unmethylated CG dinucleotide in DNA associated with the promoter region of IL-1β or unmethylated b-tubulin-4 as a reference gene as previously published (Gupta et al., 2010; Levenson et al., 2006) and are listed in **Table 2.1**. Product specificity was

determined by melt curve analysis and gel electrophoresis. For the MSP data, a methylation index was calculated by dividing the fold change value for the methylated primer set by the fold change value for the unmethylated primer as previously described (Blaze, Scheuing, & Roth, 2013; Sui, Wang, Ju, & Chen, 2012).

Target Gene	Primer Sequence (5'-3')
IL-1β Methylated	TTTTAGTTTAAGTATAAGGAGGCGA ACACATTCGCAAATATATCATCGTA
IL-1β Unmethylated	TTTTAGTTTAAGTATAAGGAGGTGA AACACATTCACAAATATATCATCATA
β –tubulin-4 Unmethylated	GGAGAGTAATATGAATGATTTGGTG CATCTCCAACTTTCCCTAACCTACTTAA

Table 2.1. Primers used in methylation-specific real-time polymerase chain reaction experiments

Global DNA Methylation Analysis

Global DNA methylation status in primary microglia was per- formed using the MethylFlash Methylated DNA Quantification Kit, an enzyme-linked immunosorbent assay used to detect the total amount of 5 mC. The assay was run according to the manufacturer's instructions (Epigentek, Farmingdale, NY, USA).

Statistical Analyses

All data were analyzed using Statistical Analysis System (SAS, Cary, NC, USA). Behavior data and data from primary microglia (not cultured) were subjected to 2-way analysis of variance for main effects of age and LPS and all 2-way interactions. Data from cell culture experiments were subjected to unpaired t-tests or 2-way analysis of variance for main effects of

5-aza and/or LPS, and all interactions. Where analysis of variance revealed a significant interaction ($p < 0.10$ unless noted elsewhere), Fisher's LSD test was used for post hoc comparisons when appropriate. All data are expressed as means ± standard error of the mean.

2.4 Results

LPS-induced sickness behavior in adult and aged mice

As previously reported in BALB/c mice (Godbout et al., 2005), aged C57BL/6 mice as well as those given LPS had a decrease in locomotor activity (**Figure 2.1**). At 4 hours, both age ($F [1,35] = 11.83$, $p = 0.001$) and LPS ($F[1,35] = 19.51$, $p < 0.0001$) produced a significant reduction in the number of line crossings during the locomotor task. At 24 hours, there was still a reduction in locomotor activity with age ($F[1,34] = 6.24$, $p = 0.018$) and LPS ($F [1,34] = 3.68$, $p = 0.063$).

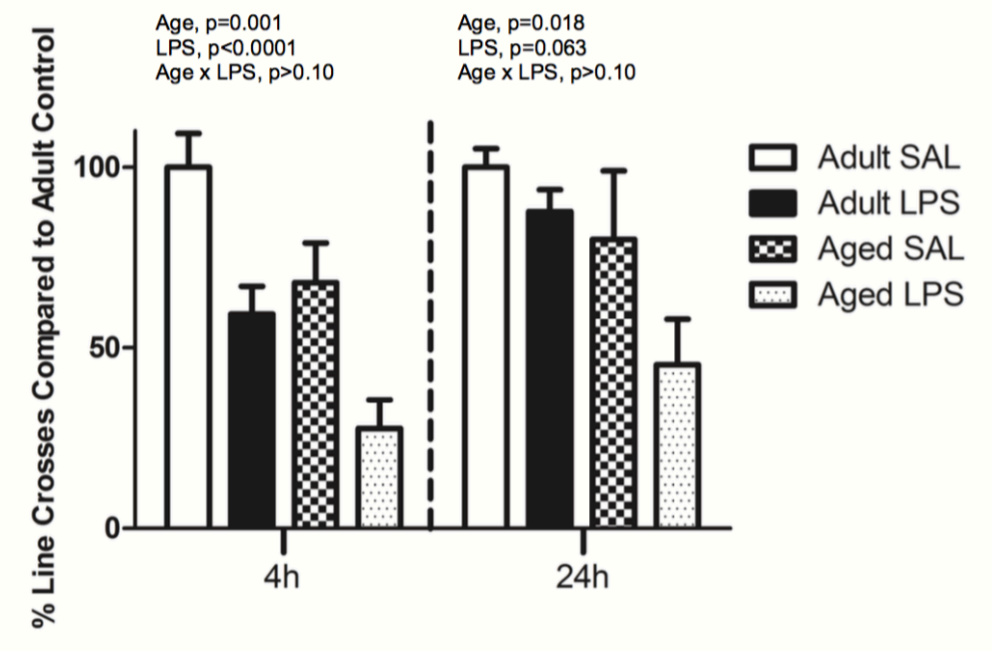

Figure 2.1. Sickness behavior in adult and aged mice after LPS. Mice were injected i.p. with sterile saline or LPS. Locomotor activity was measured at 4 and 24 hours post-injection. Activity of adult saline-treated mice at 4 hours was used for the baseline behavior. Bars represent the mean ± SEM (n = 9-10).

Primary microglia had increased MHCII expression with age and increased IL-1β expression with age and LPS

Adult and aged mice were injected with saline or LPS, and brain cells were isolated using Cd11b^{+} magnetic bead separation. These cells identified as CD11b^{+}, CD45low, and Ly6C^{-}, thought to be pre- dominantly microglia, were stained for IL-1β and major histocompatibility complex class II (MHCII) and analyzed by flow cytometry. **Figure 2.2A** and **2.2B** show representative histograms and **Figure 2.2C** and **2.2D** show the percentages of cells that were IL-1β and MHCII^{+}. A greater proportion of microglia from aged mice expressed MHCII compared with adults ($F[1,12] = 43.19$, $p < 0.0001$), whereas there was no difference between saline and LPS-treated mice, consistent with previous findings (Henry et al., 2009). Further, both aged animals and those treated with peripheral LPS had an increased percentage of IL-1β microglia

(F[1,12] = 16.82, p = 0.002 and F[1,12] = 5.66, p = 0.035), and there was an interaction in that the LPS- induced increase in IL-1β cells was greater in aged mice compared with adults (F[1, 12] = 3.42, p = 0.089).

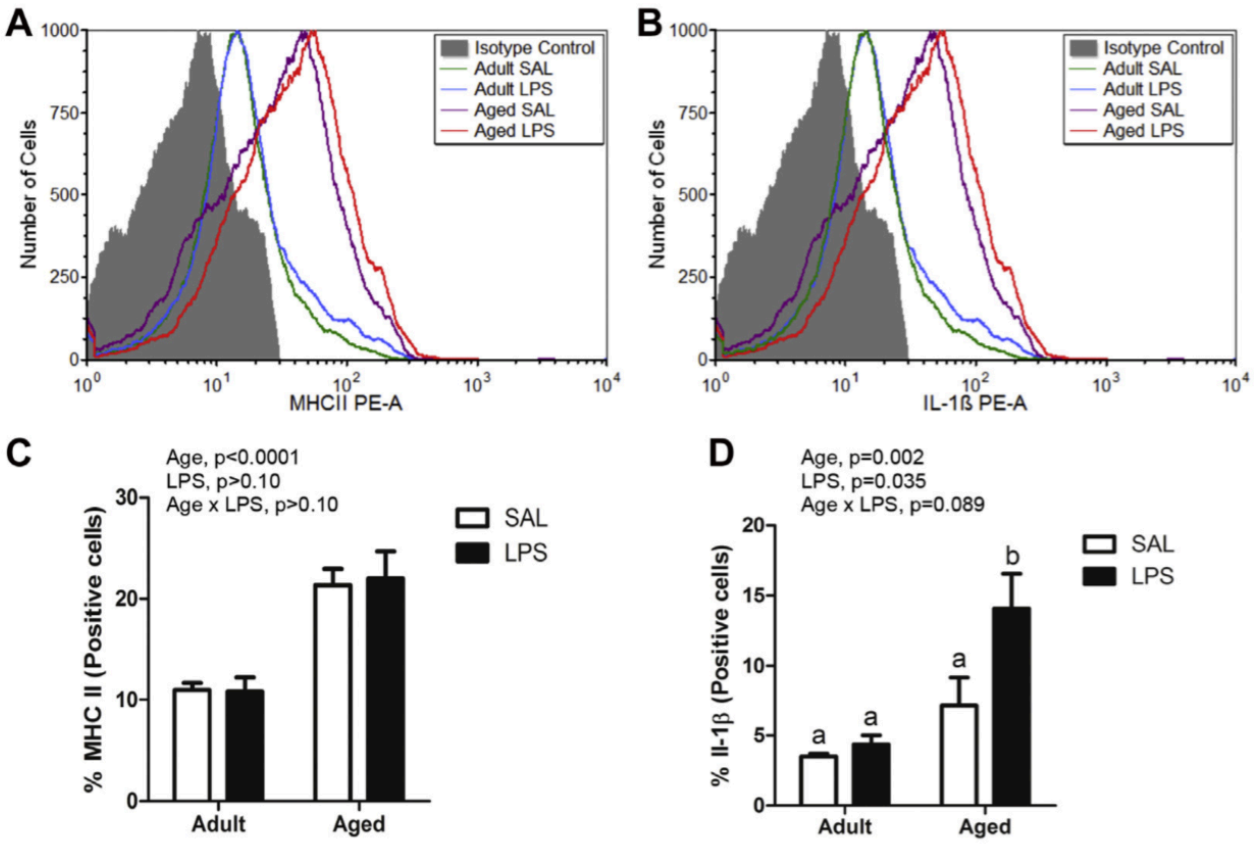

Figure 2.2. Differential expression of MHCII and IL-1β on microglial cells from saline (SAL) or LPS-treated adult and aged mice. Representative histograms of $Cd11b^{+}/CD45_{low}/Ly6C^{-}$ cells incubated with (A) anti-MHCII PE and (B) anti- IL-1β PE compared with isotype controls. Average percentage of $Cd11b^{+}/CD45_{low}/Ly6C^{-}$ cells that were (C) $MHCII^{+}$ or (D) IL-1β. Bars represent the mean ± standard error of the mean (n = 7-10). Treatment means with different letters are significantly different. Abbreviations: IL-1β, interleukin-1 beta; LPS, lipopolysaccharide; MHCII, major histocompatibility complex class II; PE, phycoerthrin.

IL-1β promoter DNA methylation decreased in aged and LPS- treated primary microglia

As expected, for IL-1β mRNA, there was a main effect of age (F[1, 26] = 16.39, p = 0.0004) and LPS (F[1, 26] = 7.51, p = 0.01) at 4 hours and main effect of age (F[1, 30] = 20.18, p < 0.0001) and LPS (F[1, 30] = 9.9, p = 0.004) at 24 hours in that aged mice, and mice given

LPS had increased IL-1β compared with adult and saline-treated mice (**Figure 2.3A**). For IL-1β promoter DNA methylation, there was a main effect of age (F[1, 3] = 6.91, p = 0.02) at 4 hours and a main effect of LPS (F[1, 17] = 6.59, p = 0.02) at 24 hours in that aged mice, and mice given LPS had decreased methylation compared with adult and saline-treated mice (**Figure 2.3B**). This coincides with the increase in IL-1β mRNA in aged and LPS-treated mice. DNA from these samples was also used to assess global methylation status, but neither age nor LPS significantly altered 5 mC content (data not shown).

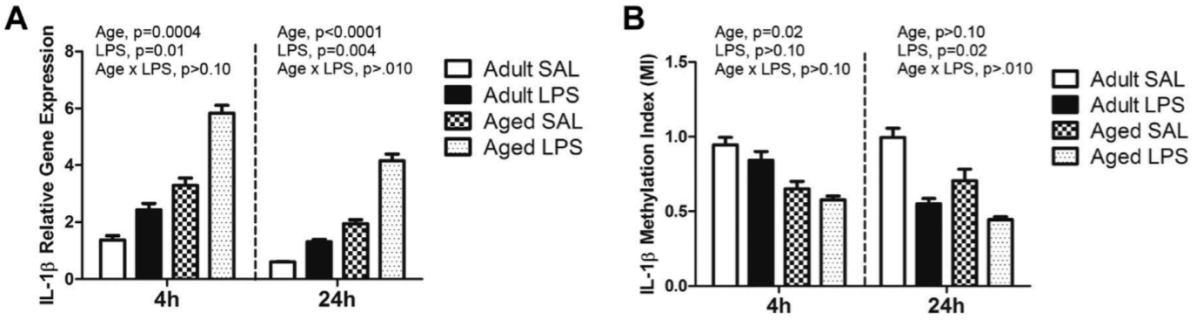

Figure 2.3. Increased microglial IL-1β gene expression in aged and LPS-treated mice coincides with decreased IL-1β promoter DNA methylation. Adult and aged mice were injected i.p. with LPS or sterile saline (SAL) and 4 or 24 hours later, brain tissue was collected for $Cd11b^{+}$ cell isolation. Bars represent the mean ± standard error of the mean (n = 7-10). (A) IL-1β gene expression at 4 hours and 24 hours, and (B) IL-1β DNA methylation at 4 hours and 24 hours. Abbreviations: IL-1β, interleukin-1 beta; LPS, lipopolysaccharide.

Epigenetic regulators are altered by age and LPS in primary microglia

To gain a broader view of the role of epigenetic regulators in neuroinflammation, mRNA for several enzymes that participate in DNA methylation was measured in microglia from adult and aged mice 4 or 24 hours after intraperitoneal injection of LPS (**Figure 2.4**). Of note, there were decreases in DNMT3a, DNMT3b, HDAC1, and MeCP2 mRNA with age and/or LPS at 4 and/or 24 hours. Both DNMT3a and MeCP2 had significant age LPS interactions at 24 hours in that aged saline-treated mice had much lower mRNA levels of DNMT3a and MeCP2 compared

to saline-treated adults. For Gadd45b, there were increases in mRNA with age at both 4 and 24 hours and with LPS at 4 hours.

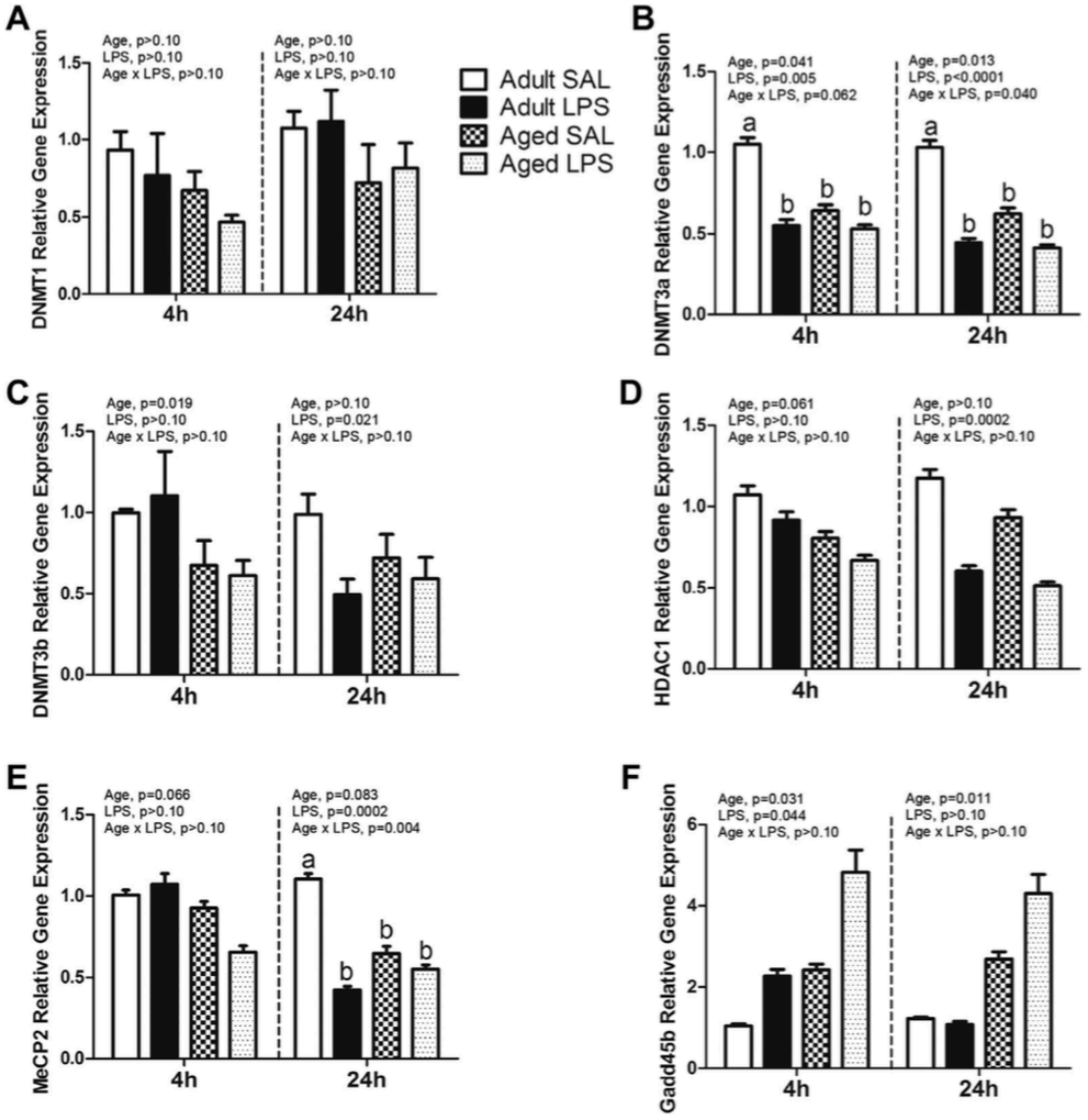

Figure 2.4. Microglial cell gene expression of epigenetic regulators 4 and 24 hours after saline (SAL) or LPS. Adult and aged mice were injected i.p. with LPS or sterile saline, and 4 or 24 hours later, brain tissue was collected for $Cd11b^{+}$ cell isolation. Data are presented as means ± standard error of the mean (n 7-10) for (A) DNMT1, (B) DNMT3a, (C) DNMT3b, (D) HDAC1, (E) MeCP2, and (F) Gadd45b gene expression. Treatment means with different letters are significantly different. Abbreviations: DNMT, DNA methyltransferase; HDAC, histone deacetylase; LPS, lipopolysaccharide; MeCP2, methyl-CpG binding protein-2.

Inhibiting DNA methylation increased IL-1β gene expression in BV2 cells and primary microglia

To demonstrate whether or not DNA methylation plays a direct role in primed microglial IL-1β mRNA expression, the BV2 immortalized murine microglial cell line was treated with 5-aza for 48 hours and/or LPS for 4 or 24 hours. IL-1β promoter DNA methylation was decreased by 5-aza treatment ($F[1, 4] = 5.18$, $p = 0.007$; **Figure 2.5A**). For IL-1β mRNA expression, there was a main effect of LPS ($F[1, 10] = 616.78$, $p < 0.0001$), 5-aza ($F[1, 10] = 26.73$, $p = 0.0004$), and a 5-aza LPS interaction ($F[1, 10] = 6.22$, $p = 0.032$) with a 4-hour LPS treatment in that 5-aza, and LPS produced a greater increase in IL-1β than 5-aza or LPS alone (**Figure 2.5B**). Similarly, for the 24-hour LPS treatment, there was a main effect of LPS ($F[1, 10] = 89$, $p < 0.0001$), 5-aza ($F[1, 10] = 25.7$, $p = 0.0005$), and a 5-aza LPS interaction ($F[1, 10] = 8.4$, $p = 0.016$) in that 5-aza, and LPS produced a greater increase in IL-1β than 5-aza or LPS alone, albeit less than at 4 hours (**Figure 2.5C**). In addition, primary microglial cells were cultured for 7-8 days and treated with 5-aza for 24 hours and/or LPS for 4 hours. IL-1β promoter DNA methylation was decreased by 5-aza and LPS treatment ($F[1, 10] = 26.27$, $p = 0.0004$) and ($F[1, 10] = 22.6$, $p = 0.0008$), and there was a 5-aza LPS interaction ($F[1, 10] = 15.08$, $p = 0.003$; **Figure 2.6A**). For IL-1β mRNA expression, there was a main effect of LPS ($F[1, 9] = 652.96$, $p < 0.0001$) and a main effect of 5-aza ($F[1, 9] = 4.49$, $p < 0.063$; **Figure 2.6B**). The increase in IL-1β mRNA was numerically greatest when LPS and 5-aza were combined, but the 5-aza LPS interaction was not significant. We also assessed mRNA for genes involved in IL-1β signaling and processing in primary microglia (**Table 2.2**). For the 3 genes assessed, there was a main effect of LPS ($F[1, 20] = 107.01$, $p < 0.0001$; $F[1, 20] = 324.97$, $p < 0.0001$; and $F[1, 20] = 588.09$, $p < 0.0001$ for Casp1, IL-1rn, and NLRP3, respectively), and for Casp1 and NLRP3,

there was a main effect of 5-aza ($F[1, 20] = 3.55$, $p = 0.074$ and $F[1, 20] = 3.44$, $p = 0.079$, respectively). No interactions were detected. These results suggest that several genes involved in IL-1β signaling and processing are affected by DNA methylation but not in the same way as IL-1β.

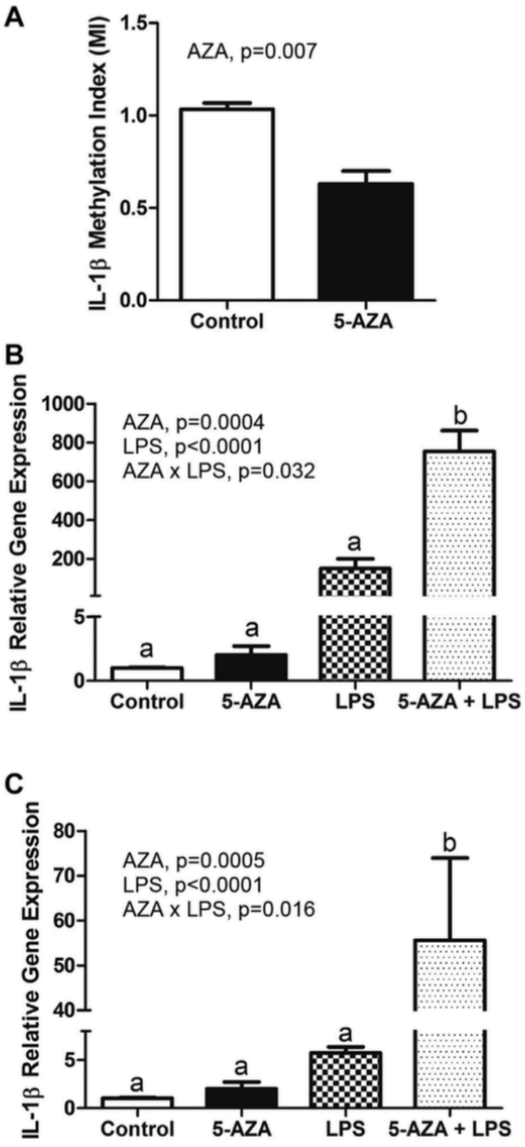

Figure 2.5. Increased IL-1β gene expression in 5-aza, and LPS-treated BV-2 cells coincide with decreased IL-1β promoter DNA methylation. BV-2 cells were treated with 5-aza for 48 hours and/or LPS for 4 or 24 hours. Bars represent the mean ± standard error of the mean (n = 3-4). (A) IL-1β promoter DNA methylation as measured by a Methylation Index (MI). (B) IL-1β mRNA expression after 4 hours LPS treatment. (C) IL-1β mRNA expression after 24 hours LPS treatment. Treatment means with different letters are significantly different. Abbreviations: 5-aza, 5-azacytidine; IL-1β, interleukin-1 beta; LPS, lipopolysaccharide.

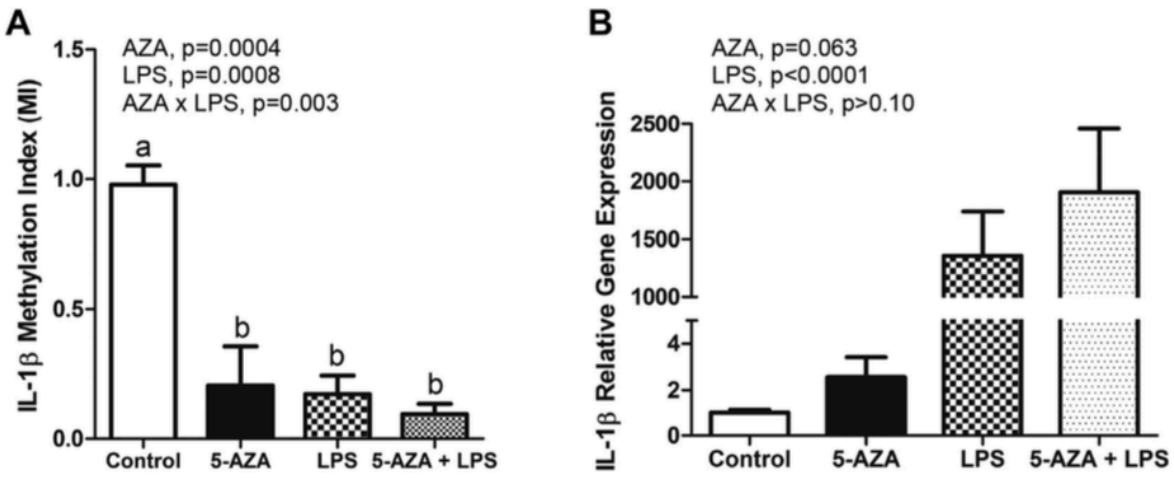

Figure 2.6. Increased IL-1β gene expression in 5-aza, and LPS-treated primary cultured microglia coincide with decreased IL-1β promoter DNA methylation. Primary-cultured microglia were treated with 5-aza for 24 hours and/or LPS for 4 hours. Bars represent the mean ± standard error of the mean (n = 3-4) for (A) IL-1β promoter DNA methylation as measured by a Methylation Index (MI) and (B) IL-1β mRNA expression. Treatment means with different letters are significantly different. Abbreviations: 5-aza, 5-azacytidine; IL-1β, interleukin-1 beta; LPS, lipopolysaccharide.

Table 2
Expression of IL-1β signaling and processing genes in 5-aza and LPS-treated primary cultured microglia

Gene	Vehicle		Aza		*p*-value		
	Control	LPS	Control	LPS	Aza	LPS	Aza × LPS
Casp1	1.04 ± 0.12	3.09 ± 0.48	0.72 ± 0.05	2.67 ± 0.17	0.074	<0.0001	0.307
IL-1Rn	1.10 ± 0.18	32.73 ± 6.79	0.95 ± 0.11	26.55 ± 2.86	0.632	<0.0001	0.962
NLRP3	1.06 ± 0.15	42.22 ± 9.60	0.68 ± 0.13	34.07 ± 2.06	0.079	<0.0001	0.285

Table 2.2. Primary cultured microglia were treated with 5-aza for 24 hours and/or LPS for 4 hours. Data represent the mean ± standard error of the mean (n = 3-4). Key: 5-aza, 5-azacytidine; IL-1β, interleukin-1 beta; LPS, lipopolysaccharide.

2.5 Discussion

The present study was designed to investigate a link between DNA methylation and the microglial phenotype of aged mice. We clearly demonstrated that age and LPS have the capacity to alter DNA methylation and expression levels of genes important for establishing, maintaining, or reversing DNA methylation in micro- glial cells. Of note, both aging and stimulation of the immune sys- tem with a proinflammatory agent (LPS) produces sickness behavior and decreases in methylation of the IL-1β promoter that coincide with increases in IL-1β gene expression and intracellular IL-1β production, suggesting that DNA methylation plays a role in the

overexpression of this proinflammatory cytokine with age. Although the percentage of IL-1β cells do not completely match previous findings (Henry et al., 2009), it is likely that our cell population is more highly purified now that the magnetic bead separation technique is used instead of the previous isolation method with a Percoll gradient (Burton, Rytych, Freund, & Johnson, 2013; Henry et al., 2009). Importantly, percentage of $Cd11b^{+}/CD45_{low}$ cells is considerably higher with the new method (Maria Nikodemova & Watters, 2012).

There are a number of possible mechanisms that could be mediating these alterations in DNA methylation with age and LPS. As nuclear factor-kB (NF-kB) activation is implicated in microglial aging (G. Zhang et al., 2013) and sickness behavior (Nadjar, Bluthe, May, Dantzer, & Parnet, 2005), NF-kB binding activity might play a role in demethylation of the IL-1β promoter. The site of methylation investigated in this study is adjacent to a canonical NF-kB-binding site (Lebedeva & Singh, 1997), and recently, the NF-kB subunit RelB at the IL-1β promoter was demonstrated to be required for the attenuated LPS response in LPS-preconditioned microglia (W. Schaafsma et al., 2015), thus providing evidence that epigenetic regulation of IL-1β in microglia from aged mice could be regulated by increased NF-kB binding that is inhibiting proper DNA methylation to be established. Further, it has been demonstrated that IL-1β induces its own expression in healthy chondrocytes and causes loss of DNA methylation (Hashimoto, Oreffo, Gibson, Goldring, & Roach, 2009). This has the potential to set up a dangerous positive feedback mechanism, and if true in vivo could partially explain the progression of neuroinflammation in aging. It should be stressed that additional studies are necessary to link these gene methylation and expression changes with histone alterations, subsequent behavioral outcomes, and to explore their reversibility.

Global DNA methylation was unchanged by age or LPS stimulation, suggesting that perhaps DNA hypomethylation is not a global phenomenon as it is in other cell types such as fibroblasts (Wilson & Jones, 1983). As epigenetic regulation of other proinflammatory genes such as tumor necrosis factor-a (TNF-a) and IL-6 have been demonstrated in other immune cell types such as natural killer cells and peripheral monocytes/macrophages (Eddy et al., 2014; Sullivan et al., 2007), it will be pertinent to explore regulation by DNA methylation and other epigenetic modifications in microglia, as well as other signature genes relevant to aging such as those recently found in the microglial sensome (Hickman et al., 2013) or other recent transcriptomic studies (Holtman et al., 2015; Orre et al., 2014).

Gene expression of epigenetic regulators was found to be altered with age and LPS and support a number of previously established findings. DNMT3a and DNMT3b mRNA decreased with age, and these genes decrease with age in fibroblasts and T cells (Lopatina et al., 2002; Z. Zhang, Deng, Lu, & Richardson, 2002). LPS decreased DNMT3a expression, and this is consistent with a previous finding that LPS downregulates DNMT3a in calf peripheral blood mononuclear cells that occurred concurrently with high expression of proinflammatory genes (Doherty, O'Farrelly, & Meade, 2013). Further, as differences in DNMT3b expression have the ability to influence adipose tissue macrophage polarization, perhaps the microglial polarization seen in aging is acting through a similar mechanism (Yang et al., 2014). LPS decreased HDAC1 expression and age also slightly decreased the expression at 4 hours ($p < 0.1$), but these results are more difficult to interpret based on existing literature. HDACs in general have been shown to be decreased with aging (Gravina & Vijg, 2010), but evidence has also shown that HDACs are increased with LPS in macrophages (Aung et al., 2006). It has been suggested that HDACs are important in limiting the inflammatory response as they have been reported to modulate Toll-like

receptor-mediated signaling and to inhibit NF-kB signaling (Aung et al., 2006), but inhibiting HDACs has also been demonstrated to suppress innate immune activation in microglia (Kannan et al., 2013). Additional work will be necessary to delineate these differential effects of HDACs in modulating inflammation, but nonetheless the current findings support the idea that decreased expression of corepressors like HDAC1 are associated with decreased IL-1β promoter DNA methylation.

The significant decreases in MeCP2 with age are interesting considering a deficiency in MeCP2 has been widely associated with Rett syndrome, a neurodevelopmental disorder causing mental retardation with early onset in childhood, and MeCP2 mutant mice have been shown to exhibit many of the same cognitive deficits and neuroanatomical abnormalities associated with Rett syndrome (Guy, Hendrich, Holmes, Martin, & Bird, 2001). Intriguingly, selective return of MeCP2 function to microglia arrests Rett syndrome pathology (Derecki, Cronk, & Kipnis, 2013). The mechanism is unclear but may relate to phagocytic ability, as microglia from Mecp2-null mice had severe impairments in phagocytic ability in vitro. The authors proposed that insufficient clearance of debris within the brains of these animals might indeed contribute to the severity of pathology, and it seems that this same phenomenon could also be a mechanism involved in aging. Gadd45b was the only gene to increase with age, but expectedly so in that it plays a major role in DNA demethylation. Previous research has demonstrated that LPS, TNF, IL-6, and other inducers of oxidative stress can increase Gadd45b. Further, NF-kB can stimulate the expression of Gadd45 and simultaneously acts as its regulatory target, thus creating a positive feedback loop (Moskalev et al., 2012).

As DNA hypomethylation is often described in context with gene activation, another important finding was to demonstrate that a demethylating drug like 5-aza has the capacity to

decrease IL-1β promoter DNA methylation and subsequently increase IL-1β mRNA in both BV2 and primary microglia, establishing that DNA methylation does indeed play a direct role in IL-1β gene regulation. This also indicates that BV2 and cultured primary microglia have the capacity to display DNA methylation patterns in a manner consistent with what was seen in freshly isolated microglia (Fig. 2). This is important because primary microglia and cell lines in culture have been shown to lose their microglial signature (Butovsky et al., 2014; Gosselin et al., 2014). The exaggerated increase in IL-1β mRNA with both 5-aza and LPS in BV2 cells suggests that DNA hypomethylation allows LPS to trigger a more pronounced immune response and is in line with previous findings in other cell lines (Kovacs, Oppenheim, Carter, & Young, 1987; Wessels, Fleischer, Rink, & Uciechowski, 2010).

It is also important to consider other factors that can lead to a heightened proinflammatory response with aging, such as expression of the endogenous receptor antagonist of IL-1β, IL-1ra (Spulber, Bartfai, & Schultzberg, 2009) or of inflammasomes (Goldberg & Dixit, 2015). As such, mRNA expression of several genes involved in IL-1β signaling and processing were also investigated in primary microglia treated with 5-aza or LPS. All IL-1β-related genes were upregulated with LPS as expected, but 5-aza decreased Casp1 and NLRP3 mRNA expression with or without LPS. This suggests that Casp1 and NLRP3 are additionally affected by DNA methylation but not in the same way as IL-1β. DNMT inhibitors in general create global demethylation of the genome, but there is some heterogeneity of response of loci (Pandiyan et al., 2013). Depending on cell type and site of methylation (e.g., promoter versus gene body methylation), DNA methylation and transcription can be positively correlated, or variable chromatin accessibility and constitutive DNA hypo- methylation can occur (Wagner et al., 2014). Histone modifications also have a close relationship with DNA methylation and could

be more influential on DNA methylation and transcription of some genes compared to others (Cedar & Bergman, 2009). More analyses of these genes involved in IL-1β signaling and processing will be necessary to understand their effects on microglial IL-1β with aging. However, the observation that 5-aza decreases IL-1β promoter DNA methylation and increases IL-1β mRNA expression (but not mRNA expression of all IL-1β signaling and processing genes) suggests that this is a specific relationship that could be important to understand the changes in IL-1β within the brain and specifically microglia from aged individuals.

Although the increase in IL-1β mRNA with 5-aza and LPS was not significantly exaggerated when combined in primary cultured microglial cells, perhaps they are not capable of the same effects in culture and cannot perform in a similar manner in isolation without the influence of other cell types within the brain. Further, the techniques we used in this study do not allow us to draw any conclusions regarding cytosine methylation verses hydroxymethylation, subregion specificity, or site-specific methylation. In the future, it will be useful to use bisulfite pyrosequencing to characterize site-specific methylation changes of the IL-1β promoter.

These findings highlight the importance of elucidating the interaction of the environment with the epigenome and its role in aging. Manipulating and understanding the epigenome holds promises for preventing and treating age-related diseases, such as restoring the DNA methylation profile of aging cells to that of young or mature cells and preventing significant age-associated demethylation. Specifically, a better understanding of how epigenetic mechanisms like DNA methylation become dysregulated with age in microglia is needed to improve our understanding of neuro- inflammatory complications and lead to the development of therapeutic interventions.

CHAPTER 3: INHIBITION OF DNA METHYLATION WITH ZEBULARINE ALTERS LIPOPOLYSACCHARIDE-INDUCED SICKNESS BEHAVIOR AND NEUROINFLAMMATION IN MICE

3.1 Abstract

Activity of DNA methyltransferases (DNMTs), the enzymes that catalyze DNA methylation, is dynamically regulated in the brain. DNMT inhibitors alter DNA methylation globally in the brain and at individual neural plasticity-associated genes, but how DNMT inhibitors centrally influence lipopolysaccharide (LPS)-induced neuroinflammation is not known. We investigated whether the DMNT inhibitor, zebularine, would alter sickness behavior, DNA methylation of the *Il1b* promoter and expression of inflammatory genes in hippocampus and microglia. Adult mice treated with an intracerebroventricular (ICV) injection of zebularine prior to LPS had faster recovery of burrowing behavior compared to mice treated with LPS. Further, genes of inflammatory markers, epigenetic regulators, and the microglial sensory apparatus (i.e. the sensome) were differentially expressed by zebularine alone or in combination with LPS. Bisulfite pyrosequencing revealed that ICV zebularine led to decreased DNA methylation of two CpG sites near the *Il1b* proximal promoter alone or in combination with LPS. Zebularine treated mice still exhibited decreased DNA methylation 48 h after treatment when LPS-induced sickness behavior as well as hippocampal and microglial gene expression were similar to control mice. Taken together, these data suggest that decreased DNA methylation, specifically of the *Il1b* promoter region, with a DNMT inhibitor in brain disrupts molecular mechanisms of neuroinflammation.

3.2 Introduction

Microglia are long-lived resident immune cells of the brain that show limited turnover (R. M. Ransohoff & Perry, 2009). They develop early in embryogenesis in the embryonic yolk sac and migrate to the central nervous system (CNS) where they remain and are rarely replaced (Ginhoux et al., 2010). Microglia are far from inactive and many recent *in vivo* observations have shown that microglia extend their processes to actively scan the microenvironment (Nimmerjahn et al., 2005; Wake et al., 2009). Despite the dynamic role of microglia in maintaining homeostasis, their long-lived nature and general inability to be replaced by circulating peripheral cells makes them particularly sensitive to oxidative stress, DNA damage, and a lifetime of inflammatory insults. Peripheral macrophage subtypes express different patterns of genes after stimulation with LPS that is linked to environmental influence of distinct epigenetic modifications during their differentiation (Kittan et al., 2013). However, little is known about the epigenetic pathways involved in the modulation of inflammatory genes in the brain and microglia. As the immune system needs to respond to rapidly changing environmental cues, the molecular regulation of inflammatory responses in the brain is also a likely target for epigenetic regulation (Garden, 2013).

DNA methylation of pro-inflammatory cytokines such as *Il1b* is a mechanism that regulates microglial reactivity and could be a therapeutic target for regulating microglia throughout the lifespan. One particularly important study determined that sirtuin 1 deficiency in aging microglia is associated with increased *Il1b* transcription and decreased methylation of CpG sites within the *Il1b* proximal promoter (Cho et al., 2015). More recently, findings from our lab (Matt, Lawson, & Johnson, 2016) indicated that aged mice had decreased methylation of the *Il1b* gene promoter in primary microglia basally or following systemic LPS that is associated with

increased *Il1b* mRNA. Further, the DNMT inhibitor 5-azacytidine increased *Il1b* gene expression and decreased DNA methylation of primary microglial cells.

DNA methylation and demethylation are dynamically regulated in the brain (Kundakovic, Chen, Guidotti, & Grayson, 2009; Roth, Lubin, Funk, & Sweatt, 2009), and it has been demonstrated that DNA methylation changes can happen in as quickly as one hour (Miller & Sweatt, 2007). The reversible nature of epigenetic aberrations contributing to human diseases makes them desirable therapeutic targets. 5-aza-2′-deoxycytidine and 5-azacytidine are DNMT inhibitors that are potential chemotherapeutic agents for cancer, and have been approved for treating myelodysplastic syndrome (Copeland, Olhava, & Scott, 2010). Both drugs act by incorporating into DNA where they bind and sequester DNMTs, which causes prevention of the maintenance methylation (Gnyszka, Jastrzebski, & Flis, 2013). However, both compounds are chemically unstable and toxic. Zebularine is a stable nucleoside analog of cytidine that is a less toxic DNMT inhibitor and the first drug in its class that can reactivate an epigenetically silenced gene by oral administration (Cheng et al., 2003). Moreover, zebularine is comparable to 5-aza-2′-deoxycytidine and 5-azacytidine in terms of its pattern of DNA demethylation (Balch et al., 2005; Griffin, Niederhuth, & Schmitz, 2016).

A significant amount of research has utilized ICV zebularine injections in rodent models, such as a cocaine-induced behavioral sensitization model (Anier, Malinovskaja, Aonurm-Helm, Zharkovsky, & Kalda, 2010), and an ischemic brain injury model (Dock, Theodorsson, & Theodorsson, 2015), to determine the relationship between DNA methylation status and disease. Since DNMT inhibition was able to demethylate the *Il1b* gene promoter and subsequently increase *Il1b* gene expression in vitro (Matt et al., 2016), the objectives of this study were to investigate whether central DNMT inhibition by zebularine causes exaggerated

neuroinflammation in microglia and hippocampus. We hypothesized that central DNMT inhibition would lead to decreased *Il1b* DNA methylation and heightened pro-inflammatory gene expression in adult mice as well as prolonged sickness behavior following central immune stimulation with LPS. Additionally, with the recent discovery of the microglial sensome (Hickman et al., 2013), a unique group of transcripts encoding proteins for sensing endogenous ligands and microbes, we hypothesized zebularine would alter genetic expression of sensome genes in microglia. Last, since DNA methylation affects other epigenetic processes such as histone modifications (Fuks, 2005), we predicted zebularine would change expression of epigenetic regulator genes within microglia.

3.3 Methods

Animals

Adult (3-6-month-old) male C57BL/6J mice (Jackson Laboratory, Bar Harbor, ME, USA) were individually housed in a temperature-controlled environment with a 12-hour reversed-phase light/dark cycle (lights on 21:00h). Mice were allowed to acclimate to these conditions for at least 3 weeks before being stereotaxically implanted with a guide cannula (Plastics One, Roanoke, VA, USA) placed to extend 1 mm dorsal to the lateral ventricle, as previously described (M. A. Lawson et al., 2013). In brief, mice were deeply anesthetized with an intraperitoneal (IP) injection of ketamine, xylazine, and buprenorphine (100, 10, and 0.05 mg/kg, respectively) all at 100µl/10g body weight and the surgical site was shaved and sterilized. Cannulae were placed at 1.5 mm lateral, 0.6 mm posterior, and 1.3 mm dorsal with respect to bregma. Guide cannulae were kept clean and covered using a screw-on dummy cannula (Plastics One). Mice were given 7 days to recover from surgery prior to ICV injections. All studies were

carried out in accordance with United States National Institutes of Health guidelines and approved by the University of Illinois Institutional Animal Care and Use Committee.

Treatments were designed in a 2 x 2 factorial arrangement and administered at the onset of the dark cycle. ICV injections were administered using a 10 µl gas-tight syringe attached to internal injector cannulae (Plastics One) that extended 1 mm beyond the tip of the guide cannula, thus penetrating the lateral ventricle. All mice received treatments in 1 µl injection volume over a 1-minute time period followed by an additional 1-minute delay to allow diffusion before removing the injector cannula. Mice were injected ICV with either saline (control) or 300ng/µl of zebularine (Sigma Aldrich, St Louis, MO, USA) and 30 minutes later with saline or LPS (10 ng/µl) from *Escherichia coli* O127:B8 (Sigma Aldrich). This dose of LPS has been previously demonstrated to induce transient sickness behavior (Huang, Henry, Dantzer, Johnson, & Godbout, 2008).

Burrowing behavior

Decreased burrowing behavior is an indicator of sickness behavior (McLinden et al., 2012). Using a similar procedure described previously (Moon et al., 2015), burrows were constructed of polyvinyl chloride (PVC) pipe fitted at one end with a PVC pipe cap (closed end). The open end was raised 1.3 cm on twin steel legs. To acclimatize mice to the burrow, mice were singly housed in cages with the burrow present for 24 hours prior to testing. Testing was initiated by adding 200 g of food pellets (Harlan Teklad 8640 chow, Madison, WI, USA) to the burrow immediately after the LPS/saline injections. Prior to replacing the burrow filled with food back into the cage, the burrow and food was weighed. Water was provided ad libitum but food was only available from the burrow. Mice were allowed to dig and/or eat the food out of the burrow for 48 h. Amount burrowed was calculated by subtracting the burrow and food weight before and

4, 8, 12, 24, and 48 hours after burrowing. Body weight was also measured at baseline and 4, 8, 12, 24, and 48 hours after the LPS/saline injections.

Microglia isolation

Microglia from mouse brains were isolated from separate groups of mice at 4 hours and 48 hours after treatment. Mice were euthanized via CO_2 asphyxiation, perfused with sterile ice-cold saline, and brain tissue (all but the hippocampus which was frozen on dry ice) was collected and used immediately for microglia isolation using a procedure adapted from Nikademova & Watters (Maria Nikodemova & Watters, 2012). Brains were enzymatically digested using the Neural Tissue Dissociation Kit (Miltenyi Biotec, Bergisch Gladbach, Germany) for 35 min at 37° C. Further processing was performed at 4° C. Tissue debris was removed by passing the cell suspension through a 40 μm cell strainer. After myelin removal using 30% Percoll Plus (GE Healthcare, Princeton, NJ, USA), cells in PBS supplemented with 0.5% BSA and 2 mM EDTA were incubated for 15 minutes with anti-Cd11b magnetic beads (Miltenyi Biotec). $CD11b^+$ cells were extensively washed and separated in a magnetic field using MS columns (Miltenyi Biotec) before being directly placed in Trizol reagent (Invitrogen, Carlsbad, CA, USA).

RNA isolation and real-time RT-PCR

Total RNA from microglia and hippocampal tissue was isolated using the Tri Reagent protocol (Invitrogen). Synthesis of cDNA was carried out using a high-capacity RT kit (Applied Biosystems, Grand Island, NY, USA) according to the manufacturer's instructions. Real-time RT-PCR was performed on an ABI PRISM 7900HT-sequence detection system (Perkin Elmer, Forest City, CA, USA). All genes were analyzed using commercially validated PrimeTime real-time RT-PCR Assays included in Table 1 (Integrated DNA Technologies, Coralville, IA, USA), and were compared with the housekeeping control gene *Gapdh* using the $2^{-\Delta\Delta Ct}$ calculation

method as previously described (Livak & Schmittgen, 2001). Data are expressed as fold change versus controls.

Fluidigm

Total RNA from microglia collected at 4 hours was isolated using the Tri Reagent protocol (Invitrogen) and synthesis of cDNA was carried out using a high-capacity RT kit (Applied Biosystems) as previously described for real-time RT-PCR. Fluidigm reactions were performed by the UIUC Functional Genomics Unit of the W.M. Keck Center using a 96 × 96 chip and included 2 technical replicates for each combination of sample and assay. Data was acquired using the Fluidigm Real-Time PCR Analysis software 3.0.2 (Fluidigm, San Francisco, CA, USA). Data from Fluidigm runs were manually checked for reaction quality before analysis, and C_t values for each gene target (see **Table 3.1**) were normalized to C_t values for the housekeeping gene *Gapdh*.

Table 3.1. Primers used in Real-time RT-PCR and Fluidigm experiments.

Gene	Assay ID
Arg1	**Mm.PT.58.8651372**
Casp1	**Mm.PT.58.13005595**
CD53	**Mm.PT.58.30699738**
CD68	**Mm.PT.58.12034788.g**
Cx3cr1	**Mm.PT.58.17555544**
Dnmt1	**Mm.PT.58.30881142**
Dnmt3a	**Mm.PT.58.13545327**
Dnmt3b	**Mm.PT.58.31955137**
Dnmt3l	**Mm.PT.58.41749889**
Gadd45b	**Mm.PT.58.10699383.g**
Gapdh	**Mm.PT.39a.1**
Gfap	**Mm.PT.58.31297710**
Gpr34	**Mm.PT.58.46001700**
Hdac1	**Mm.PT.58.43356830.g**
Hdac2	**Mm.PT.58.12358619**
Hdac3	**Mm.PT.58.11480126**
Hdac4	**Mm.PT.58.17651425**
Hdac5	**Mm.PT.58.11472897**
Hdac6	**Mm.PT.58.16685964**
Il-1β	**Mm.PT.58.41616450**
Il-1rn	**Mm.PT.58.43781580**
Il-10	**Mm.PT.58.23604055**
Il-4	**Mm.PT.58.32703659**

Gene	Assay ID
Il-6	**Mm.PT.58.13354106**
Mecp2	**Mm.PT.58.13934895.g**
P2ry12	**Mm.PT.58.43542033**
P2ry13	**Mm.PT.58.42597879.g**
Pycard	**Mm.PT.56a.42872867**
Siglech	**Mm.PT.58.45915252**
Socs1	**Mm.PT.58.11527306.g**
Socs3	**Mm.PT.58.7804681**
Stat3	**Mm.PT.58.11877007**
Tet1	**Mm.PT.58.43326803**
Tet2	**Mm.PT.58.30089849**
Tet3	**Mm.PT.58.11954119**
Tgfbr1	**Mm.PT.58.10230349**
Tlr2	**Mm.PT.58.45820113**
Tlr4	**Mm.PT.58.41643680**
Tlr7	**Mm.PT.58.10526075**
Tlr8	**Mm.PT.58.16021150**
Tmem119	**Mm.PT.58.6766267**
Trem2	**Mm.PT.58.7992121**
Tnf	**Mm.PT.58.12575861**

Table 3.1 (cont.). Primers used in Real-time RT-PCR and Fluidigm experiments.

DNA Isolation and Pyrosequencing

Total DNA from microglia and hippocampal tissue collected at both 4 and 48 hours was isolated using the Tri Reagent protocol (Invitrogen). DNA methylation for 2 CpG sites within the proximal promoter region of *Il1b* was assessed via bisulfite pyrosequencing on bisulfite modified DNA (Zymo Research, Irvine, CA, USA). Mouse *Il1b* methylation assays (ID ADS3713-RS1) were purchased from EpigenDx (Hopkinton, MA, USA) and have been previously used to assess methylation status in microglia (Cho et al., 2015). PCRs were run in duplicate and contained 20 ng of bisulfite converted DNA as starting template**.** Product specificity was determined by gel electrophoresis. Each primer was also tested using bisulfite converted DNA from high and low methylation controls (EpigenDx). Qiagen's PyroMark Q24 Advanced Pyrosequencer was used to detect DNA methylation levels following manufacturer's protocols and default settings (Qiagen, Valencia, CA), similar to a previous study (Bustamante et al., 2016).

Statistical Analyses

All data were analyzed using GraphPad Prism 7 (La Jolla, CA, USA). Behavior and change in body weight data were analyzed via a two-way repeated-measures analysis of variance (ANOVA) for main effects of zebularine and LPS, and all two-way interactions. Gene expression and pyrosequencing data from primary microglia and hippocampus were subjected to a two-way ANOVA (no repeated measures) for main effects of zebularine and LPS, and all two-way interactions. Where analysis of variance revealed a significant interaction ($p<0.05$ unless noted elsewhere), Tukey's test was used for post hoc comparisons when appropriate. All data are expressed as means ± SEM.

3.4 Results

Body weight decreases with LPS in both saline and zebularine pre-treated mice

Mice were either pre-treated ICV with saline or zebularine (ZEB), and then given an ICV injection of either saline (SAL) or LPS. For body weight, two way repeated measures ANOVA revealed main effects of both ZEB ($p<0.0001$) and LPS ($p<0.0001$), and an interaction (ZEB x LPS; $p<0.0001$) (**Figure 3.1A**). Post-hoc tests revealed that at 4 hours, all treatment groups were not different ($p>0.05$). At 8 and 12 hours, the SAL+SAL group was different from SAL+LPS ($p=0.0002$ and $p=0.0005$) and ZEB+LPS ($p=0.0006$ and $p<0.0001$), and the ZEB+SAL group was also different from SAL+LPS ($p<0.0001$ and $p<0.0001$) and ZEB+LPS ($p<0.0001$ and $p<0.0001$), in that the SAL+LPS and ZEB+LPS groups lost more weight than the SAL+SAL and ZEB+SAL groups. At 24 hours, the results were similar but the ZEB+LPS group was no longer different than the SAL+SAL group ($p=0.0651$). By 48 hours, body weight of the LPS-treated mice returned near baseline and all treatment groups were once again not different ($p>0.05$).

Zebularine pre-treated mice recover faster from central LPS-induced sickness

For burrowing behavior, two way repeated measures ANOVA revealed main effects of both ZEB ($p<0.0001$) and LPS ($p<0.0001$), and an interaction (ZEB x LPS; $p<0.0001$) (**Figure 3.1B**). Post-hoc tests revealed that at 4 and 8 hours, the SAL+SAL group was different from SAL+LPS ($p<0.0001$ and $p<0.0001$) and ZEB+LPS ($p=0.0474$ and $p<0.0001$), and the ZEB+SAL group was also different from SAL+LPS ($p<0.0001$ and $p<0.0001$) and ZEB+LPS ($p=0.006$ and $p<0.0001$), in that the SAL+LPS and ZEB+LPS groups burrowed less than the SAL+SAL and ZEB+SAL groups. At 12 and 24 hours, the results were similar but the ZEB+LPS group was now different than the SAL+LPS group ($p=0.0071$ and $p=0.0126$), in that the ZEB+LPS was burrowing more. By 48 hours, all of the mice burrowed out the majority of the food and treatment groups did not differ from one another ($p>0.05$).

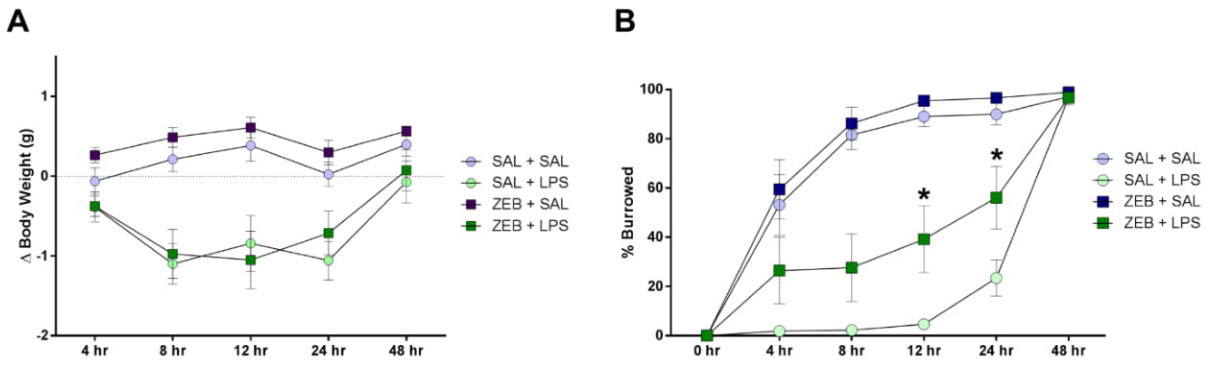

Figure 3.1. (A) Body weight was measured at baseline and 4, 8, 12, 24, and 48 hours after SAL/LPS ICV injections in adult mice pre-treated with ICV SAL/ZEB. Data are presented as means ± SEM (n=7-9). (B) Burrowing behavior was measured at 4, 8, 12, 24, and 48 hours after SAL/LPS ICV injections in adult mice pre-treated with ICV SAL/ZEB. Data are presented as means ± SEM (n=7-9). * indicates significance at $p<0.05$.

Zebularine alters LPS-induced expression of inflammatory, sensome, and epigenetic regulator genes

Fluidigm gene expression analysis on microglia was performed to gain a more comprehensive assessment of microglial gene regulation in response to zebularine. For inflammatory and regulators of inflammatory genes, there were a number of significant interactions in that ZEB decreased LPS-induced gene expression (*Il1b*, *Il-1rn, Il-10, Nlrp3, Socs1, Tlr2, Tnf*) (**Table 3.2A**). For sensome genes, there were no interactions of ZEB and LPS, but all were significantly or nearly significantly impacted by LPS, in that there were decreases compared to controls (**Table 3.2B**). Further, there were a few genes impacted by ZEB (*P2ry12, Siglech, Tgfbr1*) in that there were also decreases in gene expression. For epigenetic regulator genes, some *Dnmt*s decreased as expected (*Dnmt3a, Dnmt3b*), and *Hdacs* responded differently independently of HDAC family (i.e. *Hdac2, 3, 4, and 5* had significant effects of LPS while *Hdac1* had a very significant effect of ZEB) (**Table 3.2C**). Of note, some epigenetic regulator genes were affected slightly different in the SAL+LPS group compared to what has been demonstrated with LPS IP injections in adults (*Dnmt1, Dnmt3b, Hdac1, Mecp2*) (Matt et al., 2016). For epigenetic regulators partially responsible for DNA demethylation, *Gadd45b* increased with LPS as expected, but was decreased by zebularine and there was an interaction that zebularine decreased LPS-induced expression. For gene expression of the Tet proteins, which are responsible for DNA hydroxymethylation and influencing DNA demethylation (Kohli & Zhang, 2013), *Tet1* and *Tet2* were effected by LPS and zebularine but LPS decreased *Tet1* and increased *Tet2*, while there was no effect of either treatment on *Tet3*.

ICV zebularine decreases methylation at CpG 1 and 2 of the *Il1b* promoter in microglia at 4 hours

DNA methylation for two CpG sites within the proximal promoter region of *Il1b* was assessed via bisulfite pyrosequencing. These two sites were chosen because they have been shown to be dynamically regulated in a previous study (Cho et al., 2015). For CpG 1, main effect of ZEB ($p=0.0206$), in that ZEB decreased DNA methylation (**Figure 3.2C**). For CpG 2, there was also a main effect of ZEB ($p=0.0228$), in that zebularine decreased methylation (**Figure 3.2D**). There were no effects of LPS for either CpG site.

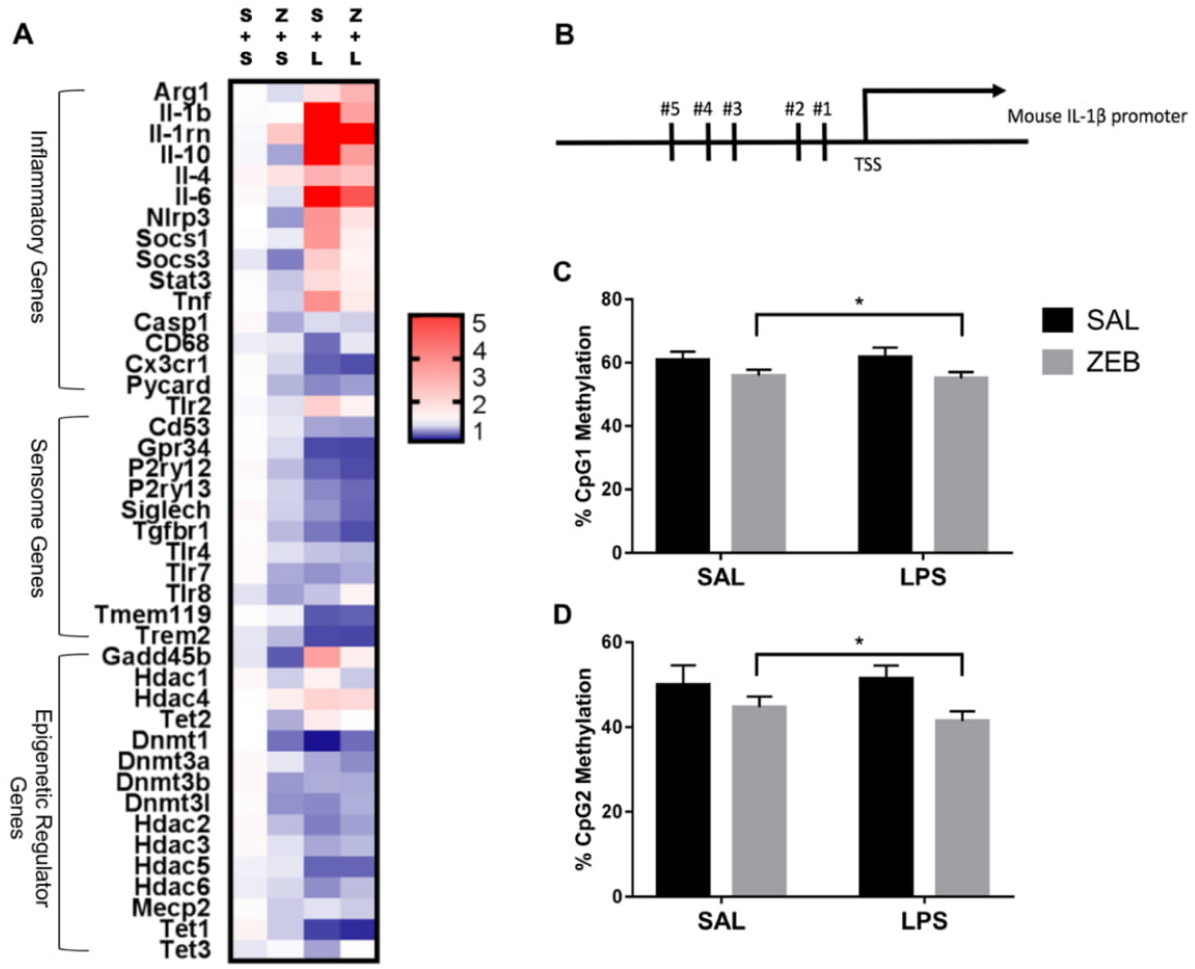

Figure 3.2. (A) Heat map visualization of relative expression (fold change) of genes in microglia analyzed by Fluidigm. Microglia were collected at 4 hours after SAL/LPS ICV injections in adult mice pre-treated with ICV SAL/ZEB. **(B)** Mouse *Il1b* promoter. DNA methylation of the *Il1b* promoter in microglia at **(C)** CpG1 and **(D)** CpG2. Data are presented as means ± SEM (n=7-9). Abbreviations: S+L, SAL+LPS; S+S, SAL+SAL; TSS, transcription start site; Z+L, ZEB+LPS; Z+S, ZEB+SAL. * indicates a main effect with significance at $p<0.05$.

Table 3.2. Expression of **(A)** inflammatory, **(B)** sensome, and **(C)** epigenetic regulator genes in microglia collected at 4 hours after SAL/LPS ICV injections in adult mice pre-treated with ICV SAL/ZEB. Data are presented as means ± SEM (n=5-7) and p-values for main effects of ZEB and LPS as well as ZEB x LPS interactions are also included.

A. Inflammatory and Regulators of Inflammatory Genes

					p-values		
Gene	**SAL + SAL**	**ZEB + SAL**	**SAL + LPS**	**ZEB + LPS**	**ZEB**	**LPS**	**ZEB x LPS**
Arg1	1.05±0.32	0.88±0.22	1.80±0.71	2.96±0.85	0.467	0.046*	0.332
Casp1	1.16±0.08	0.72±0.05	0.88±0.06	0.84±0.07	0.001*	0.236	0.006*
Cd68	0.94±0.08	0.92±0.13	0.52±0.05	0.92±0.13	0.719	<0.0001*	0.567
Cx3cr1	1.08±0.05	0.86±0.07	0.48±0.08	0.42±0.08	0.056	<0.0001*	0.305
Gene	**SAL + SAL**	**ZEB + SAL**	**SAL + LPS**	**ZEB + LPS**	**ZEB**	**LPS**	**ZEB x LPS**
Il-1β	1.08±0.24	1.05±0.14	9.31±2.18	3.46±0.88	0.012*	<0.0001*	0.013*
Il-1rn	0.98±0.41	2.46±0.68	39.00±8.37	8.86±0.68	<0.0001*	<0.0001*	<0.0001*
Il-10	0.97±0.17	0.70±0.06	7.92±1.66	3.53±0.96	0.021*	<0.0001*	0.040*
Il-4	1.23±0.47	1.72±0.32	3.04±0.94	2.57±0.52	0.994	0.072	0.504
Il-6	1.14±0.15	0.89±0.09	10.31±1.71	5.38±1.20	0.034*	<0.0001*	0.055
Nlrp3	1.00±0.18	0.66±0.06	3.74±0.97	1.75±0.34	0.022*	0.0004*	0.098
Pycard	0.99±0.06	0.75±0.02	0.61±0.07	0.68±0.03	0.097	<0.0001*	0.004*
Socs1	0.99±0.13	0.93±0.08	3.66±0.46	1.37±0.23	<0.0001*	<0.0001*	<0.0001*
Socs3	0.92±0.13	0.58±0.06	2.33±0.30	1.27±0.27	0.003*	<0.0001*	0.11
Stat3	1.10±0.09	0.81±0.06	1.91±0.22	1.43±0.18	0.016*	<0.0001*	0.534
Tlr2	0.98±0.07	0.89±0.07	2.25±0.29	1.32±0.16	0.004*	<0.0001*	0.016*
Tlr4	1.12±0.07	0.89±0.07	0.80±0.06	0.76±0.04	0.035*	0.0005*	0.136
Tlr7	1.11±0.09	0.72±0.03	0.64±0.04	0.72±0.05	0.011*	0.0002*	0.0003*
Tlr8	0.90±0.19	0.69±0.12	0.80±0.12	1.28±0.17	0.414	0.133	0.038*
Tnf	1.01±0.17	0.84±0.11	3.86±0.58	1.54±0.28	0.0004*	<0.0001*	0.002*

B. Sensome Genes

					p-values		
Gene	**SAL + SAL**	**ZEB + SAL**	**SAL + LPS**	**ZEB + LPS**	**ZEB**	**LPS**	**ZEB x LPS**
Cd53	1.01±0.18	0.92±0.19	0.70±0.06	0.68±0.16	0.738	0.081	0.8135
Gpr34	1.04±0.04	0.88±0.05	0.40±0.09	0.39±0.14	0.386	<0.0001*	0.447
P2ry12	1.14±0.09	0.78±0.08	0.49±0.09	0.41±0.12	0.035*	<0.0001*	0.17

P2ry13	**1.03±0.07**	**0.85±0.07**	**0.61±0.09**	**0.51±0.09**	**0.0787**	**<0.0001***	**0.657**
Siglech	**1.18±0.07**	**0.84±0.08**	**0.65±0.08**	**0.49±0.08**	**0.003***	**<0.0001***	**0.278**
Tgfbr1	**1.03±0.08**	**0.77±0.05**	**0.55±0.09**	**0.42±0.08**	**0.016***	**<0.0001***	**0.408**
Tmem119	**1.07±0.17**	**0.95±0.13**	**0.45±0.10**	**0.48±0.11**	**0.726**	**0.0003***	**0.601**
Trem2	**0.92±0.13**	**0.77±0.20**	**0.40±0.07**	**0.39±0.10**	**0.541**	**0.001***	**0.586**

C. Epigenetic Regulator Genes

						p-values	
Gene	**SAL + SAL**	**ZEB + SAL**	**SAL + LPS**	**ZEB + LPS**	**ZEB**	**LPS**	**ZEB x LPS**
Dnmt1	**1.00±0.18**	**0.53±0.14**	**0.24±0.09**	**0.52±0.14**	**0.524**	**0.012***	**0.013***
Dnmt3a	**1.17±0.13**	**0.92±0.04**	**0.72±0.13**	**0.62±0.07**	**0.041***	**<0.0001***	**0.369**
Gene	**SAL + SAL**	**ZEB + SAL**	**SAL + LPS**	**ZEB + LPS**	**ZEB**	**LPS**	**ZEB x LPS**
Dnmt3b	**1.17±0.10**	**0.66±0.06**	**0.73±0.20**	**0.72±0.09**	**0.044***	**0.142**	**0.049***
Dnmt3l	**1.10±0.33**	**0.64±0.11**	**0.61±0.16**	**0.74±0.13**	**0.397**	**0.324**	**0.137**
Gadd45b	**0.91±0.11**	**0.46±0.10**	**3.46±0.79**	**1.44±0.21**	**0.009***	**0.0002***	**0.015***
Hdac1	**1.17±0.11**	**0.84±0.06**	**1.36±0.18**	**0.82±0.04**	**0.0002***	**0.42**	**0.317**
Hdac2	**1.16±0.15**	**0.78±0.10**	**0.58±0.07**	**0.69±0.11**	**0.253**	**0.006***	**0.041***
Hdac3	**1.15±0.07**	**0.90±0.07**	**0.71±0.04**	**0.77±0.06**	**0.151**	**<0.0001***	**0.015***
Hdac4	**1.01±0.26**	**1.41±0.26**	**2.14±0.44**	**2.00±0.28**	**0.685**	**0.009***	**0.39**
Hdac5	**0.95±0.16**	**0.92±0.18**	**0.49±0.09**	**0.49±0.11**	**0.921**	**0.003***	**0.909**
Hdac6	**0.94±0.11**	**0.87±0.14**	**0.63±0.13**	**0.78±0.10**	**0.737**	**0.11**	**0.365**
Mecp2	**1.10±0.07**	**0.83±0.04**	**0.90±0.05**	**0.83±0.04**	**0.002***	**0.071**	**0.054**
Tet1	**1.29±0.12**	**0.83±0.07**	**0.38±0.08**	**0.31±0.11**	**0.052**	**<0.0001***	**0.2**
Tet2	**1.00±0.10**	**0.73±0.05**	**1.52±0.21**	**1.06±0.12**	**0.007***	**0.002***	**0.484**
Tet3	**0.92±0.20**	**0.98±0.23**	**0.7±0.21**	**1.07±0.33**	**0.496**	**0.836**	**0.615**

Table 3.2 (cont.). Expression of **(A)** inflammatory, **(B)** sensome, and **(C)** epigenetic regulator genes in microglia collected at 4 hours after SAL/LPS ICV injections in adult mice pre-treated with ICV SAL/ZEB. Data are presented as means ± SEM (n=5-7) and p-values for main effects of ZEB and LPS as well as ZEB x LPS interactions are also included.

Zebularine altered LPS-induced expression of inflammatory genes and *Il1b* promoter methylation in the hippocampus at 4 hours

In the hippocampus (**Figure 3.3**), for *Il1b*, there were main effects of LPS (p=0.001), ZEB (p=0.0445), and an interaction (p=0.0464) in that ZEB decreased LPS-induced *Il1b* expression. The same changes were observed for *Tnf*, with main effects of LPS (p<0.0001), ZEB (p=0.0362), and an interaction (p=0.0384). For *Il-6*, there was only a main effect of LPS (p=0.0005). For *Il-10*, main effects of LPS (p=0.0016), ZEB (p=0.0437), and an interaction (p=0.0457) in that ZEB increased LPS-induced *Il-10* expression. For *Cx3cr1*, no significant effects were observed. For *Gfap*, main effects of LPS (p=0.0006), ZEB (p=0.033), and a trending interaction (p=0.0815) in that ZEB increased LPS-induced *Gfap* expression. Increased expression with ZEB and LPS was also seen for *Socs3* (LPS (p<0.0001), ZEB (p=0.0318), and a trending interaction (p=0.0591)) and for *Stat3* (LPS (p<0.0001), ZEB (p=0.0083), and an interaction (p=0.0347)). With regards to DNA methylation, for *Il1b* CpG 1, there was a main effect of LPS (p=0.0011), in that LPS decreased DNA methylation. For *Il1b* CpG 2, there was a main effect of ZEB (p=0.0355), in that zebularine decreased methylation, and trending effect of LPS (p=0.0844), in that LPS decreased methylation.

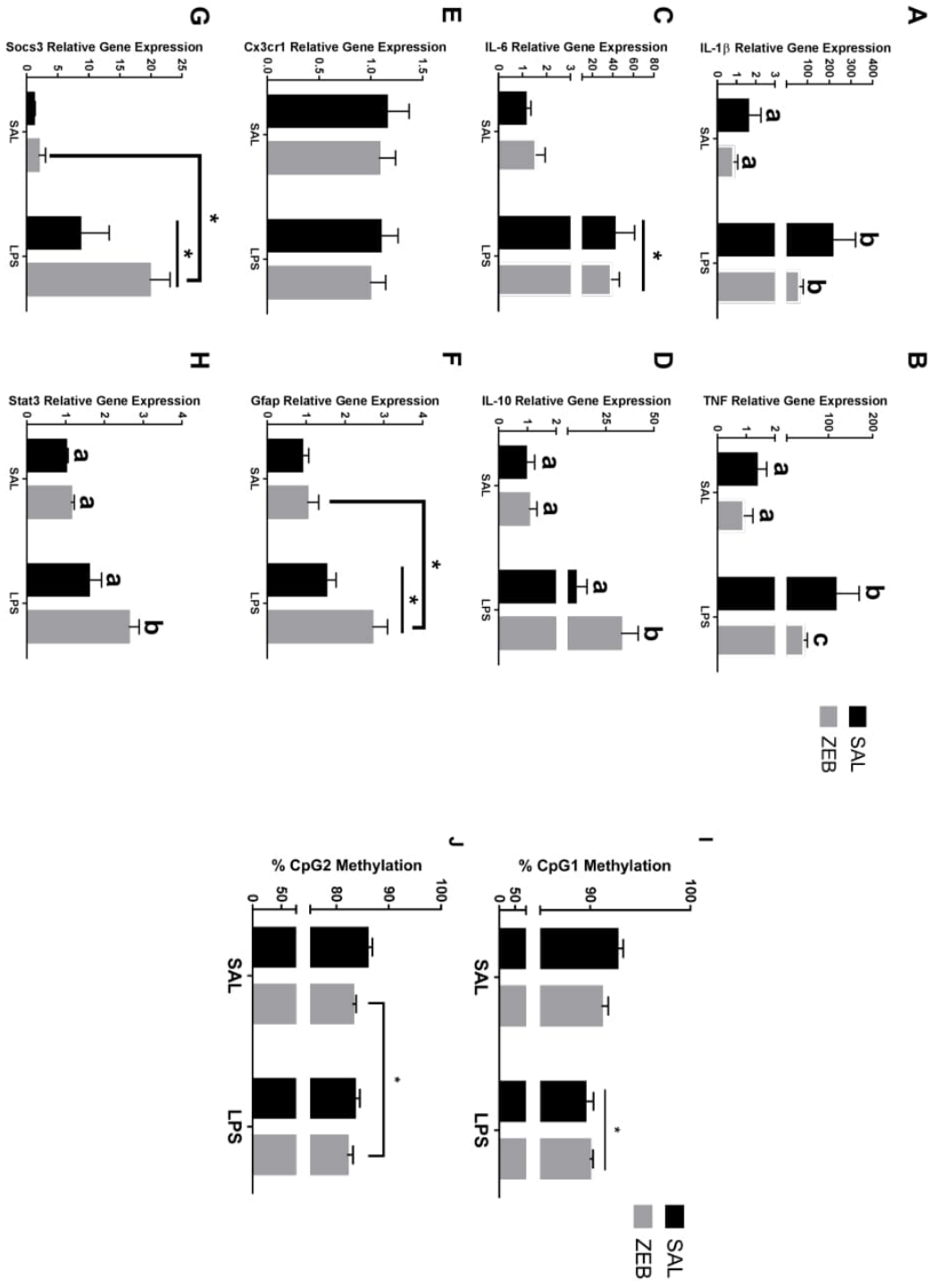

Figure 3.3. Hippocampal gene expression and DNA methylation at 4 hours after SAL/LPS ICV injections in adult mice pre-treated with ICV SAL/ZEB. Data are presented as means ± SEM (n=7-9) for **(A)** *Il1b*, **(B)** *Tnf*, **(C)** *Il-6*, **(D)** *Il-10*, **(E)** *Cx3cr1*, **(F)** *Gfap*, **(G)** *Socs3*, and **(H)** *Stat3* gene expression. Data are presented as means ± SEM (n=7-9) for DNA methylation of the *Il1b* promoter in hippocampus at **(I)** CpG1 and **(J)** CpG2. Treatment means with different letters are significantly different. * indicates a main effect with significance at $p<0.05$.

No effect of zebularine on inflammatory gene expression at 48 hours in microglia and hippocampus, but DNA methylation changes still present

Only main effects of LPS were observed at 48 hours in both microglia and hippocampus (**Figure 3.4**). For microglia, *Il1b* and *Il-6* had main effects of LPS (($p<0.0001$) and ($p<0.001$)). For hippocampus, *Il1b* and *Tnf* had main effects of LPS (($p=0.0052$) and ($p=0.0346$)). For *Il1b* DNA methylation, in microglia, *Il1b* CpG1 main effects of ZEB and LPS ($p=0.0186$ and $p=0.0484$) and *Il1b* CpG2 main effects of ZEB and LPS ($p=0.0005$ and $p=0.0021$) in that ZEB and LPS decreased DNA methylation. For hippocampus, *Il1b* CpG1 trending main effect of LPS ($p=0.0844$) *and Il1b* CpG2 main effect of ZEB ($p=0.0341$) in that ZEB and LPS decreased DNA methylation.

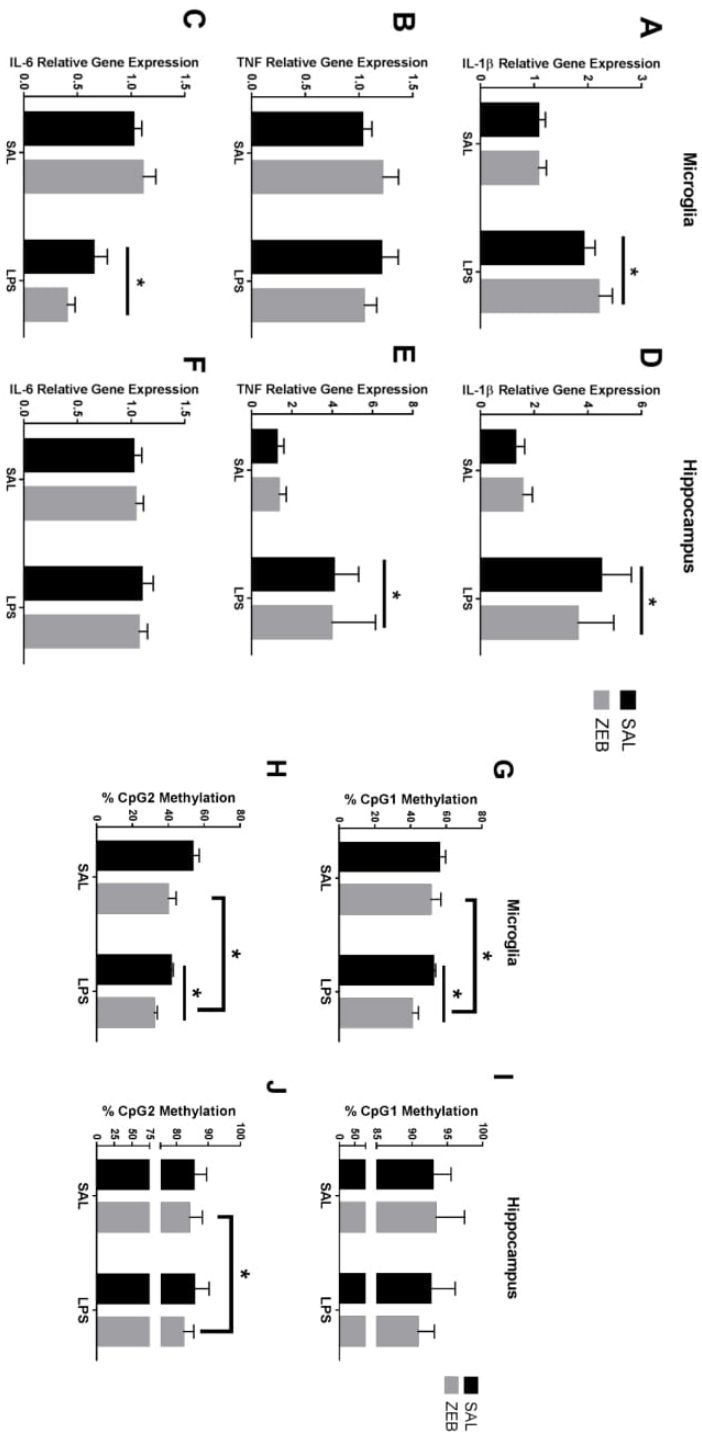

Figure 3.4. Gene expression and DNA methylation of microglia and hippocampus at 48 hours after SAL/LPS ICV injections in adult mice pre-treated with ICV SAL/ZEB. Data are presented as means ± SEM (n=7-9) for microglial **(A)** *Il1b*, **(B)** *Tnf*, **(C)** *Il-6*, and hippocampal **(D)** *Il1b*, **(E)** *Tnf*, and **(F)** *Il-6*. Data are presented as means ± SEM (n=7-9) for DNA methylation of the *Il1b* promoter in microglia at **(G)** CpG1 and **(H)** CpG2 and in hippocampus at **(I)** CpG1 and **(J)** CpG2. * indicates a main effect with significance at $p<0.05$.

3.5 Discussion

The present study was designed to investigate a link between DNA inhibition and neuroinflammation. We hypothesized that central administration of LPS and zebularine in adult mice would cause an exacerbated neuroinflammatory response, in that there would be exaggerated sickness behavior and a pro-inflammatory gene expression profile that would be associated with DNA demethylation of *Il1b*. Surprisingly, instead of intensifying the LPS-induced sickness response and increasing inflammation in the brain, zebularine led to a quicker recovery of LPS-induced sickness behavior and decreased cytokine gene expression. Results of the Fluidigm analysis indicated that DNMT inhibition created an anti-inflammatory profile in microglia at 4 hours, as many inflammatory genes were decreased by zebularine alone or in combination with LPS (*Il1b, Tnf*, etc.). Although these results do not support the original hypothesis that pharmacological DNMT inhibition in the context of central immune activation causes an exaggerated cytokine response within the adult brain, similar to what has been seen in vitro, studies have demonstrated that DNMT inhibitors have an immunosuppresive effect in other cell types. Human mesenchymal stem cells treated with a DNMT inhibitor had increased inhibitory effects on mononuclear cell proliferation and cell migration toward activated T cells, and when injected IP into mice they had a therapeutic effect in a DSS-induced mouse colitis model (Lee et al., 2015). Further, there is some indication that such anti-inflammatory effects of these drugs could translate to human disease, as patients with acute myeloid leukemia who were treated with a DNMT inhibitor after allogeneic stem cell transplantation were shown to have increased numbers of regulatory T cells, which was associated with a low incidence of graft-versus-host disease (Goodyear et al., 2012).

Novel findings using the Fluidigm analysis indicated differential expression of epigenetic regulators and sensome genes in microglia with central zebularine and LPS. Nearly all *Hdacs*

analyzed were affected by LPS, a response that has been demonstrated elsewhere (Kannan et al., 2013). Further, *Hdac1*'s significant downregulation with zebularine supports the dependency of HDAC regulation on DNA methylation (Fuks, 2005). Of note, altered gene expression of Tet proteins, which has been explored very little in microglia, indicate a role of DNA hydroxymethylation in response to DNMT inhibition and LPS. To support this, it has recently been found that Tet2 is implicated in the regulation of cytokine expression during innate as well as T-cell-mediated immune responses, and that this is controlled by an HDAC-dependent mechanism (Q. Zhang et al., 2015). Similarly, *Tet2* deficiency induced in $CD2^{+}$ T cells is associated with aberrant cytokine production and leads to increased autoimmunity in a mouse model of human multiple sclerosis (Ichiyama et al., 2015). Further, for the majority of microglial sensome genes analyzed, they decreased with zebularine and/or LPS. As it has been demonstrated that these same genes are downregulated with aging and that it would be conceptually beneficial to the brain to downregulate the ability of microglia to get activated by dying or injured cells with aging (Hickman et al., 2013), reproducing this neuroprotective phenotype with DNMT inhibition during LPS-induced inflammation could indicate therapeutic potential in other inflammatory diseases.

Expression of inflammatory genes in the hippocampus at 4 hours predominantly mirrored the anti-inflammatory changes in microglia. This included decreases in *Il1b* and *Tnf* and increases in *Socs3* and *Stat3* in mice given both zebularine and LPS. There was an opposite effect of zebularine and LPS on *Il-10* expression, but this could be explained by the increases in *Gfap* expression. Increases in *Gfap* could indicate increased astrocyte activation and modulation of microglia within heterogeneous brain tissue (Lobo-Silva, Carriche, Castro, Roque, & Saraiva, 2016; Villacampa et al., 2015). Additional studies would be useful in identifying other cell

populations such as astrocytes within the brain that are altered with DNMT inhibition during immune activation.

One particularly interesting finding was that although the effect of zebularine on gene expression disappeared at 48 hours, DNA methylation changes were still present. In fact, even more changes were present in microglia at 48 hours than at 4 hours. The functions of DNA methylation in the brain have predominantly been investigated by exploring instances where changes in methylation within gene promoters correlate with changes in gene expression. Cases where basal levels of gene expression remain unaltered following a change in DNA methylation within the corresponding gene have been largely overlooked, which has led to a limited appreciation of the functional variations in DNA methylation across the genome (Baker-Andresen, Ratnu, & Bredy, 2013; Wagner et al., 2014). However, the relationship between DNA methylation and transcriptional activity is more complex than previously realized, such as the recent discovery of hydroxymethylation or that DNA methylation can regulate alternative splicing, the development of bivalent chromatin marks, or direct nucleosome repositioning. The relevance of this expanded repertoire of epigenomic modifications, particularly within the context of microglial development and activation across the lifespan, remains to be determined. Such epigenetic modifications may persist and alter the subsequent response to immune stimulation, thus providing a form of innate cell 'memory' that can contribute to a relatively nonspecific resistance to re-infection — a phenomenon that has been termed 'trained immunity' (Netea et al., 2016). Experience-dependent variations in DNA methylation such as infection may prime the genome for response to later events by regulating transcription in response to incoming inputs, rather than by mediating enduring changes in gene expression.

In conclusion, these data do support the hypothesis that epigenetic mechanisms like DNA methylation modulate neuroinflammatory responses. Perhaps the most exciting conclusion to be drawn from this work is that modulation of DNA methylation may influence not only the molecular features, but can also affect behavioral outcomes in animals. Pharmacological strategies aimed at specifically decreasing exacerbated microglial reactivity associated with infection might be important for improving recovery from sickness and reducing neurobehavioral deficits in populations like the elderly. More precise selectivity of epigenetic drugs is increasing, and with the recent generation of small-molecule inhibitors for multiple classes of histone modifiers, we will be better able to explore epigenetic proteins and uncover selective roles in the regulation of gene expression (Tough, Lewis, Rioja, Lindon, & Prinjha, 2014; Tough, Tak, Tarakhovsky, & Prinjha, 2016). The capacity of these compounds to selectively modify gene expression and to modulate pro-inflammatory responses indicates great promise for this approach in the treatment of human disease.

CHAPTER 4: BUTYRATE AND DIETARY SOLUBLE FIBER IMPROVE NEUROINFLAMMATION ASSOCIATED WITH AGING IN MICE

4.1 Abstract

It is well accepted that aging results in chronic systemic inflammation that can alter neuroinflammation in the brain. Specifically, microglia shift to a pro-inflammatory phenotype that make them hypersensitive to signals from the peripheral immune system. It is proposed that certain nutrients can manipulate the epigenome to delay brain aging by preventing or reversing microglial aging. Butyrate, a short-chain fatty acid (SCFA) produced by bacterial fermentation of fiber in the colon, has been extensively studied pharmacologically as a histone deacetylase (HDAC) inhibitor, which has become an attractive therapeutic candidate. It is still not fully understood however, if an increase in butyrate-producing bacteria in the gut as a consequence of soluble fiber diet, could affect microglial activation, and specifically microglial activation in aging. Adult and aged mice were fed either a 1% low cellulose (non-fermentable fiber) or 5% high inulin (fermentable fiber) diet for 4 weeks. Findings indicate that mice fed inulin had an altered gut microbiome and increased butyrate, acetate, and total SCFA production. In addition, gene expression of inflammatory markers, epigenetic regulators, and the microglial sensory apparatus (i.e. the sensome) were altered by both diet and age, in that aged animals had a more anti-inflammatory microglial profile on the high fiber diet. Further, histological scoring of the distal colon demonstrated that aged animals on the low fiber diet had increased inflammatory infiltrate that was significantly decreased with the high fiber diet. Taken together, high fiber supplementation in the elderly is a non-invasive strategy to increase butyrate levels, and these data suggest that an increase in butyrate through added soluble fiber such as inulin could counterbalance the age-related microbiota dysbiosis, potentially leading to neurological benefits.

4.2 Introduction

During normal healthy aging, there is a disruption in the communication and balance between the brain and immune system. Microglia shift to a proinflammatory phenotype that make them hypersensitive to signals from the peripheral immune system (DiSabato, Quan, & Godbout, 2016; Matt & Johnson, 2016). The precise mechanisms during aging that are responsible for this detrimental transition is not known, but overproduction of IL-1β has been shown to play a role. Recently, we demonstrated that aged mice had decreased methylation of the pro-inflammatory cytokine interleukin (IL)-1β gene promoter in primary microglia basally or following systemic lipopolysaccharide (LPS) that is associated with increased *Il1b* mRNA (Matt et al., 2016). This is critical because overproduction of IL-1β has been demonstrated to produce cognitive dysfunction in rodent models (Simen et al., 2011) and increased IL-1β in aged individuals is associated with risk of neurodegenerative diseases such as Alzheimer's (W.-Y. Wang, Tan, Yu, & Tan, 2015).

Notwithstanding, it is proposed that certain nutrients can manipulate the epigenome to delay brain aging by preventing or reversing microglial aging, potentially through DNA methylation, histone modifications, and their interactions (Hoeijmakers, Heinen, van Dam, Lucassen, & Korosi, 2016). Butyrate, a short-chain fatty acid (SCFA) produced by bacterial fermentation of fiber in the colon, has been extensively studied for its beneficial effects through free fatty acid receptor signaling and metabolic regulation, but also pharmacologically as a histone deacetylase (HDAC) inhibitor. HDAC inhibitors have become an attractive therapeutic candidate due to the ability to increase histone acetylation and promote the expression of neurotrophic and anti-inflammatory genes (Huuskonen et al., 2004; Patnala et al., 2016). Although most studies using butyrate have focused on its effects on histone acetylation, there is

also evidence that butyrate can affect DNA methylation (Sarkar et al., 2011; Shin, Kim, Lee, & Lee, 2012; Wei, Melas, Wegener, Mathé, & Lavebratt, 2015).

Sodium butyrate (NaB), the sodium salt form of butyrate, is most commonly used in pharmacological studies and has been shown to decrease pro-inflammatory cytokines of microglia in vitro as well as improve learning and memory in mouse models of neurodegenerative diseases when injected intraperitoneally (i.p.) (Govindarajan et al., 2011; Kilgore et al., 2010). It has even recently been demonstrated that NaB triggers elongation of microglial processes and can abolish LPS-induced depressive like behaviors through decreasing microglial activation (P. Wang et al., 2018; Yamawaki et al., 2018).

To date, only a handful of studies have probed the mechanistic basis surrounding the beneficial neurological effects of a high fermentable fiber, which has the capacity to shift SCFA production to favor butyrate (Bourassa et al., 2016). Notably, one study found significant immune benefits in the brain of mice fed a high fermentable (soluble) fiber diet and found that they recovered faster from LPS-induced sickness (Sherry et al., 2010). After exposure to LPS, mice fed the soluble fiber diet showed an increase in IL-1RA and a decrease in IL-1β and TNF-α in the brain. Brain IL-4 mRNA was also increased, and as IL-4 expression is enhanced by increased histone acetylation, the authors hypothesized that the elevated butyrate from the dietary fiber fermentation may contribute to the immune response. It is still not fully understood however, if an increase in butyrate-producing bacteria in the gut as a consequence of soluble fiber diet, could affect microglial activation, and specifically microglial activation in aging.

SCFA concentrations are likely less than optimal in older adults, as data indicates daily dietary fiber intake for both older men and women is roughly 40% below the recommended adequate intake (King, Mainous, & Lambourne, 2012). There is also a lower capacity to produce

butyrate in the elderly gut microbiome, as suggested by the findings that there are significantly fewer copies of the butyrilCoA:acetateCoA transferase gene compared to younger adults and lower amounts of bacterial groups which are known butyrate producers (Biagi et al., 2011; Hippe et al., 2011). Therefore, the aging population is an important demographic for where increased fiber supplementation is needed. Of note, inulin has been shown to be a rich source of soluble dietary fiber that increases butyrate-producing bacteria (G. Schaafsma & Slavin, 2015). Inulin belongs to a group of non-digestible carbohydrates called fructans, and in food is considered a prebiotic (Roberfroid, 2007). Studies have specifically demonstrated that inulin is beneficial for age-related inflammation, as a nutritional supplement with inulin increased innate immunity and protection against infections in elderly people (Bunout et al., 2004). Thus, an increase in butyrate through added soluble fiber such as inulin could counterbalance the age-related microbiota dysbiosis, and potentially lead to neurological benefits.

We first wanted to determine if NaB pharmacologically has beneficial effects on microglia in aged mice with and without an immune challenge. With this being the case, we then hypothesized that butyrate derived from soluble fiber (inulin) in aged mice would promote changes in the microbiome and decreases in peripheral inflammation leading to decreased neuroinflammation. Last, we hypothesized that a high soluble fiber diet could diminish or even reverse the aging phenotype in mice following an immune challenge.

4.3 Methods

Experiment 1: Effects of intraperitoneal administration of sodium butyrate in adult and aged mice in both microglia and hippocampus in response to LPS

Animals

Adult (3-6-month-old) and aged (22-25 month-old) Balb/c male mice were reared in-house and provided with *ad libitum* access to chow (Teklad 8640, Harlan laboratories, Indianapolis, IN, USA) and water. Mice were individually housed in a temperature-controlled environment with a 12-hour reversed-phase light/dark cycle (lights on 21:00h). Treatments were designed in a 2 x 2 factorial arrangement and administered at the onset of the dark cycle. Both Escherichia coli LPS (serotype 0127:B8, Sigma, St. Louis, MO, USA) and NaB (Sigma, St. Louis, MO, USA) were dissolved in sterile saline before experimentation. Mice from both age groups were injected i.p. with either saline (control) or NaB at 1.2g/kg body weight and 2 hours later with saline or LPS at 0.33 mg/kg body weight. This dose of NaB was selected based on previous studies demonstrating significant beneficial effects in other rodent models (Blank et al., 2015; Dash, Orsi, & Moore, 2009; Govindarajan et al., 2011). This dose of LPS was selected based on previous studies demonstrating that 0.33 mg/kg LPS produced prolonged sickness behavior in aged compared with young mice (Godbout et al., 2005). Treatments were administered at 9 AM for all cohorts. Body weight was measured at baseline and 4 hours after injections as an index of sickness response.

Tissue Collection and Microglia Isolation

Animals were euthanized via CO_2 asphyxiation and animals were perfused with sterile ice-cold saline. Brain tissue (all but the hippocampus which was frozen in dry ice) was collected and used immediately for microglia isolation using a procedure adapted from Nikademova &

Watters (Maria Nikodemova & Watters, 2012). Brains were enzymatically digested using the Neural Tissue Dissociation Kit (Miltenyi Biotec, Germany) for 35 min at 37° C. Further processing was performed at 4° C. Tissue debris was removed by passing the cell suspension through a 40 μm cell strainer. After myelin removal using 30% Percoll Plus (GE Healthcare, Princeton, NJ, USA), cells in PBS supplemented with 0.5% BSA and 2 mM EDTA were incubated for 15 minutes with anti-Cd11b magnetic beads (Miltenyi Biotec, Germany). $CD11b^+$ cells were extensively washed and separated in a magnetic field using MS columns (Miltenyi Biotec, Germany) before being directly placed in Trizol reagent (Invitrogen).

RNA isolation and real-time RT-PCR

Total RNA from microglia and hippocampus was isolated using the Tri Reagent protocol (Invitrogen). Synthesis of cDNA was carried out using a high-capacity RT kit (Applied Biosystems, Grand Island, NY, USA) according to the manufacturer's instructions. Real-time RT-PCR was performed on an ABI PRISM 7900HT-sequence detection system (Perkin Elmer, Forest City, CA, USA). All genes were analyzed using PrimeTime real-time RT-PCR Assays (Integrated DNA Technologies, Coralville, IA, USA) and were compared with the housekeeping control gene GAPDH (Mm99999915_g1) using the $2^{-\Delta\Delta Ct}$ calculation method as previously described (Livak & Schmittgen, 2001). Data are expressed as fold change versus saline control adult mice.

Fluidigm

Total RNA from microglia was isolated using the Tri Reagent protocol (Invitrogen) and synthesis of cDNA was carried out using a high-capacity RT kit (Applied Biosystems) as previously described for real-time RT-PCR. Fluidigm reactions were performed by the UIUC Functional Genomics Unit of the W.M. Keck Center using a 96 × 96 chip and included 2

technical replicates for each combination of sample and assay. Data was acquired using the Fluidigm Real-Time PCR Analysis software 3.0.2 (Fluidigm, San Francisco, CA, USA). Data from Fluidigm runs were manually checked for reaction quality before analysis, and C_t values for each gene target (see **Table 4.1**) were normalized to C_t values for the housekeeping gene *Gapdh*.

Experiment 2: Effects of low and high soluble fiber diets on central and peripheral inflammation in adult and aged mice

Animals and Diet

Adult (3-6-month-old) and aged (22-25 month-old) male Balb/c mice were housed as described in Experiment 1, but were fed either AIN-93M diet with 5% cellulose (product # D10012M, Research Diets, Inc., New Brunswick, NJ, USA) or one of two AIN-93M modified diets that contained either 1% cellulose (product # D16060605, Research Diets, Inc., New Brunswick, NJ, USA) or 1% cellulose and 5% inulin (product # D16060606, Research Diets, Inc., New Brunswick, NJ, USA) for four weeks. Composition of these diets can be seen in **Table 4.2**, modified from Research Diets, Inc. Fecal samples were taken from the mice (on chow) prior to the start of the study in order to assess baseline microbiome changes between adult and aged. Body weight was measured immediately prior to euthanasia to assess any weight differences with the diets. All studies were carried out in accordance with United States National Institutes of Health guidelines and approved by the University of Illinois Institutional Animal Care and Use Committee.

Tissue Collection and Microglia Isolation

Animals were euthanized via CO_2 asphyxiation, blood was taken, and animals were perfused with sterile ice-cold saline. Samples were collected from colon, liver, mesenteric lymph nodes, and hippocampus that were frozen on dry ice. Cecal content and feces were also taken for

analysis of SFCA concentrations and microbiota compositions, respectively. Distal colon was taken for histological analysis. Brain tissue (all but the hippocampus) was collected and used immediately for microglia isolation as described in Experiment 1.

Bacterial DNA isolation and 16S rRNA sequencing

Fecal bacterial DNA was extracted using the PowerLyzer PowerSoil DNA Isolation Kit (MOBIO Laboratories, Inc.) and quality was assessed via gel electrophoresis. The DNA library was constructed using a Fluidigm Access Array system in the Functional Genomics Unit of the Roy J. Carver Biotechnology Center at the University of Illinois at Urbana (UIUC). After library construction, a 250 bp region of the 16S rRNA gene (V4) were amplified using a PCR amplification method modified from Muturi et al. (Muturi, Donthu, Fields, Moise, & Kim, 2017). Briefly, DNA samples were diluted to 2 ng/µl and amplified with Roche High Fidelity Fast Start Kit and 20x Access Array loading reagent prior to PCR. Samples were amplified using the following Access Array cycling program 50 °C for 2 minutes (1 cycle), 70 °C for 20 minutes (1 cycle), 95 °C for 10 minutes (1 cycle), followed by 10 cycles at 95 °C for 15 seconds, 60 °C for 30 seconds, and 72 °C for 1minute, 2 cycles at 95 °C for 15 seconds, 80 °C for 30 seconds, 60 °C for 30 seconds, and 72 °C for 1 minute, 8 cycles at 95 °C for 15 seconds, 60 °C for 30 seconds, and 72° for 1minute, 2 cycles at 95 °C for 15 seconds, 80 °C for 30 seconds, 60 °C for 30 seconds, and 72 °C for 1minute, 8 cycles at 95 °C for 15 seconds, 60 °C for 30 seconds, and 72 °C for 1minute, and 5 cycles at 95 °C for 15 seconds. After PCR, all samples were run on a Fragment Analyzer (Advanced Analytics, Ames, IA). Samples were then pooled in equal amounts according to PCR product concentration. The pooled products were then size selected on a 2% agarose E-gel (Life Technologies) and extracted from the isolated gel slice with Qiagen gel extraction kit (Qiagen). Cleaned size selected products were run on an Agilent Bioanalyzer

to confirm appropriate profile and determination of average size. The final library pool was spiked with 10% non-indexed PhiX control library (Illumina®) and sequenced using Illumina® MiSeq® V3 Bulk system. The libraries were sequenced from both ends of the molecules to a total read length of 250 nt from each end. High-quality (> 25) sequence data (FASTQ) from the forward read were analyzed with QIIME 2.0[54]. Quality control consisted of depleting or removing barcodes, primers, and short sequences (< 187 bp), sequences with ambiguous base calls, and sequences with homopolymer runs exceeding 6 bp. After removal of singletons, OTUs were classified using closed reference picking against Greengenes database at 97% similarity. β-diversity (weighted and unweighted UniFrac distances) were computed at an even sampling depth of 10,048 sequences per sample based on α-diversity (Chao1) rarefaction plots (**Supplementary Figure 4.3**)

Short chain fatty acid analysis

SCFAs were analyzed by dry matter content as described previously by Panasevich et al (Panasevich, Allen, Wallig, Woods, & Dilger, 2015). To calculator dry matter percentage, a portion (~0.08-0.15 grams) of wet cecal contents were weighed and then heated in oven for 24 hours to dry samples. Resulting dry matter percentage was calculated as [weight of dry sample/weight (g) of wet sample (g) *100]. The rest of the cecal contents (~0.05-0.15 grams) were acidified immediately after collection in 6.25% meta-phosphoric acid solution and stored at −20°C until analysis. After thawing, samples were spun down at 10,000 rpm for 8 minutes and supernatant was collected for analysis. SCFA concentrations (wet) were determined by gas chromatography by using a gas chromatograph (Hewlett-Packard 5890A Series II) and a glass column (180 cm × 4 mm i.d.), packed with 10% SP-1200/1% H3PO4 on 80/100 + mesh Chromosorb WAW (Supelco, Inc.). Nitrogen was the carrier gas with a flow rate of 75 mL/min.

Oven, detector, and injector temperatures were 125°, 175°, and 180°C, respectively. Acetic, n-butyric, and propionic acid solutions (Sigma-Aldrich) were used as standards.

RNA isolation and real-time RT-PCR

Total RNA from microglia, hippocampus, colon, liver, and mesenteric lymph nodes was isolated and synthesis of cDNA was carried out as described in Experiment 1. Real-time RT-PCR was performed also as described in Experiment 1 with the exception that data are expressed as fold change versus control adult mice on AIN-93M diet.

Fluidigm

As described in Experiment 1.

DNA Isolation and Pyrosequencing

Total DNA from microglia and hippocampus tissue was isolated using the Tri Reagent protocol (Invitrogen). DNA methylation for 2 CpG sites within the proximal promoter region of *Il1b* was assessed via bisulfite pyrosequencing on bisulfite modified DNA (Zymo Research, Irvine, CA, USA). The mouse *Il1b* methylation assay (ID ADS3713-RS1 was purchased from EpigenDx (Hopkinton, MA, USA) and has been previously used to assess methylation status in microglia (Cho et al., 2015). PCRs were run in duplicate and contained 20 ng of bisulfite converted DNA as starting template**.** Product specificity was determined by gel electrophoresis. The primer was also tested using bisulfite converted DNA from high and low methylation controls (EpigenDx, Hopkinton, MA, USA). Qiagen's PyroMark Q24 Advanced Pyrosequencer was used to detect DNA methylation levels following manufacturer's protocols and default settings (Qiagen, Valencia, CA), similar to a previous study (Bustamante et al., 2016).

Distal Colon Histology

Distal colon was fixed in Methacarn (60% methanol, 30% chloroform, 10% acetic acid) for 72 hours and then placed in 100% ethanol until tissue embedding. Distal colon tissue was paraffin embedded, and 5µm sections mounted on glass slides were stained with hematoxylin and eosin (H&E) for assessment of intestinal morphology. Histology was scored by a trained, blinded observer on a modified version of a published scoring (Erben et al., 2014) system that considers four criteria: inflammatory cell infiltration (0-4), goblet cell mucus depletion (0-4); destruction of architecture (0-4) and crypt abscesses (0-4). Overall histology score was quantified using an aggregate of these scores.

LPS Binding Protein (LBP) Assay

LBP was quantified in serum samples using the Mouse LBP enzyme-linked immunosorbent assay (ELISA) Kit (catalog #: HK205-02, Hycult Biotech Inc., Plymouth Meeting, PA, USA). The assay was run according to the manufacturer's instructions.

Experiment 3: Effects of low and high soluble fiber diets on central and peripheral inflammation in adult and aged mice stimulated with LPS

Animals and Diet

Adult (3-6-month-old) and aged (22-25 month-old) male Balb/c mice were housed and fed diets as described in Experiment 2. Mice were injected i.p. with LPS at 0.33 mg/kg body weight as described in Experiment 1. Body weight was measured at baseline and 4 hours after injections as an index of sickness response. All studies were carried out in accordance with United States National Institutes of Health guidelines and approved by the University of Illinois Institutional Animal Care and Use Committee.

Tissue Collection and Microglia Isolation

Animals were euthanized via CO_2 asphyxiation, blood was taken, and animals were perfused with sterile ice-cold saline. Samples were collected from colon, liver, mesenteric lymph nodes, and hippocampus that were frozen on dry ice. Brain tissue (all but the hippocampus) was collected and used immediately for microglia isolation as described in Experiment 1 and 2.

RNA isolation and real-time RT-PCR

Isolation of RNA, cDNA synthesis, and Real-time RT-PCR were performed as described in Experiment 2.

DNA Isolation and Pyrosequencing

As described in Experiment 2.

LPS Binding Protein (LBP) Assay

As described in Experiment 2.

Statistical Analyses

Body weight, gene expression (including Fluidigm), SCFA analysis, pyrosequencing, colon histology scoring, and LBP data were analyzed using Statistical Analysis System (SAS, Cary, NC, USA) and were subjected to 2-way analysis of and all interactions. Where analysis of variance revealed a significant interaction ($p < 0.05$), Fisher's LSD test was used for post hoc comparisons when appropriate. Microbiome community compositions (β- diversity; weighted Unifrac) were compared across ages and diets with permutational analysis of variance analysis (PERMANOVA). Next, to unbiasedly identify key features of the gut microbiota that are affected by age and fiber diets, Random Forest (RF) alongside Boruta feature selection was performed Boruta selection uses RF to iteratively compare importance of independent variables with that of pseudo-random (shadow) attributes (Kursa, 2014). Variables 'confirmed' by Boruta

feature selection had significantly higher RF importance scores than 'shadow' attributes and could therefore delineate between diet and age. Analysis was performed on R random forest package with 1000 trees and all other default values. All data are expressed as means ± SEM.

Table 4.1. Primers used in Real-time RT-PCR and Fluidigm experiments.

Gene	Assay ID
Arg1	**Mm.PT.58.8651372**
Casp1	**Mm.PT.58.13005595**
CD53	**Mm.PT.58.30699738**
CD68	**Mm.PT.58.12034788.g**
Cx3cr1	**Mm.PT.58.17555544**
Dnmt1	**Mm.PT.58.30881142**
Dnmt3a	**Mm.PT.58.13545327**
Dnmt3b	**Mm.PT.58.31955137**
Dnmt3l	**Mm.PT.58.41749889**
Ffar2	**Mm.PT.58.32870135**
Gadd45b	**Mm.PT.58.10699383.g**
Gapdh	**Mm.PT.39a.1**
Gfap	**Mm.PT.58.31297710**
Gpr34	**Mm.PT.58.46001700**
Hdac1	**Mm.PT.58.43356830.g**
Hdac2	**Mm.PT.58.12358619**
Hdac3	**Mm.PT.58.11480126**
Hdac4	**Mm.PT.58.17651425**
Hdac5	**Mm.PT.58.11472897**
Hdac6	**Mm.PT.58.16685964**
Il-1β	**Mm.PT.58.41616450**
Il-1rn	**Mm.PT.58.43781580**
Il-10	**Mm.PT.58.23604055**
Il-17	**Mm.PT.58.6531092**
Il-23	**Mm.PT.58.10594618.g**
Il-4	**Mm.PT.58.32703659**
Il-6	**Mm.PT.58.13354106**
Mct1	**Mm.PT.58.7080950**
Mecp2	**Mm.PT.58.13934895.g**
Muc2	**Mm.PT.58.29496069.g**
Nlrp3	**Mm.PT.58.13974318**
Ocln	**Mm.PT.58.30118962**
P2ry12	**Mm.PT.58.43542033**
P2ry13	**Mm.PT.58.42597879.g**
Pycard	**Mm.PT.56a.42872867**
Siglech	**Mm.PT.58.45915252**
Socs1	**Mm.PT.58.11527306.g**
Socs3	**Mm.PT.58.7804681**
Stat3	**Mm.PT.58.11877007**
Tet1	**Mm.PT.58.43326803**
Tet2	**Mm.PT.58.30089849**
Tet3	**Mm.PT.58.11954119**
Tff3	**Mm.PT.58.43353357**
Tgfbr1	**Mm.PT.58.10230349**
Tjp1	**Mm.PT.58.29459730**

Gene	Assay ID
Tjp2	**Mm.PT.58.16834535**
Tlr2	**Mm.PT.58.45820113**
Tlr4	**Mm.PT.58.41643680**
Tlr7	**Mm.PT.58.10526075**
Tlr8	**Mm.PT.58.16021150**
Tmem119	**Mm.PT.58.6766267**
Trem2	**Mm.PT.58.7992121**
Tnf	**Mm.PT.58.12575861**

Table 4.1 (cont.). Primers used in Real-time RT-PCR and Fluidigm experiments.

Table 4.2. AIN-93M Mature Rodent Diet and Modified AIN-93M Diets with 10 gm Cellulose or 10 gm Cellulose + 50 gm Inulin per 3850 kcal.

Product #	**D10012M**		**D16060605**		**D16060606**	
	AIN-93M		*10 gm Cellulose/3850kcal*		*10 gm cellulose + 50 gm Inulin/3850kcal*	
	gm%	*kcal%*	gm%	*kcal%*	gm%	*kcal%*
Protein	14	*15*	15	*15*	14	*15*
Carbohydrate	73	*76*	76	*76*	72	*74*
Fat	4	*9*	4	*9*	4	*9*
Total		*100*		*100*		*98*
kcal/gm	3.85		4.01		3.88	
Ingredient	**gm**	***kcal***	**gm**	***kcal***	**gm**	***kcal***
Casein	140	*560*	140	*560*	140	*560*
L-Cystine	1.8	*7*	1.8	*7*	1.8	*7*
Corn Starch	495.692	*1983*	495.692	*1983*	**476.942**	***1908***
Maltodextrin 10	125	*500*	125	*500*	125	*500*
Sucrose	100	*400*	100	*400*	100	*400*
Cellulose, BW200	50	*0*	**10**	*0*	**10**	*0*

Product #	**D10012M**		**D16060605**		**D16060606**	
Inulin	0	*0*	0	*0*	**50**	**75**
Soybean Oil	40	*360*	40	*360*	40	*360*
t-Butylhydroquinone	0.008	*0*	0.008	*0*	0.008	*0*
Mineral Mix S10022M	35	*0*	35	*0*	35	*0*
Vitamin Mix V10037	10	*40*	10	*40*	10	*40*
Choline Bitartrate	2.5	*0*	2.5	*0*	2.5	*0*
FD&C Yellow Dye #5	0	*0*	0 0.05 0	*0*	0 0.025 0.025	*0*
FD&C Red Dye #40	0	*0*		*0*		*0*
FD&C Blue Dye #1	0	*0*		*0*		*0*
Total	**1000**	***3850***	**960.05**	***3850***	**991.3**	***3850***
Cellulose (gm/kg diet)	50.0		10.4		10.1	
Inulin (gm/kg diet)	0.0		0.0		50.4	

Table 4.2 (cont). AIN-93M Mature Rodent Diet and Modified AIN-93M Diets with 10 gm Cellulose or 10 gm Cellulose + 50 gm Inulin per 3850 kcal.

4.4 Results

Sodium butyrate downregulates *Il1b* gene expression in response to LPS in adult and aged microglia and hippocampus

Mice were either pre-treated i.p. with saline (SAL) or NaB, and then given an i.p. injection of either SAL or LPS two hours later. For body weight, LPS-treated adult and aged mice lost more weight (main effect of LPS, $p=0.0052$ and $p<0.0001$) as expected, but there was

also an interaction (NaB x LPS, p=0.0391) with the aged mice in that NaB pre-treated mice with LPS did not lose as much weight as the SAL pre-treated mice with LPS (data not shown).

Fluidigm gene expression analysis on microglia was performed to gain a more comprehensive assessment of microglial gene regulation in response to NaB (**Table 4.3** and **Table 4.4**). However, there were very few changes associated with NaB in the majority of genes analyzed, so we chose to focus on pro-inflammatory cytokine gene expression (**Figure 4.1A-C**). In adult microglia, for *Il1b*, there were main effects of LPS (p=0.0005), NaB (p=0.0447), and a trending interaction (p=0.0774) in that NaB decreased LPS-induced *Il1b* expression. In aged microglia, for *Il1b*, there were main effects of LPS (p<0.0001), NaB (p=0.0497), and an interaction (p=0.0178) in that NaB decreased LPS-induced *Il1b* expression. For microglial *Tnf*, there were only main effects of LPS in both adult and aged mice (p=0.02 and p=0.003). For microglial *Il-6*, there was only a main effect of LPS in aged mice (p<0.0001).

Similar changes were also observed in the hippocampus (**Figure 4.1D-F**). In the adult hippocampus, for *Il1b*, there was only a main effect of LPS (p=0.0018). But in the aged hippocampus, for *Il1b*, there were main effects of LPS (p<0.0001), NaB (p=0.0246), and an interaction (p=0.0257) in that NaB decreased LPS-induced *Il1b* expression. For hippocampal *Tnf* and *Il-6*, there were only main effects of LPS in both adult and aged mice (p=0.0031 and p<0.0001 and p=0.0475 and p=0.0069).

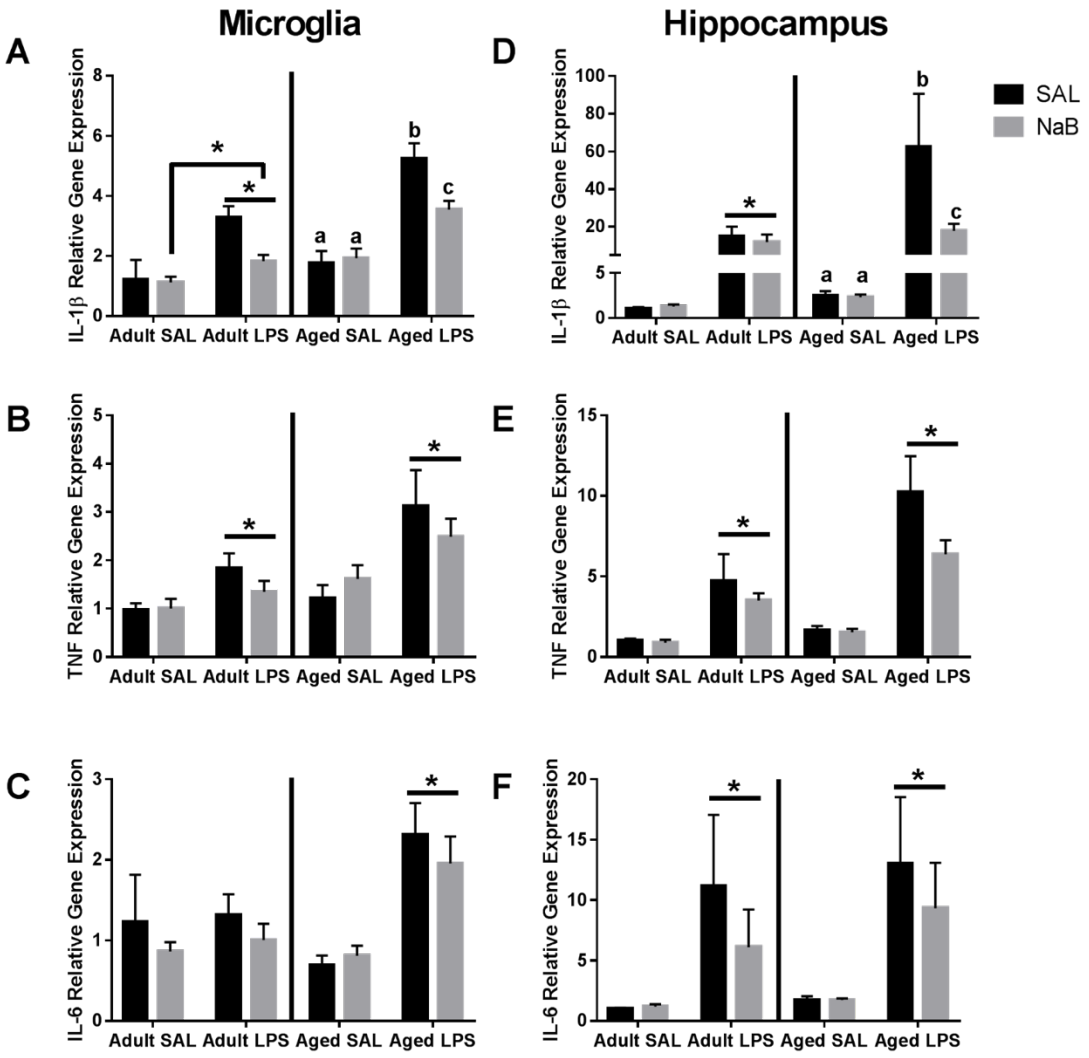

Figure 4.1. Microglial and hippocampal gene expression 4 hours after SAL/LPS i.p. injections in adult and aged mice pre-treated with i.p. SAL/NaB. Data are presented as means ± SEM (n=7-10) for microglial **(A)** *Il1b*, **(B)** *Tnf*, **(C)** *Il-6* and hippocampal **(D)** *Il1b*, **(E)** *Tnf*, and **(F)** *Il-6* gene expression. Treatment means with different letters are significantly different. * indicates a main effect with significance at $p<0.05$.

Table 4.3. Expression of **(A)** inflammatory, **(B)** sensome, and **(C)** epigenetic regulator genes in microglia collected at 4 hours after SAL/LPS i.p. injections in adult mice pre-treated with i.p. SAL/NaB. Data are presented as means ± SEM (n=7-10) and p-values for main effects of NaB and LPS as well as NaB x LPS interactions are also included.

A. Inflammatory and Regulators of Inflammatory Genes

					p-values		
Gene	**SAL + SAL**	**NaB + SAL**	**SAL + LPS**	**NaB + LPS**	**NaB**	**LPS**	**NaB x LPS**
Arg1	1.21±0.31	1.21±0.61	2.09±0.39	0.94±0.24	0.161	0.454	0.165
Casp1	0.95±0.19	1.21±0.25	0.77±0.14	0.52±0.10	0.98	0.029*	0.193
Cd68	0.91±0.13	1.08±0.20	0.56±0.08	0.37±0.04	0.929	0.0003*	0.188
Cx3cr1	0.97±0.17	0.97±0.13	0.41±0.06	0.23±0.02	0.378	<0.0001*	0.373
Gene	**SAL + SAL**	**ZEB + SAL**	**SAL + LPS**	**ZEB + LPS**	**ZEB**	**LPS**	**ZEB x LPS**
HIF-1α	0.88±0.02	1.18±0.25	1.52±0.41	0.93±0.23	0.720	0.624	0.262
Igf1	1.06±0.31	1.32±0.25	0.37±0.12	0.21±0.03	0.809	<0.0001*	0.269
Il-1β	1.22±0.65	1.13±0.18	3.29±0.37	1.83±0.21	0.045*	0.0005*	0.077
Il-1rn	0.99±0.35	0.81±0.11	19.03±3.82	14.91±3.25	0.436	<0.0001*	0.474
Il-10	1.10±0.35	0.80±0.16	5.19±0.77	2.21±0.56	0.004*	<0.0001*	0.017*
Il-6	1.23±0.59	0.86±0.12	1.32±0.25	1.01±0.20	0.277	0.709	0.934
Niarc1	1.16±0.55	1.09±0.20	6.67±1.52	5.41±1.09	0.529	<0.0001*	0.578
Nlrp3	0.84±0.07	1.59±0.52	1.05±0.25	0.80±0.21	0.548	0.484	0.234
Pycard	0.99±0.06	0.75±0.02	0.61±0.07	0.68±0.03	0.097	<0.0001*	0.004*
Socs1	1.01±0.25	1.74±0.28	1.39±0.17	1.40±0.26	0.143	0.947	0.148
Socs3	0.98±0.23	1.82±0.55	3.86±0.95	3.20±0.72	0.914	0.011*	0.361
Stat3	0.87±0.06	0.92±0.11	2.69±0.32	2.10±0.28	0.345	<0.0001*	0.264
Tlr2	0.94±0.15	1.13±0.18	1.78±0.38	1.71±0.41	0.877	0.062	0.730
Tlr4	1.02±0.14	1.01±0.16	0.47±0.06	0.36±0.04	0.599	<0.0001*	0.656
Tlr7	0.86±0.04	0.92±0.13	1.32±0.16	1.00±0.12	0.444	0.128	0.275
Tlr8	0.94±0.18	1.01±0.17	1.35±0.21	0.89±0.12	0.323	0.447	0.177
Tnf	0.97±0.14	1.01±0.20	1.84±0.31	1.35±0.23	0.371	0.02*	0.306

B. Sensome Genes

					p-values		
Gene	**SAL + SAL**	**NaB + SAL**	**SAL + LPS**	**NaB + LPS**	**NaB**	**LPS**	**NaB x LPS**
Cd53	0.92±0.09	0.96±0.13	0.93±0.12	0.71±0.08	0.475	0.340	0.300

Gpr34	**0.96±0.12**	**1.14±0.22**	**0.20±0.05**	**0.08±0.02**	**0.822**	**<0.0001***	**0.338**
P2ry12	**1.18±0.49**	**0.88±0.09**	**0.31±0.06**	**0.17±0.02**	**0.312**	**0.0004***	**0.69**
P2ry13	**0.93±0.12**	**0.90±0.12**	**0.43±0.05**	**0.28±0.02**	**0.299**	**<0.0001***	**0.509**
Siglech	**0.94±0.13**	**1.07±0.18**	**0.53±0.08**	**0.32±0.04**	**0.781**	**<0.0001***	**0.192**
Tgfbr1	**0.93±0.18**	**1.19±0.24**	**0.53±0.08**	**0.34±0.04**	**0.842**	**0.0003***	**0.170**
Tmem119	**1.09±0.27**	**2.04±0.62**	**0.55±0.11**	**0.32±0.05**	**0.362**	**0.005***	**0.133**
Trem2	**0.93±0.31**	**2.16±0.61**	**0.86±0.19**	**0.62±0.14**	**0.192**	**0.035***	**0.053**

C. Epigenetic Regulator Genes

					p-values		
Gene	**SAL + SAL**	**NaB + SAL**	**SAL + LPS**	**NaB + LPS**	**NaB**	**LPS**	**NaB x LPS**
Hdac2	**0.97±0.21**	**1.27±0.25**	**0.99±0.18**	**0.71±0.13**	**0.958**	**0.226**	**0.195**
Hdac3	**0.91±0.13**	**1.00±0.16**	**0.76±0.10**	**0.58±0.08**	**0.725**	**0.031***	**0.305**
Hdac4	**0.93±0.29**	**1.61±0.32**	**3.67±0.92**	**3.16±0.73**	**0.902**	**0.004***	**0.404**
Hdac5	**0.99±0.26**	**1.82±0.41**	**0.54±0.12**	**0.32±0.05**	**0.247**	**0.0004***	**0.0457***
Hdac6	**0.97±0.27**	**1.76±0.38**	**1.87±0.40**	**1.19±0.24**	**0.883**	**0.673**	**0.059**
Tet1	**0.94±0.07**	**1.00±0.16**	**0.29±0.07**	**0.12±0.02**	**0.621**	**<0.0001***	**0.313**
Tet2	**1.03±0.18**	**1.23±0.23**	**1.32±0.29**	**1.23±0.25**	**0.855**	**0.633**	**0.641**
Tet3	**1.03±0.27**	**2.42±0.69**	**0.81±0.19**	**0.57±0.14**	**0.167**	**0.013***	**0.049***

Table 4.3 (cont.). Expression of **(A)** inflammatory, **(B)** sensome, and **(C)** epigenetic regulator genes in microglia collected at 4 hours after SAL/LPS i.p. injections in adult mice pre-treated with i.p. SAL/NaB. Data are presented as means ± SEM (n=7-10) and p-values for main effects of NaB and LPS as well as NaB x LPS interactions are also included.

Table 4.4. Expression of **(A)** inflammatory, **(B)** sensome, and **(C)** epigenetic regulator genes in microglia collected at 4 hours after SAL/LPS i.p. injections in aged mice pre-treated with i.p. SAL/NaB. Data are presented as means ± SEM (n=7-10) and p-values for main effects of NaB and LPS as well as NaB x LPS interactions are also included.

A. Inflammatory and Regulators of Inflammatory Genes

					p-values		
Gene	**SAL + SAL**	**NaB + SAL**	**SAL + LPS**	**NaB + LPS**	**NaB**	**LPS**	**NaB x LPS**
Arg1	**2.82±1.46**	**1.38±0.55**	**5.65±1.37**	**4.69±0.75**	**0.252**	**0.005***	**0.812**
Casp1	**0.62±0.13**	**0.73±0.13**	**0.45±0.10**	**0.49±0.07**	**0.482**	**0.053**	**0.790**
Cd68	**0.74±0.15**	**0.93±0.16**	**0.47±0.09**	**0.44±0.05**	**0.508**	**0.0016***	**0.364**
Cx3cr1	**0.51±0.09**	**0.58±0.07**	**0.18±0.02**	**0.18±0.02**	**0.582**	**<0.0001***	**0.576**
HIF-1α	**0.76±0.17**	**0.95±0.19**	**2.14±0.57**	**2.09±0.40**	**0.850**	**0.0013***	**0.744**
Igf1	**1.15±0.33**	**1.55±0.33**	**0.26±0.07**	**0.24±0.04**	**0.360**	**<0.0001***	**0.304**
Il-1β	**1.77±0.40**	**1.93±0.31**	**5.24±0.52**	**3.54±0.30**	**0.050***	**<0.0001***	**0.018***
Il-1rn	**2.81±0.50**	**3.07±0.36**	**38.12±3.75**	**27.25±2.91**	**0.036***	**<0.0001***	**0.028***
Il-10	**1.42±0.39**	**2.23±0.59**	**12.67±3.90**	**7.28±1.44**	**0.239**	**<0.0001***	**0.113**
Il-6	**0.70±0.12**	**0.81±0.12**	**2.32±0.39**	**1.96±0.33**	**0.659**	**<0.0001***	**0.398**
Niarc1	**1.34±0.26**	**1.52±0.27**	**7.38±1.53**	**8.21±1.43**	**0.656**	**<0.0001***	**0.771**
Nlrp3	**1.02±0.34**	**1.14±0.29**	**1.26±0.45**	**1.16±0.24**	**0.964**	**0.699**	**0.744**
Pycard	**0.99±0.06**	**0.75±0.02**	**0.61±0.07**	**0.68±0.03**	**0.097**	**<0.0001***	**0.004***
Socs1	**1.71±0.18**	**2.05±0.19**	**1.69±0.31**	**1.41±0.25**	**0.899**	**0.176**	**0.205**
Socs3	**1.16±0.30**	**1.21±0.22**	**5.53±1.57**	**4.21±0.85**	**0.488**	**0.0001***	**0.460**
Stat3	**0.59±0.08**	**0.55±0.06**	**2.36±0.32**	**1.98±0.22**	**0.306**	**<0.0001***	**0.411**
Tlr2	**0.90±0.16**	**1.09±0.16**	**3.05±0.66**	**2.41±0.35**	**0.566**	**<0.0001***	**0.294**
Tlr4	**0.62±0.12**	**0.66±0.10**	**0.41±0.06**	**0.33±0.03**	**0.816**	**0.0014***	**0.510**
Tlr7	**0.55±0.08**	**0.54±0.07**	**0.96±0.14**	**0.88±0.08**	**0.657**	**0.0002***	**0.700**
Tlr8	**1.34±0.27**	**1.41±0.28**	**2.30±0.51**	**1.89±0.26**	**0.612**	**0.035***	**0.486**
Tnf	**1.23±0.26**	**1.62±0.28**	**3.13±0.74**	**2.49±0.37**	**0.783**	**0.003***	**0.257**

B. Sensome Genes

					p-values		
Gene	**SAL + SAL**	**NaB + SAL**	**SAL + LPS**	**NaB + LPS**	**NaB**	**LPS**	**NaB x LPS**
Cd53	**0.54±0.10**	**0.55±0.08**	**0.64±0.08**	**0.74±0.007**	**0.487**	**0.093**	**0.571**

Gpr34	**0.54±0.01**	**0.60±0.11**	**0.05±0.01**	**0.06±0.01**	**0.681**	**<0.0001***	**0.727**
P2ry12	**0.48±0.07**	**0.52±0.07**	**0.12±0.01**	**0.11±0.01**	**0.706**	**0.0004***	**0.629**
P2ry13	**0.48±0.09**	**0.50±0.06**	**0.25±0.04**	**0.24±0.02**	**0.938**	**<0.0001***	**0.849**
Siglech	**0.56±0.12**	**0.55±0.09**	**0.28±0.05**	**0.28±0.04**	**0.946**	**0.0006***	**0.957**
Gene	**SAL + SAL**	**ZEB + SAL**	**SAL + LPS**	**ZEB + LPS**	**ZEB**	**LPS**	**ZEB x LPS**
Tgfbr1	**0.61±0.13**	**0.73±0.13**	**0.27±0.06**	**0.31±0.04**	**0.439**	**0.0002***	**0.679**
Tmem119	**1.06±0.35**	**1.36±0.40**	**0.27±0.09**	**0.31±0.08**	**0.506**	**0.0006***	**0.613**
Trem2	**1.52±0.48**	**2.07±0.49**	**0.68±0.24**	**0.68±0.14**	**0.449**	**0.0025***	**0.439**

C. Epigenetic Regulator Genes

					p-values		
Gene	**SAL + SAL**	**NaB + SAL**	**SAL + LPS**	**NaB + LPS**	**NaB**	**LPS**	**NaB x LPS**
Hdac2	**0.78±0.17**	**0.84±0.16**	**0.61±0.11**	**0.62±0.07**	**0.802**	**0.138**	**0.842**
Hdac3	**0.59±0.11**	**0.65±0.10**	**0.53±0.08**	**0.52±0.06**	**0.750**	**0.278**	**0.677**
Hdac4	**1.09±0.26**	**1.11±0.22**	**2.32±0.52**	**3.00±0.57**	**0.432**	**0.0008***	**0.452**
Hdac5	**1.14±0.32**	**1.67±0.33**	**0.28±0.07**	**0.27±0.05**	**0.257**	**<0.0001***	**0.247**
Hdac6	**0.83±0.22**	**1.06±0.21**	**1.43±0.37**	**1.20±0.21**	**0.997**	**0.149**	**0.360**
Tet1	**0.48±0.08**	**0.51±0.07**	**0.07±0.01**	**0.07±0.01**	**0.747**	**<0.0001***	**0.808**
Tet2	**0.86±0.18**	**0.89±0.16**	**1.34±0.28**	**1.40±0.27**	**0.843**	**0.040***	**0.962**
Tet3	**1.16±0.35**	**1.65±0.43**	**0.71±0.20**	**0.65±0.09**	**0.466**	**0.014***	**0.348**

Table 4.4 (cont.). Expression of **(A)** inflammatory, **(B)** sensome, and **(C)** epigenetic regulator genes in microglia collected at 4 hours after SAL/LPS i.p. injections in aged mice pre-treated with i.p. SAL/NaB. Data are presented as means ± SEM (n=7-10) and p-values for main effects of NaB and LPS as well as NaB x LPS interactions are also included.

Significant shifts in the microbiome associated with age

At baseline, β-diversity analysis revealed that gut microbiota composition was different between adult (3-6 months) and aged (22-25 months) mice fed a normal chow diet (PERMANOVA $p<0.05$). Random forest analysis with Boruta feature selection identified lower levels of *Mucuspirillum spp.* and *Odoribacter spp*., and higher levels of in *Ruminococcus spp., Coprococcus spp*., and *Rikenellaceae* in aged versus adult mice.

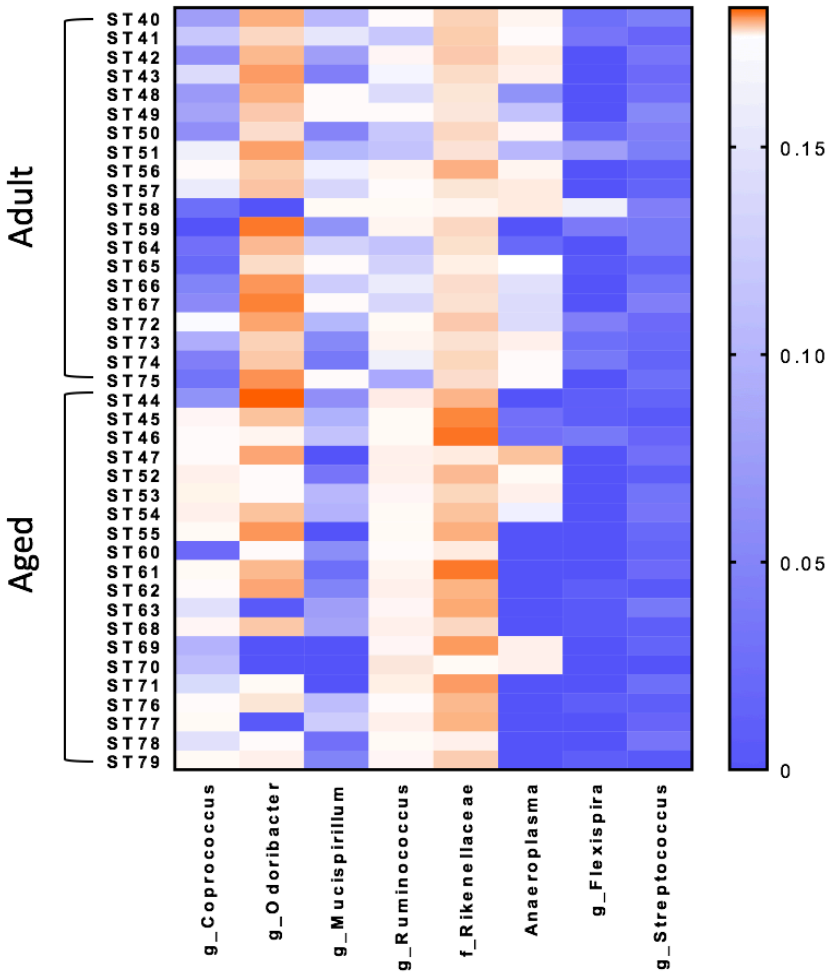

Figure 4.2. Random forest analysis with Boruta feature identifies eight bacterial genera within the fecal microbiome that discriminate between adult and aged mice fed a normal chow diet. Scale bar represents relative abundance. N=20 per group.

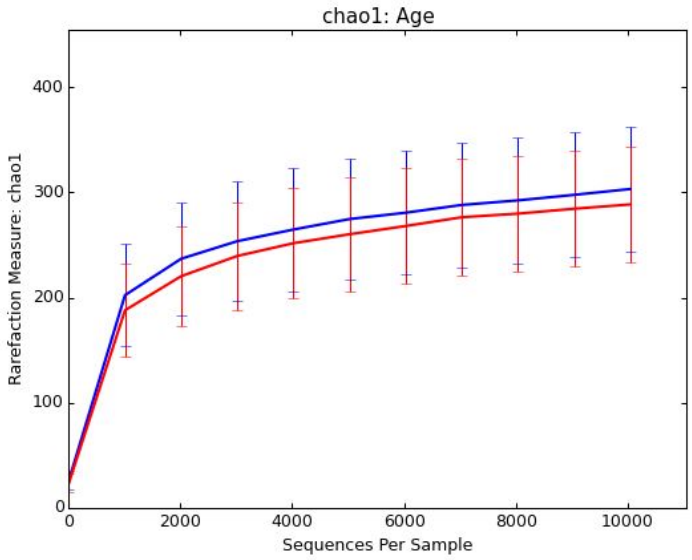

Figure 4.3. α-diversity rarefaction plots as determined by Chao1. No differences in α- diversity were observed as a result of age (blue: adult mice red: aged mice; shown above) or fiber feeding (data not shown).

High soluble fiber diet alters microbiota and increases production of SCFA's

Adult and aged mice were fed either a low fiber (1% cellulose) or high fiber (1% cellulose + 5% inulin) diet for 4 weeks. For body weight, there were no differences in body weight for age or diet ($p>0.05$, data not shown).

β-diversity analysis revealed a robust effect of 4 weeks of soluble fiber feeding on gut microbiota composition (PERMANOVA $p<0.05$; **Supplementary Figure 4.4**). Of note, inulin feeing led to lower abundances of *Ruminococcus spp*. and f. Rikenellaceae, two taxa that were more highly represented in aged mice fed a chow diet. Cecal contents were analyzed for SCFA concentrations to assess the magnitude and profile of fermentation end products (**Figure 4.5**). Inulin feeding led to an increase in cecal acetate ($p=0.0066$) and butyrate ($p=0.009$), and total SCFAs ($p=0.0107$), irrespective of age. Propionate concentrations were not responsive to diet nor affected by age ($p>0.05$; Figure **4.5C**).

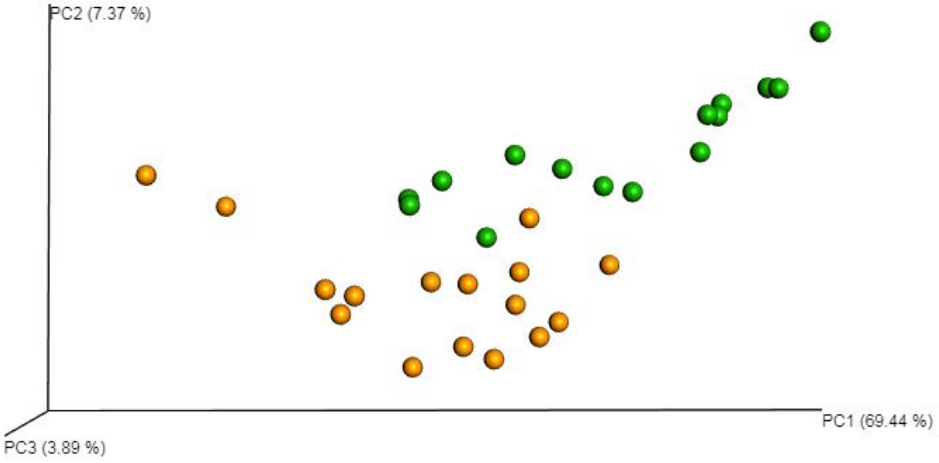

Figure 4.4. β-diversity analysis (weighted Unifrac) reveals differences in gut microbiota community composition between high fiber-fed (green) and low fiber-fed (orange) mice after 4 weeks of feeding.

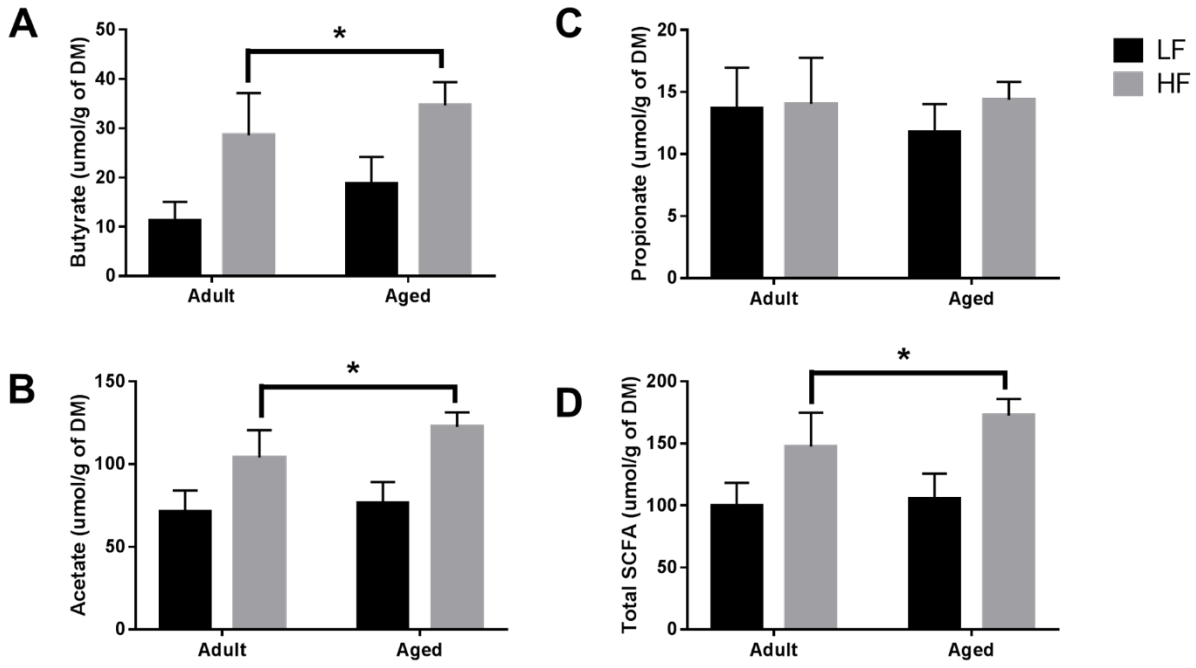

Figure 4.5. Cecal content concentrations of **(A)** butyrate, **(B)** acetate, **(C)** propionate, and **(D)** total SCFAs in adult and aged mice fed a LF (1% cellulose) or HF (1% cellulose and 5% inulin) diet. Data are presented as means ± SEM (n=6-8). * indicates a main effect with significance at $p<0.05$.

Fiber alters expression of inflammatory, sensome, and epigenetic regulator genes in adult and aged microglia and butyrate correlates positively with reduced microglial inflammatory gene expression

Fluidigm gene expression analysis on microglia was performed to gain a more comprehensive assessment of microglial gene regulation in response to diets with low and high fiber (**Figure 4.6A**). For inflammatory and regulators of inflammatory genes, there were a number of significant main effects of diet in that high fiber decreased gene expression (*Il1b*, *Il-1rn, Il-6, Nlrp3, Tlr4, Tnf*) (**Table 4.5A**). For sensome genes, there were main effects of diet for all genes analyzed (see **Table 4.5B**), as well as an interaction with *Trem2* in which aged mice on the low fiber diet had the highest expression but decreased to levels similar to the adult groups with the high fiber diet. For epigenetic regulator genes, there were also main effects of almost all genes analyzed, in that high fiber decreased expression (**Table 4.5C**). Of note, some epigenetic regulator genes were affected by age similar to what has been demonstrated previously (*Hdac1, Gadd45b*) (Matt et al., 2016).

We also wanted to determine if the increased butyrate seen with the high fiber diet is related to the anti-inflammatory effect seen in the brain. Correlating microglial *Il1b*, *Il-6,* and *Tnf* with concentrations of butyrate demonstrated that for *Il1b* and *Tnf* (trend for *Il-6*), higher butyrate correlated with lower pro-inflammatory gene expression (**Figure 4.6B-D**).

Fiber does not alter expression of inflammatory genes or *Il1b* DNA methylation in adult and aged hippocampus

Only main effects of age were observed in the hippocampus of adult and aged mice fed low and high fiber diets (*Il1b*, $p=0.0074$, *Tnf,* $p=0.0145$, and *Il-6*, $p>0.05$) (**Figure 4.6E-G**). Due to low DNA yield, we were not able to assess *Il1b* DNA methylation in microglia. However, in the

hippocampus (**Figure 4.6H-I**), analysis of *Il1b* DNA methylation revealed a main effect of age in *Il1b* CpG1 ($p=0.0395$). There were no changes in *Il1b* CpG2.

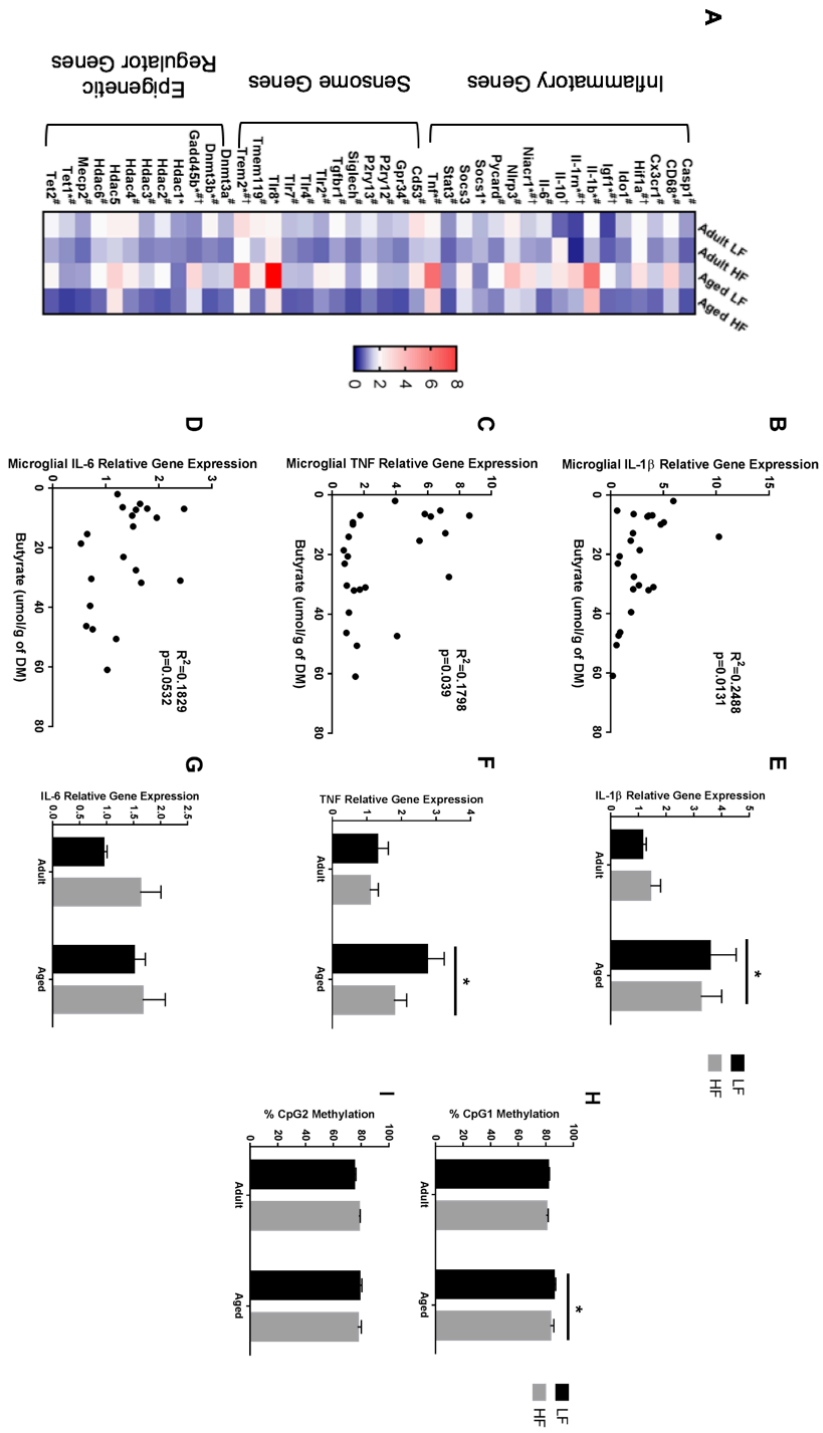

Figure 4.6. (A) Heat map visualization of relative expression of genes in microglia analyzed by Fluidigm. Microglia were collected from adult and aged mice fed a LF (1% cellulose) or HF (1% cellulose and 5% inulin) diet. Correlational analyses were performed between cecal concentrations of butyrate and microglial **(B)** *Il1b*, **(C)** *Tnf*, **(D)** *Il-6*. Hippocampal **(E)** *Il1b*, **(F)** *Tnf*, **(G)** *Il-6* gene expression and DNA methylation of the *Il1b* promoter at **(H)** CpG1 and **(I)** CpG2. Data are presented as means ± SEM (n=6-8). * indicates a main effect with significance at $p<0.05$.

Table 4.5. Expression of **(A)** inflammatory, **(B)** sensome, and **(C)** epigenetic regulator genes in microglia collected from adult and aged mice fed low and or high fiber diets. Data are presented as means ± SEM (n=7-10) and p-values for main effects of Age and Diet as well as Age x Diet interactions are also included.

A. Inflammatory and Regulators of Inflammatory Genes

					p-values		
Gene	**Adult LF**	**Adult HF**	**Aged LF**	**Aged HF**	**Age**	**Diet**	**Age x Diet**
Casp1	**1.10±0.15**	**0.68±0.12**	**1.28±0.15**	**0.59±0.09**	**0.734**	**<0.0001***	**0.315**
Cd68	**1.80±0.32**	**1.27±0.22**	**3.24±0.46**	**1.42±0.32**	**0.025***	**0.0012***	**0.067**
Cx3cr1	**1.38±0.22**	**0.96±0.21**	**1.46±0.23**	**0.72±0.17**	**0.695**	**0.0079***	**0.447**
HIF-1α	**1.96±0.35**	**1.89±0.59**	**2.74±0.33**	**0.85±0.15**	**0.753**	**0.019***	**0.028***
Ido1	**1.37±0.21**	**0.94±0.27**	**1.26±0.17**	**0.76±0.16**	**0.491**	**0.0279***	**0.872**
Igf1	**0.49±0.09**	**0.68±0.22**	**1.95±0.30**	**0.74±0.15**	**0.0013***	**0.0276***	**0.0027***
Il-1β	**1.91±0.30**	**1.30±0.29**	**6.34±0.68**	**4.03±0.84**	**<0.0001***	**0.012***	**0.134**
Il-1rn	**0.48±0.06**	**0.25±0.07**	**3.35±3.51**	**1.26±0.19**	**<0.0001***	**0.0002***	**0.0023***
Il-10	**0.70±0.18**	**2.22±0.64**	**2.57±0.48**	**1.07±0.32**	**0.512**	**0.989**	**0.0094***
Il-6	**1.62±0.17**	**1.08±0.23**	**1.63±0.17**	**0.70±0.14**	**0.327**	**0.0002***	**0.300**
Niarc1	**1.44±0.15**	**1.13±0.08**	**2.65±0.30**	**1.46±0.20**	**0.0002***	**0.0004***	**0.0293**
Nlrp3	**2.24±0.27**	**1.55±0.39**	**3.87±0.56**	**1.57±0.40**	**0.060**	**0.001***	**0.066**
Pycard	**1.58±0.25**	**0.93±0.19**	**1.87±0.25**	**0.91±0.19**	**0.539**	**0.0007***	**0.506**
Socs1	**1.30±0.08**	**1.29±0.05**	**0.93±0.11**	**1.14±0.06**	**0.0022***	**0.246**	**0.187**
Socs3	**1.71±0.30**	**1.11±0.27**	**2.27±0.44**	**1.60±0.51**	**0.181**	**0.105**	**0.918**
Stat3	**1.03±0.16**	**0.72±0.13**	**1.04±0.13**	**0.58±0.10**	**0.617**	**0.0051***	**0.577**
Tlr2	**1.21±0.19**	**0.73±0.14**	**2.24±0.33**	**1.04±0.22**	**0.0048***	**0.0006***	**0.125**
Tlr4	**1.40±0.17**	**0.85±0.18**	**1.31±0.17**	**0.67±0.13**	**0.419**	**0.0006***	**0.762**
Tlr7	**1.35±0.14**	**1.02±0.24**	**1.35±0.17**	**0.65±0.11**	**0.302**	**0.0048***	**0.293**
Tlr8	**2.10±0.46**	**2.30±0.59**	**8.72±1.55**	**2.60±0.52**	**0.089**	**0.113**	**0.013***
Tnf	**2.09±0.29**	**1.46±0.47**	**6.42±0.93**	**3.17±1.03**	**0.0001***	**0.011***	**0.081**

B. Sensome Genes

					p-values		
Gene	**Adult LF**	**Adult HF**	**Aged LF**	**Aged HF**	**Age**	**Diet**	**Age x Diet**
Cd53	**2.67±0.59**	**1.40±0.28**	**2.53±0.47**	**1.08±0.21**	**0.602**	**0.003***	**0.851**
Gpr34	**1.46±0.16**	**0.87±0.22**	**1.26±0.15**	**0.54±0.11**	**0.119**	**0.0003***	**0.698**

P2ry12	**1.05±0.22**	**1.05±0.22**	**1.29±0.17**	**0.60±0.11**	**0.134**	**0.005***	**0.267**
P2ry13	**1.66±0.28**	**1.26±0.30**	**1.95±0.31**	**0.87±0.21**	**0.876**	**0.011***	**0.231**
Siglech	**1.43±0.16**	**0.81±0.18**	**1.18±0.14**	**0.54±0.11**	**0.089**	**<0.0001***	**0.933**
Tgfbr1	**1.84±0.32**	**1.14±0.22**	**2.10±0.28**	**0.81±0.19**	**0.891**	**0.0003***	**0.262**
Tmem119	**2.15±0.38**	**1.36±0.38**	**2.36±0.34**	**0.82±0.25**	**0.636**	**0.0014***	**0.283**
Trem2	**2.80±0.61**	**1.82±0.33**	**6.23±1.04**	**1.99±0.53**	**0.011***	**0.0004***	**0.021***

C. Epigenetic Regulator Genes

					p-values		
Gene	**Adult LF**	**Adult HF**	**Aged LF**	**Aged HF**	**Age**	**Diet**	**Age x Diet**
Dnmt3a	**1.28±0.19**	**0.83±0.18**	**1.49±0.18**	**0.77±0.16**	**0.681**	**0.0019***	**0.456**
Dnmt3b	**2.01±0.31**	**0.96±0.20**	**1.41±0.21**	**0.63±0.12**	**0.046***	**0.0002***	**0.566**
Gadd45b	**1.01±0.12**	**0.81±0.22**	**3.04±0.35**	**1.60±0.40**	**<0.0001***	**0.006***	**0.033***
Hdac1	**1.11±0.02**	**0.95±0.07**	**0.83±0.04**	**0.82±0.03**	**<0.0001***	**0.068**	**0.106**
Hdac2	**1.67±0.30**	**1.00±0.22**	**1.87±0.23**	**0.63±0.14**	**0.704**	**0.0001***	**0.224**
Hdac3	**1.22±0.17**	**0.94±0.18**	**1.50±0.20**	**0.71±0.12**	**0.855**	**0.0029***	**0.145**
Hdac4	**2.20±0.47**	**1.27±0.33**	**2.25±0.38**	**0.93±0.73**	**0.699**	**0.0037***	**0.595**
Hdac5	**2.13±0.38**	**1.48±0.41**	**3.18±0.65**	**2.60±1.04**	**0.100**	**0.350**	**0.957**
Hdac6	**1.91±0.27**	**1.38±0.39**	**1.86±0.29**	**0.74±0.17**	**0.256**	**0.0085***	**0.331**
Mecp2	**1.13±0.17**	**0.77±0.16**	**1.13±0.17**	**0.54±0.10**	**0.429**	**0.0019***	**0.457**
Tet1	**1.49±0.17**	**1.01±0.20**	**1.09±0.15**	**0.44±0.09**	**0.004***	**0.001***	**0.609**
Tet2	**1.75±0.27**	**1.22±0.23**	**1.97±0.24**	**0.64±0.10**	**0.422**	**0.0001***	**0.080**
Tet3	**3.54±0.70**	**1.90±0.50**	**5.55±1.09**	**5.55±2.23**	**0.021***	**0.488**	**0.489**

Table 4.5 (cont). Expression of **(A)** inflammatory, **(B)** sensome, and **(C)** epigenetic regulator genes in microglia collected from adult and aged mice fed low and or high fiber diets. Data are presented as means ± SEM (n=7-10) and p-values for main effects of Age and Diet as well as Age x Diet interactions are also included.

Feeding a diet supplemented with soluble fiber significantly reduces signs of inflammation specifically in the aged but does not alter LBP

Representative images of the cecum and colon from mice fed low fiber and high fiber diets reveal increased cecal size with the high fiber diet, indicative of increased fermentation (**Figure 4.7A**). Distal colon samples were stained with H&E to examine morphological changes

due to age and fiber diet. Representative pictures (**Figure 4.7B-C**) indicate severe inflammation associated with leukocyte infiltration in aged animals on a low fiber diet. Scoring of histology sections for inflammatory infiltrate reveal that there is a main effect of diet ($p=0.0499$) and an interaction ($p=0.0499$) in that aged mice on the high fiber diet have decreased inflammatory infiltrate, with scoring not significantly different from either low fiber or high fiber adult groups (**Figure 4.7D**). With regards to total histological scoring, there is a trending main effect for diet ($p=0.088$) in that diet decreased total score (**Figure 4.7E**). Lastly, we assessed LBP in serum of adult and aged animals fed low and high fiber diets (**Figure 4.7F**). We found a main effect of age ($p=0.0298$) which matches previous findings from our lab (unpublished results), but no significant effect of diet.

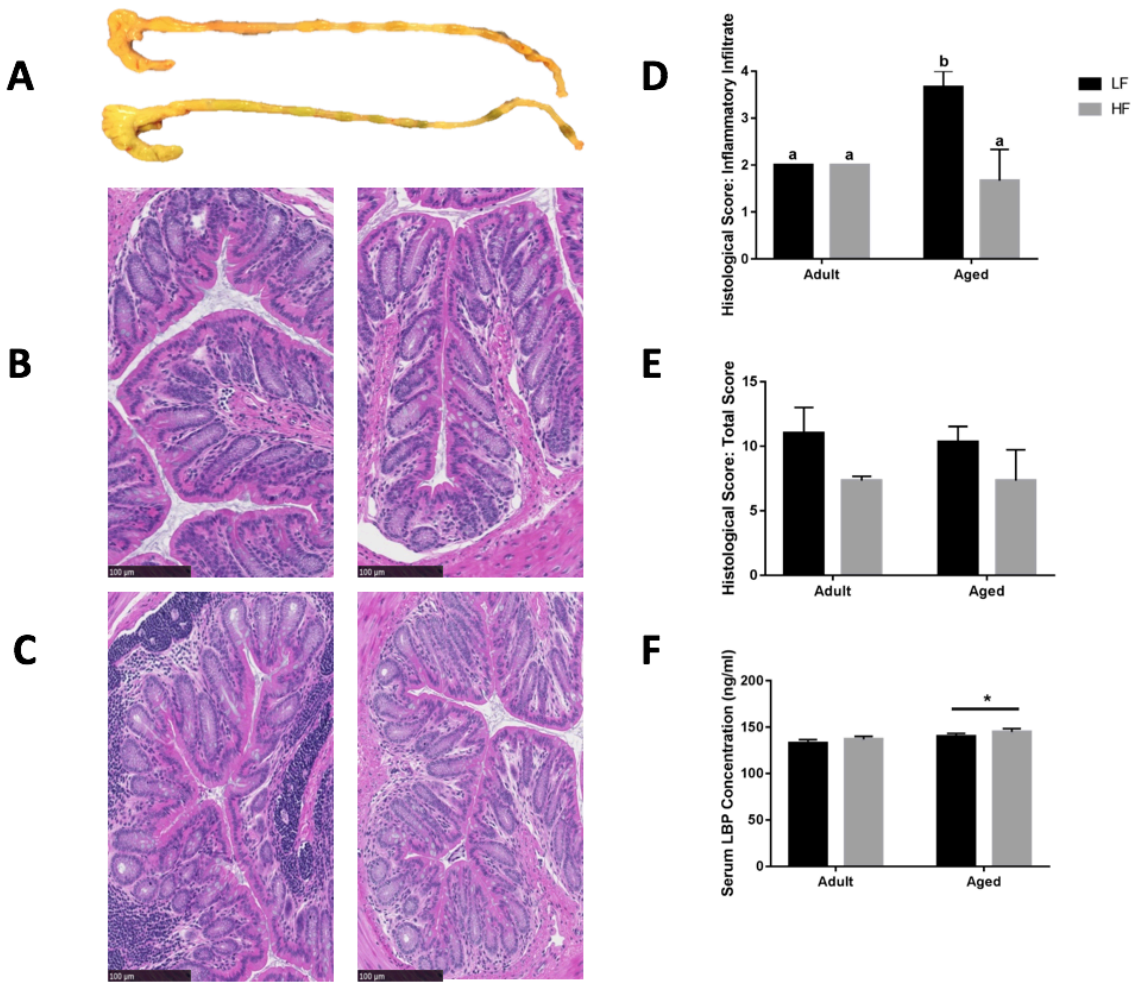

Figure 4.7. (A) Representative images of cecum and colon in mice fed either a low (top) or high (bottom) fiber diet. Representative sections of the distal colon of 4-month old **(B)** and 24-month old **(C)** mice fed either a low (left) or a high (right) diet. Sections were stained with hematoxylin and eosin (H&E). Scale bar = 100 µM. Blinded histological scoring of distal colons: **(D)** inflammatory cell infiltration (score 0-4) and **(E)** total histology score (0-16) (includes aggregate scores of inflammatory cell infiltration (0-4), goblet cell mucus depletion (0-4; data not shown), destruction of architecture (0-4; data not shown) and crypt abscesses (0-4; data not shown). Data are presented as means ± SEM (n=3). Bars with no SEM indicate identical scoring for all mice in the group. Treatment means with different letters are significantly different. **(F)** Serum LBP measured in adult and aged mice fed low or high fiber diets. Data are presented as means ± SEM (n=7-10). * indicates a main effect with significance at $p<0.05$.

Peripheral gene expression does not mirror microglial changes but Tjp2 and FFAR2 expression are affected by high soluble fiber diet

Gene expression for the pro-inflammatory cytokines *Il1b* and *Tnf*, other inflammatory regulators including *Il-10* and *Il-1rn*, *Il-17*, and *Il-23*, the histone deacetylase *Hdac3*, tight

junction proteins/intestinal markers *Tjp1, Tjp2, Tff3, Ocln, Mct1*, and *Muc2*, as well as the FFARs *Ffar2* and *Gpr109a* were measured in colon (**Figure 4.8A**). There were no significant changes in any of the genes analyzed in adult mice (data not shown), so we chose to focus on aged animals. Surprisingly, there were no effects of diet on pro-inflammatory gene expression, but there was an effect of diet for *Tjp2* (p=0.0396) and *Ffar2* (p=0.0319). There were also trending effects of diet for *Tjp1* (0.0738) and *Ocln* (p=0.0857). Gene expression for the pro-inflammatory cytokines *Il1b, Tnf*, and *Il-6* were assessed in lymph nodes and liver, but there were no differences between low fiber and high fiber groups in adult (data no shown) or aged mice (**Figure 4.8B**).

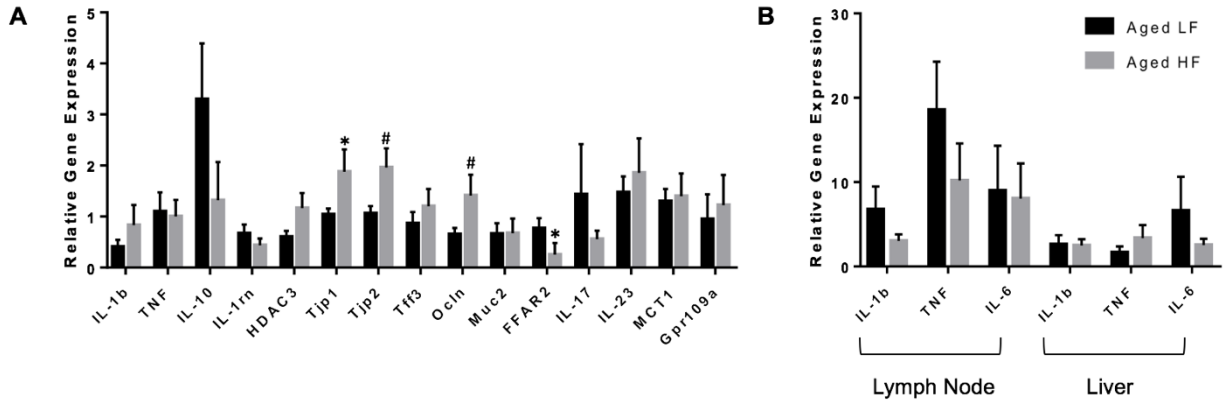

Figure 4.8. Gene expression of **(A)** colon and **(B)** lymph node and liver samples from aged mice fed either a low or high fiber diet. Data are presented as means ± SEM (n=7-10). * indicates significance at p<0.05 and # indicates significance at p<0.1.

Minimal changes in LPS-treated mice fed low and high fiber diets

For Experiment 3, the treatments were identical to Experiment 2 except that mice were injected i.p. with LPS in order to characterize changes in immune stimulus associated with diet. For body weight, LPS decreased body weight as expected (1-2 grams on average, data not shown), and there were no differences in body weight for age or diet (p>0.05, data not shown).

Fluidigm analysis from microglia is shown in **Table 4.6**. Interestingly, the majority of the diet main effects and interactions were seen in the sensome (*Cd53, Siglech, P2ry12, P2ry13, Trem2, Tmem119*). For the hippocampus, only one main effect of age was observed in adult and aged mice fed low and high fiber diets (*Il1b*, p=0.0325, *Tnf,* p=>0.05, and *Il-6*, p>0.05) (**Figure 9A-C**). Due to low DNA yield, we were not able to assess *Il1b* DNA methylation in microglia. However, in the hippocampus (**Figure 4.9D-E**), analysis of *Il1b* DNA methylation revealed a main effect of age in *Il1b* CpG2 (p=0.001) and an interaction (p=0.0064) in that aged mice had less DNA methylation than both adult groups but adult mice with the high fiber diet had increased DNA methylation compared to adult mice with the low fiber diet. There were no changes in *Il1b* CpG1. With regards to the periphery, colon, lymph nodes, and liver gene expression were analyzed in the same way as **Figure 8**. The only effect of diet was *Ffar2* colon gene expression (p=0.0179), in that *Ffar2* increased in aged animals with the high fiber compared to the low fiber diet (data not shown). There were also no differences in LBP (data not shown).

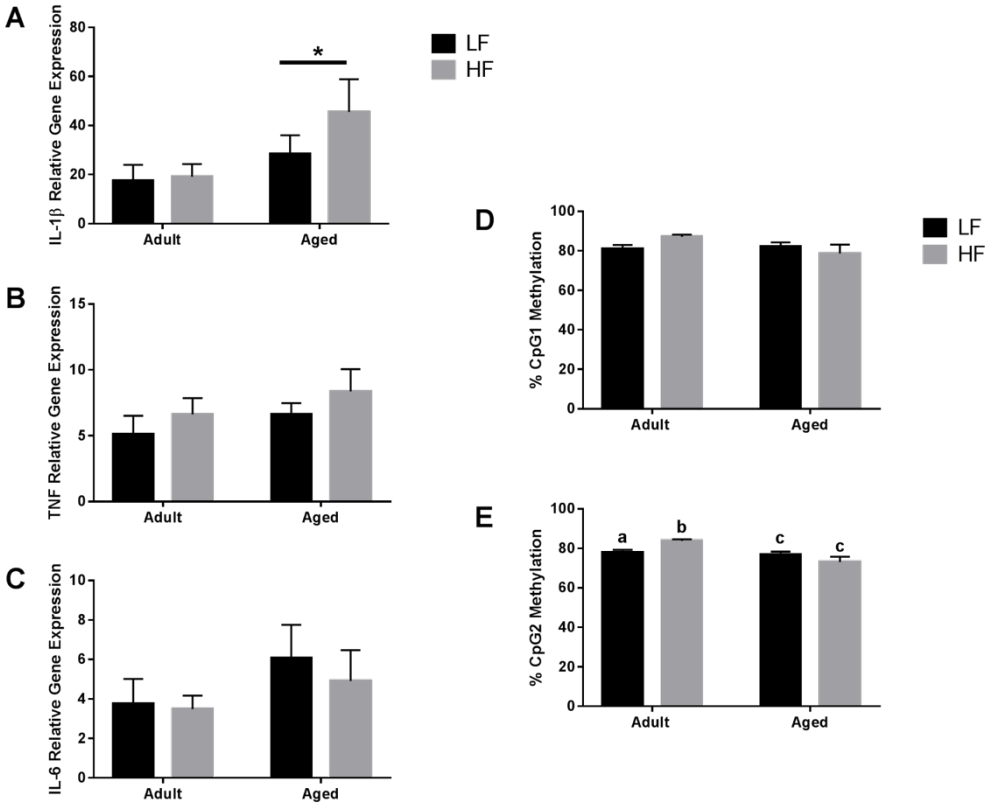

Figure 4.9. Hippocampal gene expression and DNA methylation at 4 hours after i.p. LPS injections in adult and aged mice fed either a low or high fiber diet. Data are presented as means ± SEM (n=7-10) for **(A)** *Il1b*, **(B)** *Tnf*, and **(C)** *Il-6* gene expression. Data are presented as means ± SEM (n=7-10) for DNA methylation of the *Il1b* promoter in hippocampus at **(D)** CpG1 and **(E)** CpG2. Treatment means with different letters are significantly different. * indicates a main effect with significance at $p<0.05$.

Table 4.6. Expression of **(A)** inflammatory, **(B)** sensome, and **(C)** epigenetic regulator genes in microglia collected at 4 hours after SAL/LPS i.p. injections in aged mice pre-treated with i.p. SAL/NaB. Data are presented as means ± SEM (n=7-10) and p-values for main effects of NaB and LPS as well as NaB x LPS interactions are also included.

A. Inflammatory and Regulators of Inflammatory Genes

					p-values		
Gene	**Adult LF**	**Adult HF**	**Aged LF**	**Aged HF**	**Age**	**Diet**	**Age x Diet**
Casp1	**0.89±0.11**	**1.10±0.13**	**0.98±0.11**	**0.84±0.09**	**0.415**	**0.744**	**0.127**
Cd68	**1.40±0.13**	**1.70±0.14**	**2.03±0.19**	**1.68±0.20**	**0.075**	**0.882**	**0.058**
Cx3cr1	**0.53±0.06**	**0.80±0.09**	**0.59±0.06**	**0.54±0.06**	**0.166**	**0.131**	**0.025***
HIF-1α	**3.40±0.71**	**3.07±0.41**	**3.00±0.932**	**2.96±0.36**	**0.697**	**0.780**	**0.831**
Ido1	**1.95±0.28**	**1.78±0.28**	**2.36±0.50**	**2.37±0.42**	**0.191**	**0.839**	**0.813**
Igf1	**0.45±0.17**	**0.40±0.12**	**2.08±0.77**	**1.36±0.75**	**0.018***	**0.468**	**0.522**
Il-1β	**7.17±1.04**	**8.01±0.80**	**12.41±1.07**	**14.55±2.10**	**<0.0001***	**0.252**	**0.614**
Il-1rn	**10.38±1.94**	**8.31±1.48**	**15.19±3.22**	**18.89±3.59**	**0.005***	**0.761**	**0.280**
Gene	**SAL + SAL**	**ZEB + SAL**	**SAL + LPS**	**ZEB + LPS**	**ZEB**	**LPS**	**ZEB x LPS**
Il-10	**7.42±1.88**	**5.46±0.72**	**9.64±1.93**	**9.38±1.67**	**0.070**	**0.507**	**0.609**
Il-6	**3.00±0.40**	**3.24±0.40**	**2.77±0.30**	**3.60±0.33**	**0.858**	**0.150**	**0.423**
Niarc1	**11.79±1.88**	**15.09±2.05**	**11.96±0.88**	**13.03±2.22**	**0.604**	**0.232**	**0.540**
Nlrp3	**2.56±0.37**	**2.87±0.36**	**2.45±0.27**	**2.65±0.45**	**0.649**	**0.485**	**0.887**
Pycard	**2.14±0.25**	**2.62±0.34**	**2.31±0.19**	**2.26±0.22**	**0.704**	**0.401**	**0.314**
Socs1	**1.13±0.05**	**1.02±0.07**	**0.97±0.05**	**0.99±0.08**	**0.163**	**0.474**	**0.280**
Socs3	**8.86±0.97**	**8.37±0.67**	**11.08±1.11**	**9.33±1.48**	**0.153**	**0.312**	**0.566**
Stat3	**4.08±0.50**	**4.32±0.53**	**3.62±0.34**	**3.06±0.41**	**0.064**	**0.722**	**0.385**
Tlr2	**3.03±0.51**	**2.58±0.32**	**3.17±0.29**	**3.44±0.56**	**0.250**	**0.832**	**0.399**
Tlr4	**0.72±0.07**	**1.00±0.14**	**0.80±0.06**	**0.77±0.06**	**0.439**	**0.171**	**0.097**
Tlr7	**2.35±0.27**	**3.24±0.50**	**1.87±0.19**	**1.67±0.16**	**0.002***	**0.280**	**0.091**
Tlr8	**3.51±0.59**	**4.56±0.97**	**6.07±1.21**	**4.36±0.71**	**0.208**	**0.723**	**0.142**
Tnf	**4.77±0.64**	**6.65±0.79**	**7.02±0.75**	**7.66±0.81**	**0.034***	**0.100**	**0.411**

B. Sensome Genes

						p-values	
Gene	**Adult LF**	**Adult HF**	**Aged LF**	**Aged HF**	**Age**	**Diet**	**Age x Diet**
Cd53	**1.83±0.27**	**3.19±0.87**	**0.91±0.17**	**2.67±0.73**	**0.297**	**0.028***	**0.778**

Gpr34	**0.23±0.04**	**0.40±0.08**	**0.20±0.03**	**0.21±0.06**	**0.064**	**0.119**	**0.167**
P2ry12	**0.45±0.06**	**0.71±0.12**	**0.41±0.05**	**0.33±0.06**	**0.011***	**0.263**	**0.047***
P2ry13	**1.03±0.09**	**1.61±0.23**	**0.97±0.09**	**0.82±0.07**	**0.004***	**0.136**	**0.013***
Siglech	**0.71±0.07**	**1.04±0.15**	**0.67±0.05**	**0.59±0.05**	**0.010***	**0.199**	**0.035***
Tgfbr1	**1.04±0.12**	**1.80±0.36**	**1.02±0.14**	**0.96±0.15**	**0.054**	**0.120**	**0.065**
Tmem119	**1.00±0.17**	**2.36±0.49**	**1.28±0.25**	**1.34±0.32**	**0.271**	**0.036***	**0.056**
Trem2	**1.73±0.19**	**2.66±0.33**	**2.03±1.34**	**1.46±0.25**	**0.123**	**0.527**	**0.011***

C. Epigenetic Regulator Genes

					p-values		
Gene	**Adult LF**	**Adult HF**	**Aged LF**	**Aged HF**	**Age**	**Diet**	**Age x Diet**
Dnmt3a	**0.74±0.08**	**0.94±0.12**	**0.93±0.10**	**0.86±0.09**	**0.577**	**0.509**	**0.185**
Dnmt3b	**1.80±0.12**	**2.40±0.36**	**1.76±0.14**	**1.74±0.20**	**0.142**	**0.212**	**0.187**
Gadd45b	**3.83±0.62**	**4.75±0.57**	**6.27±0.68**	**7.25±1.03**	**0.0012***	**0.006***	**0.033***
Hdac1	**0.90±0.03**	**0.81±0.04**	**0.75±0.04**	**0.78±0.04**	**0.012***	**0.375**	**0.101**
Gene	**SAL + SAL**	**ZEB + SAL**	**SAL + LPS**	**ZEB + LPS**	**ZEB**	**LPS**	**ZEB x LPS**
Hdac2	**2.15±0.40**	**2.45±0.33**	**2.46±0.60**	**1.75±0.54**	**0.680**	**0.678**	**0.297**
Hdac3	**1.33±0.14**	**1.61±0.23**	**1.34±0.10**	**1.16±0.10**	**0.162**	**0.776**	**0.149**
Hdac4	**7.70±1.19**	**8.46±1.38**	**5.70±0.90**	**5.22±1.52**	**0.043***	**0.913**	**0.624**
Hdac5	**0.45±0.08**	**1.33±0.30**	**0.61±0.12**	**0.70±0.18**	**0.236**	**0.015***	**0.045***
Hdac6	**3.44±0.45**	**3.79±0.80**	**3.38±0.76**	**3.33±0.94**	**0.735**	**0.841**	**0.800**
Mecp2	**1.42±0.16**	**1.76±0.20**	**1.35±0.11**	**1.22±0.12**	**0.052**	**0.498**	**0.140**
Tet1	**0.30±0.09**	**0.65±0.12**	**0.34±0.06**	**0.47±0.12**	**0.512**	**0.023***	**0.279**
Tet2	**2.74±0.37**	**3.21±0.45**	**2.24±0.30**	**2.18±0.38**	**0.050***	**0.589**	**0.492**
Tet3	**5.85±1.77**	**6.35±2.44**	**1.20±0.35**	**5.67±1.95**	**0.250**	**0.284**	**0.390**

Table 4.6 (cont.). Expression of **(A)** inflammatory, **(B)** sensome, and **(C)** epigenetic regulator genes in microglia collected at 4 hours after SAL/LPS i.p. injections in aged mice pre-treated with i.p. SAL/NaB. Data are presented as means ± SEM (n=7-10) and p-values for main effects of NaB and LPS as well as NaB x LPS interactions are also included.

4.5 Conclusion

These studies tested the hypotheses that (1) NaB pharmacologically could be anti-inflammatory for aged microglia, (2) a high soluble fiber diet has the potential to be anti-

inflammatory for aged microglia through increases in butyrate and changes in the microbiome/periphery, and that (3) a high soluble fiber diet could diminish the aged microglial phenotype seen during an immune challenge.

First, we demonstrated that LPS-induced *Il1b* gene expression was decreased in microglia and hippocampus in NaB-pretreated aged mice. There were similar trending effects in adult mice, but effects were much more pronounced in the aged. This may be due to the fact that HDAC inhibitor effectiveness on controlling epigenetic regulation in the brain may vary widely depending on experience (Sewal et al., 2015). Nonetheless, our results support the fact that butyrate can decrease pro-inflammatory cytokine expression in microglia, similar to previous findings (Huuskonen et al., 2004; Patnala et al., 2016). Because NaB exerted an anti-inflammatory effect on microglia in our aged mouse model, we wanted to determine whether an increase in butyrate through a high soluble fiber diet has the potential to alter neuroinflammation.

Before starting the diet study, we performed a microbiome analysis between adult and aged mice to determine whether aged mice had an altered microbiome, a finding that has been shown previously and reported to be related to increased inflammation seen with aging (Langille et al., 2014; Thevaranjan et al., 2017). Of note, there were lower levels of *Mucuspirillum spp.* and *Odoribacter spp*., and higher levels of in *Ruminococcus spp., Coprococcus spp*., and *Rikenellaceae* in aged versus adult mice. Increases in *Ruminococcus spp* has been shown in elderly humans that was associated with high frailty scores (van Tongeren, Slaets, Harmsen, & Welling, 2005) and increases in *Rikenellaceae* have been shown in aged mice compared to adult mice (Neyrinck et al., 2017). Interestingly, when we performed a microbiome analysis at the end of the diet study (4 weeks), high fiber decreased both *Ruminococcus spp* and *Rikenellaceae*, indicative of a potential beneficial effect. Although we did not find any specific species effects,

fermentation of fiber is thought to contribute significantly to butyrate production in the colon and is dominated by *Ruminococcus bromii* (Ze, Duncan, Louis, & Flint, 2012). Surprisingly, we saw no differences in the butyryl-CoA:acetate CoA-transferase gene (data not shown), a gene that is thought to be a valuable marker for gastrointestinal microbiota function and increased butyrate production/butyrate producing bacteria (Hippe et al., 2011). However, SCFA analysis did reveal significant increases in butyrate along with acetate and total SCFA production with the high fiber diet. This discrepancy in results may be due to the fact that mice were only on low and high fiber diets for 4 weeks. A 2 or 3 month diet intervention may be necessary to see more pronounced changes.

Results of the Fluidigm gene expression analysis indicated that a high fiber diet created an anti-inflammatory profile in microglia, as many inflammatory genes were decreased by diet or in combination with age (*Il1b*, *Il-1rn, Il-6, Nlrp3, Tlr4, Tnf*). Novel findings also indicated changes in sensome and epigenetic regulator genes, suggesting that high fiber can promote changes in a microglial-specific and epigenetic-dependent manner. Since *Il1b, Tnf,* and *Il-6* gene expression was strongly decreased by diet, we correlated these genes with corresponding concentrations of butyrate in the mice. For *Il1b* and *Tnf* (trend for *Il-6*), higher butyrate correlated with lower pro-inflammatory gene expression. The mechanisms behind such an association are unclear, but many possible explanations exist, including regulation of FFARs on peripheral immune cells signaling to the brain or differential activation of the vagus nerve (Mu, Yang, & Zhu, 2016).

Since DNA methylation has been shown to be affected by butyrate and other dietary factors (vel Szic, Declerck, Vidaković, & Vanden Berghe, 2015), *Il1b* DNA methylation in the hippocampus was measured. There were no DNA methylation changes related to diet, but as

there were no significant effects of diet in the pro-inflammatory genes measured in the hippocampus, this is not surprising. This strengthens the ideas that the anti-inflammatory changes seen with diet are microglial-specific. We hypothesize that DNA methylation changes would be observed in microglia, but this was not able to be measured due to low DNA yield. It will be important to confirm these results in the future, along with histone modifications and DNA hydroxymethylation changes that are known to be affected in *Il1b* (Haseeb, Makki, & Haqqi, 2014; W. Schaafsma et al., 2015). Furthermore, it is exciting that newly discovered histone modifications such as histone propionylation and butyrylation could have the potential to be regulated by dietary fiber (Kebede et al., 2017).

A surprising finding was that although significant pro-inflammatory gene expression changes with diet were observed in microglia, these changes were not mirrored in the colon, lymph nodes, or liver. This could be due to length of the diet as mention previously, or effects have potentially been masked due to the heterogeneous mix of cells in colon tissue. There were however effects of diet in the colon for *Tjp2* and trending effects for *Tjp1* and *Ocln* in that high fiber diet increased all of the genes, indicating a beneficial change in gut permeability. Higher tight junction protein expression would be expected as increases in butyrate have been shown to upregulate tight junction proteins (Bordin, Atri, Guillemot, & Citi, 2005). There was also a significant decrease in *Ffar2*, which may be related to decreased neutrophil infiltration (Fournier & Parkos, 2012). Scoring of histology sections for inflammatory infiltrate revealed that aged mice on a low fiber diet had dramatically increased leukocyte infiltration, and that aged mice on the high fiber diet have decreased inflammatory infiltrate, with scoring not significantly different from either low fiber or high fiber adult groups. This demonstrates that a low fiber diet creates an

increased inflammatory environment that is more pronounced in aged, and that a high fiber diet has a potential to decrease these inflammatory changes.

Our last experiment was designed to determine whether a high fiber diet could diminish the exaggerated inflammatory response in aged mice during an immune challenge. We found that when both adult and aged mice were fed low and high fiber diets and injected with LPS, there were minimal effects of diet on both the brain and the periphery at the peak immune response (4 hours). However, it is interesting to note that there was an interaction of age x diet in one of the CpG sites analyzed for *Il1b* DNA methylation, in that aged mice had less DNA methylation than both adult groups, but adult mice with the high fiber diet had increased DNA methylation compared to adult mice with the low fiber diet. This may indicate that DNA methylation is more dynamic and responsive to a dietary intervention in adults (Jones, Goodman, & Kobor, 2015), but the mechanism of this is unclear. Using a lower dose of LPS or an infection such as influenza to more accurately mimic a typical immune response in humans may be necessary to see more nuanced changes and understand the epigenetic mechanisms involved in the inflammatory response of aged individuals.

In conclusion, data thus far supports a role of high fermentable fiber in altering the microbiome and potentially immune infiltration/gut permeability, which supports beneficial microglial function in aged mice. More work needs to be performed to examine the mode of action of butyrate-producing diets in the brain and whether or not these changes relate to the beneficial effects seen with NaB. The characteristic that butyrate is synthesized endogenously via fermentation of non-digestible fibers by bacteria in the colon makes the prevention or at least suppression of neuroinflammatory conditions such as aging possible (Bourassa et al., 2016).

High fiber supplementation in the elderly therefore may be a non-invasive strategy to increase butyrate levels and support an environment with decreased chronic neuroinflammation.

CHAPTER 5: CONCLUSIONS AND FUTURE DIRECTIONS

The studies in this dissertation sought to examine the role of epigenetic mechanisms in microglia during aging. Our findings demonstrated that microglia of aged mice do indeed have differential epigenetic regulation, including decreased methylation of the *Il1b* gene basally or following LPS, as well as changes in gene expression of epigenetic regulators (Matt et al., 2016). Furthermore, we found that inhibiting DNA methylation increased *Il1b* gene expression and decreased DNA methylation of BV2 and primary microglial cells similar to microglia from aged mice.

Since inhibiting DNA methylation was able to produce a heightened pro-inflammatory response in microglia in vitro, we investigated whether inhibiting DNA methylation in the brain of adult mice would alter sickness behavior, DNA methylation of the *Il1b* promoter and expression of inflammatory genes in microglia similar to aged mice. Instead, we found that inhibiting DNA methylation with a DNMT inhibitor produced anti-inflammatory effects in vivo, including decreased sickness behavior when injected with LPS and decreased gene expression of inflammatory markers. Interestingly, DNA methylation of *Il1b* proximal promoter was changed by inhibiting DNA methylation alone or in combination with LPS, and these changes persisted 48 hours after LPS treatment, when gene expression changes were no longer present.

Lastly, we were interested in examining the effects of butyrate in microglia of aged mice, using both injections of butyrate and increases in butyrate through a highly fermentable diet. We found that both pre-treatment of NaB and a 4-week feeding of a high fiber diet decreased gene expression of inflammatory markers in microglia, and that this was more pronounced in aged animals. We also found that epigenetic regulators and the microglial sensome were altered by both diet and age.

In order to move forward with the findings from this dissertation, it is important to discuss the limitations of these studies and suggest several lines of research to pursue. First, the focus of epigenetic findings in this dissertation was limited to DNA methylation, so it will be important to characterize other epigenetic mechanisms altered in healthy aging microglia. These include changes in DNA hydroxymethylation, histone modifications, and microRNAs. As a number of epigenetic signatures have been found for age-related diseases in microglia (Coppieters et al., 2014; Tang et al., 2014; Thome, Harms, Volpicelli-Daley, & Standaert, 2016; Zhu et al., 2017), it would be beneficial to make comparisons.

In Chapter 3, although we found the DNMT inhibitor to be overall anti-inflammatory when we measured sickness behavior and microglial transcriptional activity, we did not look at the role of the peripheral immune system in this model. An essential next step would be to determine the role of DNMT inhibition in response to peripheral immune stimulation (giving mice an i.p. LPS injection instead of an i.c.v. injection). As the brain and peripheral immune system have many routes of communication (Dilger & Johnson, 2008), extending the findings of this study could uncover specific pathways involved in regulating DNA methylation in microglia. Further, combined treatments of epigenetic drugs such as DNMT inhibitors and HDAC inhibitors could elicit even more favorable microglia activity, as in vitro studies from our lab suggest (unpublished data).

In Chapter 4, we found increases in butyrate with a highly fermentable diet along with anti-inflammatory effects in microglia. However, we found limited effects in the periphery, and specifically we surprisingly found very few changes in butyrate-producing bacteria with our microbiome analysis. This suggests that a longer diet (2-3 month) study might be necessary to further increase butyrate and uncover additional benefits. It would also be important to take a

more mechanistic approach in order to understand how the microbiome is communicating with the immune system and specifically microglia in the brain. Utilization of transgenic mice to specifically knock out HDACs or FFARs in microglia, gut epithelial cells, or peripheral immune cells (Abram, Roberge, Hu, & Lowell, 2014; Feng et al., 2013; Parkhurst et al., 2013; Yona et al., 2013), or utilization of germ free mice and then recolonizing with specific butyrate producing bacteria to manipulate the microbiome (Donohoe et al., 2011) are invaluable tools necessary to better understand our findings.

Lastly, another limitation is that microglial morphology was not quantified in these studies. Altered microglial morphology has been reported extensively in both aged human and rodent brains (Davies, Ma, Jegathees, & Goldsbury, 2017; Norden & Godbout, 2013; Streit, Sammons, Kuhns, & Sparks, 2004). Therefore, using immunohistochemistry, valuable findings could be obtained to understand whether or not our transcriptional changes found with epigenetic modifiers correlate with changes in microglial morphology or if colocalization of proteins of interest exist.

Collectively, the aforementioned experiments suggest that epigenetic modifications are altered in aged microglia and have the ability to induce different microglial phenotypes. As stated at the beginning of this dissertation, it is still not completely understood whether inflammatory pathways become more activated with age, or whether the immune system fails to mount appropriate inflammatory responses due to age-related deterioration (Lucin & Wyss-Coray, 2009). The studies presented herein suggest that there could be a combination of both scenarios, as heightened inflammation is present in aged animals but the transcripts encoding proteins and receptors involved in detecting ligands and microbes (sensome genes) are consistently downregulated. Our findings also suggest that using both pharmacological agents

and non-pharmacological interventions like a high soluble fiber diet that act as epigenetic modifiers may potentially modulate this imbalance in microglial cell function. It will be important in the future to better understand these responses to epigenetic modifiers, through diet or pharmacological agents, and to create a personalized approach of combination therapy in order to accurately treat age-related diseases.

REFERENCES

Abraham, J., & Johnson, R. W. (2009). Central inhibition of interleukin-1β ameliorates sickness behavior in aged mice. *Brain, behavior, and immunity, 23*(3), 396-401. doi:10.1016/j.bbi.2008.12.008

Abram, C. L., Roberge, G. L., Hu, Y., & Lowell, C. A. (2014). Comparative analysis of the efficiency and specificity of myeloid-Cre deleting strains using ROSA-EYFP reporter mice. *Journal of immunological methods, 408*, 89-100. doi:10.1016/j.jim.2014.05.009

Anier, K., Malinovskaja, K., Aonurm-Helm, A., Zharkovsky, A., & Kalda, A. (2010). DNA Methylation Regulates Cocaine-Induced Behavioral Sensitization in Mice. *Neuropsychopharmacology, 35*(12), 2450-2461. doi:10.1038/npp.2010.128

Aspelund, A., Antila, S., Proulx, S. T., Karlsen, T. V., Karaman, S., Detmar, M., . . . Alitalo, K. (2015). A dural lymphatic vascular system that drains brain interstitial fluid and macromolecules. *The Journal of Experimental Medicine, 212*(7), 991-999. doi:10.1084/jem.20142290

Aung, H. T., Schroder, K., Himes, S. R., Brion, K., van Zuylen, W., Trieu, A., . . . Ravasi, T. (2006). LPS regulates proinflammatory gene expression in macrophages by altering histone deacetylase expression. *FASEB J, 20*(9), 1315-1327. doi:10.1096/fj.05-5360com

Baker-Andresen, D., Ratnu, V. S., & Bredy, T. W. (2013). Dynamic DNA methylation: a prime candidate for genomic metaplasticity and behavioral adaptation. *Trends Neurosci, 36*(1), 3-13. doi:10.1016/j.tins.2012.09.003

Balch, C., Yan, P., Craft, T., Young, S., Skalnik, D. G., Huang, T. H., & Nephew, K. P. (2005). Antimitogenic and chemosensitizing effects of the methylation inhibitor zebularine in ovarian cancer. *Mol Cancer Ther, 4*(10), 1505-1514. doi:10.1158/1535-7163.mct-05-0216

Bannister, A. J., & Kouzarides, T. (2011). Regulation of chromatin by histone modifications. *Cell Research, 21*(3), 381-395. doi:10.1038/cr.2011.22

Bercik, P., Park, A. J., Sinclair, D., Khoshdel, A., Lu, J., Huang, X., . . . Verdu, E. F. (2011). The anxiolytic effect of Bifidobacterium longum NCC3001 involves vagal pathways for gut-brain communication. *Neurogastroenterol Motil, 23*(12), 1132-1139. doi:10.1111/j.1365-2982.2011.01796.x

Biagi, E., Candela, M., Franceschi, C., & Brigidi, P. (2011). The aging gut microbiota: new perspectives. *Ageing Res Rev, 10*(4), 428-429. doi:10.1016/j.arr.2011.03.004

Biagi, E., Candela, M., Turroni, S., Garagnani, P., Franceschi, C., & Brigidi, P. (2013). Ageing and gut microbes: perspectives for health maintenance and longevity. *Pharmacol Res, 69*(1), 11-20. doi:10.1016/j.phrs.2012.10.005

Bird, A. (2002). DNA methylation patterns and epigenetic memory. *Genes Dev, 16*.

Bird, A. (2007). Perceptions of epigenetics. *Nature, 447*(7143), 396-398. doi:10.1038/nature05913

Bischoff, S. C., Barbara, G., Buurman, W., Ockhuizen, T., Schulzke, J.-D., Serino, M., . . . Wells, J. M. (2014). Intestinal permeability – a new target for disease prevention and therapy. *BMC Gastroenterology, 14*(1), 189. doi:10.1186/s12876-014-0189-7

Blank, M., Werenicz, A., Velho, L. A., Pinto, D. F., Fedi, A. C., Lopes, M. W., . . . Roesler, R. (2015). Enhancement of memory consolidation by the histone deacetylase inhibitor sodium butyrate in aged rats. *Neuroscience Letters, 594*, 76-81. doi:https://doi.org/10.1016/j.neulet.2015.03.059

Blaze, J., Scheuing, L., & Roth, T. L. (2013). Differential methylation of genes in the medial prefrontal cortex of developing and adult rats following exposure to maltreatment or nurturing care during infancy. *Dev Neurosci, 35*(4), 306-316. doi:10.1159/000350716

Bollati, V., Schwartz, J., Wright, R., Litonjua, A., Tarantini, L., Suh, H., . . . Baccarelli, A. (2009). Decline in genomic DNA methylation through aging in a cohort of elderly subjects. *Mech Ageing Dev, 130*(4), 234-239. doi:10.1016/j.mad.2008.12.003

Bordin, M., Atri, F., Guillemot, L., & Citi, S. (2005). Histone Deacetylase Inhibitors Up-Regulate the Expression of Tight Junction Proteins¹1Swiss Cancer League, Swiss National Science Foundation, Ministry for Italian University and Research, ERASMUS Program (M. Bordin), and Roche Research Foundation fellowship (L. Guillemot). *Molecular Cancer Research, 2*(12), 692.

Bourassa, M. W., Alim, I., Bultman, S. J., & Ratan, R. R. (2016). Butyrate, neuroepigenetics and the gut microbiome: Can a high fiber diet improve brain health? *Neuroscience Letters, 625*, 56-63. doi:http://dx.doi.org/10.1016/j.neulet.2016.02.009

Bracken, A. P., Kleine-Kohlbrecher, D., Dietrich, N., Pasini, D., Gargiulo, G., Beekman, C., . . . Helin, K. (2007). The Polycomb group proteins bind throughout the INK4A-ARF locus and are disassociated in senescent cells. *Genes & Development, 21*(5), 525-530. doi:10.1101/gad.415507

Braniste, V., Al-Asmakh, M., Kowal, C., Anuar, F., Abbaspour, A., Toth, M., . . . Pettersson, S. (2014). The gut microbiota influences blood-brain barrier permeability in mice. *Sci Transl Med, 6*(263), 263ra158. doi:10.1126/scitranslmed.3009759

Bunout, D., Barrera, G., Hirsch, S., Gattas, V., de la Maza, M. P., Haschke, F., . . . Munoz, C. (2004). Effects of a nutritional supplement on the immune response and cytokine production in free-living Chilean elderly. *Journal of Parenteral and Enteral Nutrition, 28*(5), 348-354. doi:10.1177/0148607104028005348

Burton, M. D., Rytych, J. L., Amin, R., & Johnson, R. W. (2016). Dietary Luteolin Reduces Proinflammatory Microglia in the Brain of Senescent Mice. *Rejuvenation Res, 19*(4), 286-292. doi:10.1089/rej.2015.1708

Burton, M. D., Rytych, J. L., Freund, G. G., & Johnson, R. W. (2013). Central inhibition of interleukin-6 trans-signaling during peripheral infection reduced neuroinflammation and sickness in aged mice. *Brain Behav Immun, 30*, 66-72. doi:10.1016/j.bbi.2013.01.002

Bustamante, A. C., Aiello, A. E., Galea, S., Ratanatharathorn, A., Noronha, C., Wildman, D. E., & Uddin, M. (2016). Glucocorticoid receptor DNA methylation, childhood maltreatment and major depression. *J Affect Disord, 206*, 181-188. doi:10.1016/j.jad.2016.07.038

Butovsky, O., Jedrychowski, M. P., Moore, C. S., Cialic, R., Lanser, A. J., Gabriely, G., . . . Weiner, H. L. (2014). Identification of a unique TGF-[beta]-dependent molecular and functional signature in microglia. *Nat Neurosci, 17*(1), 131-143. doi:10.1038/nn.3599

http://www.nature.com/neuro/journal/v17/n1/abs/nn.3599.html - supplementary-information

Byun, C. J., Seo, J., Jo, S. A., Park, Y. J., Klug, M., Rehli, M., . . . Jo, I. (2012). DNA methylation of the 5'-untranslated region at +298 and +351 represses BACE1 expression in mouse BV-2 microglial cells. *Biochem Biophys Res Commun, 417*(1), 387-392. doi:10.1016/j.bbrc.2011.11.123

Cedar, H., & Bergman, Y. (2009). Linking DNA methylation and histone modification: patterns and paradigms. *Nat Rev Genet, 10*(5), 295-304.

Chapman, T. R., Barrientos, R. M., Ahrendsen, J. T., Maier, S. F., & Patterson, S. L. (2010). Synaptic Correlates Of Increased Cognitive Vulnerability With Aging: Peripheral Immune Challenge and Aging Interact to Disrupt Theta-Burst L-LTP in Hippocampal Area CA1. *The Journal of neuroscience : the official journal of the Society for Neuroscience, 30*(22), 7598-7603. doi:10.1523/JNEUROSCI.5172-09.2010

Chen, J., Buchanan, J. B., Sparkman, N. L., Godbout, J. P., Freund, G. G., & Johnson, R. W. (2008). Neuroinflammation and disruption in working memory in aged mice after acute stimulation of the peripheral innate immune system. *Brain, behavior, and immunity, 22*(3), 301-311. doi:10.1016/j.bbi.2007.08.014

Cheng, J. C., Matsen, C. B., Gonzales, F. A., Ye, W., Greer, S., Marquez, V. E., . . . Selker, E. U. (2003). Inhibition of DNA methylation and reactivation of silenced genes by zebularine. *J Natl Cancer Inst, 95*(5), 399-409.

Cherry, J. D., Olschowka, J. A., & O'Banion, M. K. (2014). Neuroinflammation and M2 microglia: the good, the bad, and the inflamed. *Journal of Neuroinflammation, 11*(1), 98. doi:10.1186/1742-2094-11-98

Cho, S. H., Chen, J. A., Sayed, F., Ward, M. E., Gao, F., Nguyen, T. A., . . . Gan, L. (2015). SIRT1 deficiency in microglia contributes to cognitive decline in aging and neurodegeneration via epigenetic regulation of IL-1beta. *J Neurosci, 35*(2), 807-818. doi:10.1523/jneurosci.2939-14.2015

Chung, H. Y., Cesari, M., Anton, S., Marzetti, E., Giovannini, S., Seo, A. Y., . . . Leeuwenburgh, C. (2009). Molecular inflammation: underpinnings of aging and age-related diseases. *Ageing Res Rev, 8*(1), 18-30. doi:10.1016/j.arr.2008.07.002

Conde, J. R., & Streit, W. J. (2006). Microglia in the aging brain. *J Neuropathol Exp Neurol, 65*(3), 199-203. doi:10.1097/01.jnen.0000202887.22082.63

Copeland, R. A., Olhava, E. J., & Scott, M. P. (2010). Targeting epigenetic enzymes for drug discovery. *Curr Opin Chem Biol, 14*(4), 505-510. doi:10.1016/j.cbpa.2010.06.174

Coppieters, N., Dieriks, B. V., Lill, C., Faull, R. L., Curtis, M. A., & Dragunow, M. (2014). Global changes in DNA methylation and hydroxymethylation in Alzheimer's disease human brain. *Neurobiol Aging, 35*(6), 1334-1344. doi:10.1016/j.neurobiolaging.2013.11.031

Corrêa-Oliveira, R., Fachi, J. L., Vieira, A., Sato, F. T., & Vinolo, M. A. R. (2016). Regulation of immune cell function by short-chain fatty acids. *Clinical & Translational Immunology, 5*(4), e73. doi:10.1038/cti.2016.17

Damani, M. R., Zhao, L., Fontainhas, A. M., Amaral, J., Fariss, R. N., & Wong, W. T. (2011). Age-related alterations in the dynamic behavior of microglia. *Aging Cell, 10*(2), 263-276. doi:10.1111/j.1474-9726.2010.00660.x

Dantzer, R. (2001). Cytokine-induced sickness behavior: where do we stand? *Brain Behav Immun, 15*(1), 7-24. doi:10.1006/brbi.2000.0613

Dantzer, R. (2009). Cytokine, sickness behavior, and depression. *Immunol Allergy Clin North Am, 29*(2), 247-264. doi:10.1016/j.iac.2009.02.002

Dantzer, R., O'Connor, J. C., Freund, G. G., Johnson, R. W., & Kelley, K. W. (2008). From inflammation to sickness and depression: when the immune system subjugates the brain. *Nat Rev Neurosci, 9*(1), 46-56. doi:10.1038/nrn2297

Dash, P. K., Orsi, S. A., & Moore, A. N. (2009). Histone deactylase inhibition combined with behavioral therapy enhances learning and memory following traumatic brain injury. *Neuroscience, 163*(1), 1-8. doi:10.1016/j.neuroscience.2009.06.028

Davies, D. S., Ma, J., Jegathees, T., & Goldsbury, C. (2017). Microglia show altered morphology and reduced arborization in human brain during aging and Alzheimer's disease. *Brain Pathology, 27*(6), 795-808. doi:10.1111/bpa.12456

Derecki, N. C., Cronk, J. C., & Kipnis, J. (2013). The role of microglia in brain maintenance: implications for Rett syndrome. *Trends in immunology, 34*(3), 144-150. doi:10.1016/j.it.2012.10.002

Derrien, M., & van Hylckama Vlieg, J. E. (2015). Fate, activity, and impact of ingested bacteria within the human gut microbiota. *Trends Microbiol, 23*(6), 354-366. doi:10.1016/j.tim.2015.03.002

Dilger, R. N., & Johnson, R. W. (2008). Aging, microglial cell priming, and the discordant central inflammatory response to signals from the peripheral immune system. *J Leukoc Biol, 84*(4), 932-939. doi:10.1189/jlb.0208108

DiSabato, D. J., Quan, N., & Godbout, J. P. (2016). Neuroinflammation: the devil is in the details. *J Neurochem, 139 Suppl 2*, 136-153. doi:10.1111/jnc.13607

Dock, H., Theodorsson, A., & Theodorsson, E. (2015). DNA Methylation Inhibitor Zebularine Confers Stroke Protection in Ischemic Rats. *Transl Stroke Res, 6*(4), 296-300. doi:10.1007/s12975-015-0397-7

Doherty, R., O'Farrelly, C., & Meade, K. G. (2013). Epigenetic regulation of the innate immune response to LPS in bovine peripheral blood mononuclear cells (PBMC). *Veterinary Immunology and Immunopathology, 154*(3–4), 102-110. doi:http://dx.doi.org/10.1016/j.vetimm.2013.05.004

Donohoe, D. R., Garge, N., Zhang, X., Sun, W., O'Connell, T. M., Bunger, M. K., & Bultman, S. J. (2011). The microbiome and butyrate regulate energy metabolism and autophagy in the mammalian colon. *Cell Metab, 13*(5), 517-526. doi:10.1016/j.cmet.2011.02.018

Doran, K. S., Banerjee, A., Disson, O., & Lecuit, M. (2013). Concepts and mechanisms: crossing host barriers. *Cold Spring Harb Perspect Med, 3*(7). doi:10.1101/cshperspect.a010090

Dorfel, M. J., & Huber, O. (2012). Modulation of tight junction structure and function by kinases and phosphatases targeting occludin. *J Biomed Biotechnol, 2012*, 807356. doi:10.1155/2012/807356

Durham, B. S., Grigg, R., & Wood, I. C. (2017). Inhibition of histone deacetylase 1 or 2 reduces induced cytokine expression in microglia through a protein synthesis independent mechanism. *J Neurochem, 143*(2), 214-224. doi:10.1111/jnc.14144

Eddy, J. L., Krukowski, K., Janusek, L., & Mathews, H. L. (2014). Glucocorticoids regulate natural killer cell function epigenetically. *Cell Immunol, 290*(1), 120-130. doi:10.1016/j.cellimm.2014.05.013

El Aidy, S., Dinan, T. G., & Cryan, J. F. (2014). Immune modulation of the brain-gut-microbe axis. *Front Microbiol, 5*, 146. doi:10.3389/fmicb.2014.00146

Erben, U., Loddenkemper, C., Doerfel, K., Spieckermann, S., Haller, D., Heimesaat, M. M., . . . Kühl, A. A. (2014). A guide to histomorphological evaluation of intestinal inflammation in mouse models. *International Journal of Clinical and Experimental Pathology, 7*(8), 4557-4576.

Erny, D., Hrabe de Angelis, A. L., Jaitin, D., Wieghofer, P., Staszewski, O., David, E., . . . Prinz, M. (2015). Host microbiota constantly control maturation and function of microglia in the CNS. *Nat Neurosci, 18*(7), 965-977. doi:10.1038/nn.4030

http://www.nature.com/neuro/journal/v18/n7/abs/nn.4030.html - supplementary-information

Feng, Y., Sentani, K., Wiese, A., Sands, E., Green, M., Bommer, G. T., . . . Fearon, E. R. (2013). Sox9 induction, ectopic Paneth cells, and mitotic spindle axis defects in mouse colon adenomatous epithelium arising from conditional biallelic Apc inactivation. *Am J Pathol, 183*(2), 493-503. doi:10.1016/j.ajpath.2013.04.013

Fournier, B. M., & Parkos, C. A. (2012). The role of neutrophils during intestinal inflammation. *Mucosal Immunol, 5*(4), 354-366. doi:10.1038/mi.2012.24

Franceschi, C., & Campisi, J. (2014). Chronic inflammation (inflammaging) and its potential contribution to age-associated diseases. *J Gerontol A Biol Sci Med Sci, 69 Suppl 1*, S4-9. doi:10.1093/gerona/glu057

Frank, D. N., & Pace, N. R. (2008). Gastrointestinal microbiology enters the metagenomics era. *Curr Opin Gastroenterol, 24*(1), 4-10. doi:10.1097/MOG.0b013e3282f2b0e8

Fuks, F. (2005). DNA methylation and histone modifications: teaming up to silence genes. *Curr Opin Genet Dev, 15*(5), 490-495. doi:10.1016/j.gde.2005.08.002

Garden, G. A. (2013). Epigenetics and the Modulation of Neuroinflammation. *Neurotherapeutics, 10*(4), 782-788. doi:10.1007/s13311-013-0207-4

Ginhoux, F., Greter, M., Leboeuf, M., Nandi, S., See, P., Gokhan, S., . . . Merad, M. (2010). Fate mapping analysis reveals that adult microglia derive from primitive macrophages. *Science, 330*(6005), 841-845. doi:10.1126/science.1194637

Gnyszka, A., Jastrzebski, Z., & Flis, S. (2013). DNA methyltransferase inhibitors and their emerging role in epigenetic therapy of cancer. *Anticancer Res, 33*(8), 2989-2996.

Godbout, J. P., Chen, J., Abraham, J., Richwine, A. F., Berg, B. M., Kelley, K. W., & Johnson, R. W. (2005). Exaggerated neuroinflammation and sickness behavior in aged mice following activation of the peripheral innate immune system. *FASEB J, 19*(10), 1329-1331. doi:10.1096/fj.05-3776fje

Goehler, L. E., Gaykema, R. P., Opitz, N., Reddaway, R., Badr, N., & Lyte, M. (2005). Activation in vagal afferents and central autonomic pathways: early responses to intestinal infection with Campylobacter jejuni. *Brain Behav Immun, 19*(4), 334-344. doi:10.1016/j.bbi.2004.09.002

Goldberg, E. L., & Dixit, V. D. (2015). Drivers of age-related inflammation and strategies for healthspan extension. *Immunol Rev, 265*(1), 63-74. doi:10.1111/imr.12295

Goodyear, O. C., Dennis, M., Jilani, N. Y., Loke, J., Siddique, S., Ryan, G., . . . Craddock, C. F. (2012). Azacitidine augments expansion of regulatory T cells after allogeneic stem cell transplantation in patients with acute myeloid leukemia (AML). *Blood, 119*(14), 3361-3369. doi:10.1182/blood-2011-09-377044

Gosselin, D., Link, V. M., Romanoski, C. E., Fonseca, G. J., Eichenfield, D. Z., Spann, N. J., . . . Glass, C. K. (2014). Environment drives selection and function of enhancers controlling tissue-specific macrophage identities. *Cell, 159*(6), 1327-1340. doi:10.1016/j.cell.2014.11.023

Govindarajan, N., Agis-Balboa, R. C., Walter, J., Sananbenesi, F., & Fischer, A. (2011). Sodium butyrate improves memory function in an Alzheimer's disease mouse model when administered at an advanced stage of disease progression. *J Alzheimers Dis, 26*(1), 187-197. doi:10.3233/jad-2011-110080

Gravina, S., & Vijg, J. (2010). Epigenetic factors in aging and longevity. *Pflugers Arch, 459*(2), 247-258. doi:10.1007/s00424-009-0730-7

Griffin, P. T., Niederhuth, C. E., & Schmitz, R. J. (2016). A Comparative Analysis of 5-Azacytidine and Zebularine induced DNA Demethylation. *G3: Genes|Genomes|Genetics*.

Guigoz, Y., Dore, J., & Schiffrin, E. J. (2008). The inflammatory status of old age can be nurtured from the intestinal environment. *Curr Opin Clin Nutr Metab Care, 11*(1), 13-20. doi:10.1097/MCO.0b013e3282f2bfdf

Gupta, S., Kim, S. Y., Artis, S., Molfese, D. L., Schumacher, A., Sweatt, J. D., . . . Lubin, F. D. (2010). Histone methylation regulates memory formation. *J Neurosci, 30*(10), 3589-3599. doi:10.1523/jneurosci.3732-09.2010

Guy, J., Hendrich, B., Holmes, M., Martin, J. E., & Bird, A. (2001). A mouse Mecp2-null mutation causes neurological symptoms that mimic Rett syndrome. *Nat Genet, 27*(3), 322-326. doi:10.1038/85899

Haley, M. J., Brough, D., Quintin, J., & Allan, S. M. (2017). Microglial Priming as Trained Immunity in the Brain. *Neuroscience*. doi:10.1016/j.neuroscience.2017.12.039

Haseeb, A., Makki, M. S., & Haqqi, T. M. (2014). Modulation of ten-eleven translocation 1 (TET1), Isocitrate Dehydrogenase (IDH) expression, alpha-Ketoglutarate (alpha-KG), and DNA hydroxymethylation levels by interleukin-1beta in primary human chondrocytes. *J Biol Chem, 289*(10), 6877-6885. doi:10.1074/jbc.M113.512269

Hashimoto, K., Oreffo, R. O., Gibson, M. B., Goldring, M. B., & Roach, H. I. (2009). DNA demethylation at specific CpG sites in the IL1B promoter in response to inflammatory cytokines in human articular chondrocytes. *Arthritis Rheum, 60*(11), 3303-3313. doi:10.1002/art.24882

Heerboth, S., Lapinska, K., Snyder, N., Leary, M., Rollinson, S., & Sarkar, S. (2014). Use of Epigenetic Drugs in Disease: An Overview. *Genetics & Epigenetics, 6*, 9-19. doi:10.4137/GEG.S12270

Henry, C. J., Huang, Y., Wynne, A. M., & Godbout, J. P. (2009). Peripheral lipopolysaccharide (LPS) challenge promotes microglial hyperactivity in aged mice that is associated with exaggerated induction of both pro-inflammatory IL-1β and anti-inflammatory IL-10 cytokines. *Brain, behavior, and immunity, 23*(3), 309-317. doi:http://dx.doi.org/10.1016/j.bbi.2008.09.002

Hernandez, D. G., Nalls, M. A., Gibbs, J. R., Arepalli, S., van der Brug, M., Chong, S., . . . Singleton, A. B. (2011). Distinct DNA methylation changes highly correlated with chronological age in the human brain. *Hum Mol Genet, 20*(6), 1164-1172. doi:10.1093/hmg/ddq561

Hickman, S. E., Kingery, N. D., Ohsumi, T., Borowsky, M., Wang, L.-c., Means, T. K., & Khoury, J. E. (2013). The Microglial Sensome Revealed by Direct RNA Sequencing. *Nature neuroscience, 16*(12), 1896-1905. doi:10.1038/nn.3554

Hippe, B., Zwielehner, J., Liszt, K., Lassl, C., Unger, F., & Haslberger, A. G. (2011). Quantification of butyryl CoA:acetate CoA-transferase genes reveals different butyrate production capacity in individuals according to diet and age. *FEMS Microbiology Letters, 316*(2), 130-135. doi:10.1111/j.1574-6968.2010.02197.x

Hoeijmakers, L., Heinen, Y., van Dam, A.-M., Lucassen, P. J., & Korosi, A. (2016). Microglial Priming and Alzheimer's Disease: A Possible Role for (Early) Immune Challenges and Epigenetics? *Frontiers in Human Neuroscience, 10*, 398. doi:10.3389/fnhum.2016.00398

Holtman, I. R., Raj, D. D., Miller, J. A., Schaafsma, W., Yin, Z., Brouwer, N., . . . Eggen, B. J. (2015). Induction of a common microglia gene expression signature by aging and neurodegenerative conditions: a co-expression meta-analysis. *Acta Neuropathol Commun, 3*, 31. doi:10.1186/s40478-015-0203-5

Huang, Y., Henry, C. J., Dantzer, R., Johnson, R. W., & Godbout, J. P. (2008). Exaggerated sickness behavior and brain proinflammatory cytokine expression in aged mice in response to intracerebroventricular lipopolysaccharide. *Neurobiol Aging, 29*(11), 1744-1753. doi:10.1016/j.neurobiolaging.2007.04.012

Huuskonen, J., Suuronen, T., Nuutinen, T., Kyrylenko, S., & Salminen, A. (2004). Regulation of microglial inflammatory response by sodium butyrate and short-chain fatty acids. *Br J Pharmacol, 141*(5), 874-880. doi:10.1038/sj.bjp.0705682

Ichiyama, K., Chen, T., Wang, X., Yan, X., Kim, B.-S., Tanaka, S., . . . Dong, C. (2015). The methylcytosine dioxygenase Tet2 promotes DNA demethylation and activation of cytokine gene expression in T cells. *Immunity, 42*(4), 613-626. doi:10.1016/j.immuni.2015.03.005

Ivanisevic, J., Stauch, K. L., Petrascheck, M., Benton, H. P., Epstein, A. A., Fang, M., . . . Siuzdak, G. (2016). Metabolic drift in the aging brain. *Aging (Albany NY), 8*(5), 1000-1013. doi:10.18632/aging.100961

Ivanov, A. I., Parkos, C. A., & Nusrat, A. (2010). Cytoskeletal regulation of epithelial barrier function during inflammation. *Am J Pathol, 177*(2), 512-524. doi:10.2353/ajpath.2010.100168

Jaenisch, R., & Bird, A. (2003). Epigenetic regulation of gene expression: how the genome integrates intrinsic and environmental signals. *Nat Genet, 33 Suppl*, 245-254. doi:10.1038/ng1089

Jin, B., Li, Y., & Robertson, K. D. (2011). DNA Methylation: Superior or Subordinate in the Epigenetic Hierarchy? *Genes & Cancer, 2*(6), 607-617. doi:10.1177/1947601910393957

Johansson, M. E., Larsson, J. M., & Hansson, G. C. (2011). The two mucus layers of colon are organized by the MUC2 mucin, whereas the outer layer is a legislator of host-microbial interactions. *Proc Natl Acad Sci U S A, 108 Suppl 1*, 4659-4665. doi:10.1073/pnas.1006451107

Jones, M. J., Goodman, S. J., & Kobor, M. S. (2015). DNA methylation and healthy human aging. *Aging Cell, 14*(6), 924-932. doi:10.1111/acel.12349

Jurkowski, T. P., Meusburger, M., Phalke, S., Helm, M., Nellen, W., Reuter, G., & Jeltsch, A. (2008). Human DNMT2 methylates tRNA(Asp) molecules using a DNA methyltransferase-like catalytic mechanism. *Rna, 14*(8), 1663-1670. doi:10.1261/rna.970408

Kannan, V., Brouwer, N., Hanisch, U. K., Regen, T., Eggen, B. J., & Boddeke, H. W. (2013). Histone deacetylase inhibitors suppress immune activation in primary mouse microglia. *J Neurosci Res, 91*(9), 1133-1142. doi:10.1002/jnr.23221

Kawakami, K., Nakamura, A., Ishigami, A., Goto, S., & Takahashi, R. (2009). Age-related difference of site-specific histone modifications in rat liver. *Biogerontology, 10*(4), 415-421. doi:10.1007/s10522-008-9176-0

Kebede, A. F., Nieborak, A., Shahidian, L. Z., Le Gras, S., Richter, F., Gomez, D. A., . . . Schneider, R. (2017). Histone propionylation is a mark of active chromatin. *Nat Struct Mol Biol, 24*(12), 1048-1056. doi:10.1038/nsmb.3490

Kelly, J. R., Kennedy, P. J., Cryan, J. F., Dinan, T. G., Clarke, G., & Hyland, N. P. (2015). Breaking down the barriers: the gut microbiome, intestinal permeability and stress-related psychiatric disorders. *Frontiers in Cellular Neuroscience, 9*, 392. doi:10.3389/fncel.2015.00392

Kilgore, M., Miller, C. A., Fass, D. M., Hennig, K. M., Haggarty, S. J., Sweatt, J. D., & Rumbaugh, G. (2010). Inhibitors of class 1 histone deacetylases reverse contextual memory deficits in a mouse model of Alzheimer's disease. *Neuropsychopharmacology, 35*(4), 870-880. doi:10.1038/npp.2009.197

King, D. E., Mainous, A. G., 3rd, & Lambourne, C. A. (2012). Trends in dietary fiber intake in the United States, 1999-2008. *J Acad Nutr Diet, 112*(5), 642-648. doi:10.1016/j.jand.2012.01.019

Kittan, N. A., Allen, R. M., Dhaliwal, A., Cavassani, K. A., Schaller, M., Gallagher, K. A., . . . Hogaboam, C. M. (2013). Cytokine Induced Phenotypic and Epigenetic Signatures Are Key to Establishing Specific Macrophage Phenotypes. *PLoS One, 8*(10), e78045. doi:10.1371/journal.pone.0078045

Kohli, R. M., & Zhang, Y. (2013). TET enzymes, TDG and the dynamics of DNA demethylation. *Nature, 502*(7472), 472-479. doi:10.1038/nature12750

Kouzarides, T. (2007). Chromatin modifications and their function. *Cell, 128*(4), 693-705. doi:10.1016/j.cell.2007.02.005

Kovacs, E. J., Oppenheim, J. J., Carter, D. B., & Young, H. A. (1987). Enhanced interleukin-1 production by human monocyte cell lines following treatment with 5-azacytidine. *J Leukoc Biol, 41*(1), 40-46.

Kristensen, L. S., Nielsen, H. M., & Hansen, L. L. (2009). Epigenetics and cancer treatment. *Eur J Pharmacol, 625*(1-3), 131-142. doi:10.1016/j.ejphar.2009.10.011

Kundakovic, M., Chen, Y., Guidotti, A., & Grayson, D. R. (2009). The reelin and GAD67 promoters are activated by epigenetic drugs that facilitate the disruption of local repressor complexes. *Mol Pharmacol, 75*(2), 342-354. doi:10.1124/mol.108.051763

Kursa, M. B. (2014). Robustness of Random Forest-based gene selection methods. *BMC Bioinformatics, 15*(1), 8. doi:10.1186/1471-2105-15-8

Langille, M. G., Meehan, C. J., Koenig, J. E., Dhanani, A. S., Rose, R. A., Howlett, S. E., & Beiko, R. G. (2014). Microbial shifts in the aging mouse gut. *Microbiome, 2*(1), 50. doi:10.1186/s40168-014-0050-9

Lavin, Y., Winter, D., Blecher-Gonen, R., David, E., Keren-Shaul, H., Merad, M., . . . Amit, I. (2014). Tissue-Resident Macrophage Enhancer Landscapes Are Shaped by the Local Microenvironment. *Cell, 159*(6), 1312-1326. doi:10.1016/j.cell.2014.11.018

Lawson, L. J., Perry, V. H., Dri, P., & Gordon, S. (1990). Heterogeneity in the distribution and morphology of microglia in the normal adult mouse brain. *Neuroscience, 39*(1), 151-170.

Lawson, M. A., Parrott, J. M., McCusker, R. H., Dantzer, R., Kelley, K. W., & O'Connor, J. C. (2013). Intracerebroventricular administration of lipopolysaccharide induces indoleamine-2,3-dioxygenase-dependent depression-like behaviors. *Journal of Neuroinflammation, 10*, 87-87. doi:10.1186/1742-2094-10-87

Lebedeva, T. V., & Singh, A. K. (1997). Constitutive activity of the murine IL-1 beta promoter is regulated by a transcriptional repressor. *Biochim Biophys Acta, 1353*(1), 32-38.

Lee, S., Kim, H.-S., Roh, K.-H., Lee, B.-C., Shin, T.-H., Yoo, J.-M., . . . Seo, K.-W. (2015). DNA methyltransferase inhibition accelerates the immunomodulation and migration of human mesenchymal stem cells. *Scientific Reports, 5*, 8020. doi:10.1038/srep08020

http://www.nature.com/articles/srep08020 - supplementary-information

Levenson, J. M., Roth, T. L., Lubin, F. D., Miller, C. A., Huang, I. C., Desai, P., . . . Sweatt, J. D. (2006). Evidence that DNA (cytosine-5) methyltransferase regulates synaptic plasticity in the hippocampus. *J Biol Chem, 281*(23), 15763-15773. doi:10.1074/jbc.M511767200

Li, L. C., & Dahiya, R. (2002). MethPrimer: designing primers for methylation PCRs. *Bioinformatics, 18*(11), 1427-1431.
Livak, K. J., & Schmittgen, T. D. (2001). Analysis of relative gene expression data using real-time quantitative PCR and the 2(-Delta Delta C(T)) Method. *Methods, 25*(4), 402-408. doi:10.1006/meth.2001.1262
Lobo-Silva, D., Carriche, G. M., Castro, A. G., Roque, S., & Saraiva, M. (2016). Balancing the immune response in the brain: IL-10 and its regulation. *Journal of Neuroinflammation, 13*(1), 297. doi:10.1186/s12974-016-0763-8
Lopatina, N., Haskell, J. F., Andrews, L. G., Poole, J. C., Saldanha, S., & Tollefsbol, T. (2002). Differential maintenance and de novo methylating activity by three DNA methyltransferases in aging and immortalized fibroblasts. *Journal of Cellular Biochemistry, 84*(2), 324-334. doi:10.1002/jcb.10015
Louveau, A., Smirnov, I., Keyes, T. J., Eccles, J. D., Rouhani, S. J., Peske, J. D., . . . Kipnis, J. (2015). Structural and functional features of central nervous system lymphatic vessels. *Nature, 523*(7560), 337-341. doi:10.1038/nature14432
http://www.nature.com/nature/journal/v523/n7560/abs/nature14432.html - supplementary-information
Lucin, K. M., & Wyss-Coray, T. (2009). Immune activation in brain aging and neurodegeneration: too much or too little? *Neuron, 64*(1), 110-122. doi:10.1016/j.neuron.2009.08.039
Ma, D. K., Guo, J. U., Ming, G. L., & Song, H. (2009). DNA excision repair proteins and Gadd45 as molecular players for active DNA demethylation. *Cell Cycle, 8*(10), 1526-1531.
Matcovitch-Natan, O., Winter, D. R., Giladi, A., Vargas Aguilar, S., Spinrad, A., Sarrazin, S., . . . Amit, I. (2016). Microglia development follows a stepwise program to regulate brain homeostasis. *Science, 353*(6301), aad8670. doi:10.1126/science.aad8670
Matt, S. M., & Johnson, R. W. (2016). Neuro-immune dysfunction during brain aging: new insights in microglial cell regulation. *Curr Opin Pharmacol, 26*, 96-101. doi:10.1016/j.coph.2015.10.009
Matt, S. M., Lawson, M. A., & Johnson, R. W. (2016). Aging and peripheral lipopolysaccharide can modulate epigenetic regulators and decrease IL-1beta promoter DNA methylation in microglia. *Neurobiol Aging, 47*, 1-9. doi:10.1016/j.neurobiolaging.2016.07.006
McCabe, M. T., Brandes, J. C., & Vertino, P. M. (2009). Cancer DNA methylation: molecular mechanisms and clinical implications. *Clin Cancer Res, 15*(12), 3927-3937. doi:10.1158/1078-0432.ccr-08-2784
McLinden, K. A., Kranjac, D., Deodati, L. E., Kahn, M., Chumley, M. J., & Boehm, G. W. (2012). Age exacerbates sickness behavior following exposure to a viral mimetic. *Physiol Behav, 105*(5), 1219-1225. doi:10.1016/j.physbeh.2011.04.024
Miller, C. A., & Sweatt, J. D. (2007). Covalent modification of DNA regulates memory formation. *Neuron, 53*(6), 857-869. doi:10.1016/j.neuron.2007.02.022
Mittelbronn, M., Dietz, K., Schluesener, H. J., & Meyermann, R. (2001). Local distribution of microglia in the normal adult human central nervous system differs by up to one order of magnitude. *Acta Neuropathol, 101*(3), 249-255.
Montagne, A., Barnes, S. R., Sweeney, M. D., Halliday, M. R., Sagare, A. P., Zhao, Z., . . . Zlokovic, B. V. (2015). Blood-Brain Barrier Breakdown in the Aging Human Hippocampus. *Neuron, 85*(2), 296-302. doi:10.1016/j.neuron.2014.12.032

Moon, M. L., Joesting, J. J., Blevins, N. A., Lawson, M. A., Gainey, S. J., Towers, A. E., . . . Freund, G. G. (2015). IL-4 Knock out Mice Display Anxiety-like Behavior. *Behavior genetics, 45*(4), 451-460. doi:10.1007/s10519-015-9714-x

Moore, L. D., Le, T., & Fan, G. (2013). DNA methylation and its basic function. *Neuropsychopharmacology, 38*(1), 23-38. doi:10.1038/npp.2012.112

Morrison, J. H., & Hof, P. R. (2002). Selective vulnerability of corticocortical and hippocampal circuits in aging and Alzheimer's disease. *Prog Brain Res, 136*, 467-486.

Moskalev, A. A., Smit-McBride, Z., Shaposhnikov, M. V., Plyusnina, E. N., Zhavoronkov, A., Budovsky, A., . . . Fraifeld, V. E. (2012). Gadd45 proteins: relevance to aging, longevity and age-related pathologies. *Ageing Res Rev, 11*(1), 51-66. doi:10.1016/j.arr.2011.09.003

Mu, C., Yang, Y., & Zhu, W. (2016). Gut Microbiota: The Brain Peacekeeper. *Front Microbiol, 7*, 345. doi:10.3389/fmicb.2016.00345

Muturi, E. J., Donthu, R. K., Fields, C. J., Moise, I. K., & Kim, C. H. (2017). Effect of pesticides on microbial communities in container aquatic habitats. *Sci Rep, 7*, 44565. doi:10.1038/srep44565

Nadjar, A., Bluthe, R. M., May, M. J., Dantzer, R., & Parnet, P. (2005). Inactivation of the cerebral NFkappaB pathway inhibits interleukin-1beta-induced sickness behavior and c-Fos expression in various brain nuclei. *Neuropsychopharmacology, 30*(8), 1492-1499. doi:10.1038/sj.npp.1300755

Netea, M. G., Joosten, L. A. B., Latz, E., Mills, K. H. G., Natoli, G., Stunnenberg, H. G., . . . Xavier, R. J. (2016). Trained immunity: A program of innate immune memory in health and disease. *Science, 352*(6284). doi:10.1126/science.aaf1098

Neyrinck, A. M., Taminiau, B., Walgrave, H., Daube, G., Cani, P. D., Bindels, L. B., & Delzenne, N. M. (2017). Spirulina Protects against Hepatic Inflammation in Aging: An Effect Related to the Modulation of the Gut Microbiota? *Nutrients, 9*(6), 633. doi:10.3390/nu9060633

Nikodemova, M., Small, A. L., Kimyon, R. S., & Watters, J. J. (2016). Age-dependent differences in microglial responses to systemic inflammation are evident as early as middle age. *Physiol Genomics, 48*(5), 336-344. doi:10.1152/physiolgenomics.00129.2015

Nikodemova, M., & Watters, J. (2012). Efficient isolation of live microglia with preserved phenotypes from adult mouse brain. *Journal of Neuroinflammation, 9*(1), 147.

Nimmerjahn, A., Kirchhoff, F., & Helmchen, F. (2005). Resting microglial cells are highly dynamic surveillants of brain parenchyma in vivo. *Science, 308*(5726), 1314-1318. doi:10.1126/science.1110647

Norden, D. M., & Godbout, J. P. (2013). Microglia of the Aged Brain: Primed to be Activated and Resistant to Regulation. *Neuropathology and applied neurobiology, 39*(1), 19-34. doi:10.1111/j.1365-2990.2012.01306.x

O'Hara, A. M., & Shanahan, F. (2006). The gut flora as a forgotten organ. *EMBO Reports, 7*(7), 688-693. doi:10.1038/sj.embor.7400731

Ooi, S. K., Qiu, C., Bernstein, E., Li, K., Jia, D., Yang, Z., . . . Bestor, T. H. (2007). DNMT3L connects unmethylated lysine 4 of histone H3 to de novo methylation of DNA. *Nature, 448*(7154), 714-717. doi:10.1038/nature05987

Orre, M., Kamphuis, W., Osborn, L. M., Melief, J., Kooijman, L., Huitinga, I., . . . Hol, E. M. (2014). Acute isolation and transcriptome characterization of cortical astrocytes and

microglia from young and aged mice. *Neurobiol Aging, 35*(1), 1-14. doi:10.1016/j.neurobiolaging.2013.07.008
Pal, S., & Tyler, J. K. (2016). Epigenetics and aging. *Science Advances, 2*(7), e1600584. doi:10.1126/sciadv.1600584
Panasevich, M. R., Allen, J. M., Wallig, M. A., Woods, J. A., & Dilger, R. N. (2015). Moderately Fermentable Potato Fiber Attenuates Signs and Inflammation Associated with Experimental Colitis in Mice. *J Nutr, 145*(12), 2781-2788. doi:10.3945/jn.115.218578
Pandiyan, K., You, J. S., Yang, X., Dai, C., Zhou, X. J., Baylin, S. B., . . . Liang, G. (2013). Functional DNA demethylation is accompanied by chromatin accessibility. *Nucleic Acids Research, 41*(7), 3973-3985. doi:10.1093/nar/gkt077
Parkhurst, C. N., Yang, G., Ninan, I., Savas, J. N., Yates, J. R., Lafaille, J. J., . . . Gan, W.-B. (2013). Microglia promote learning-dependent synapse formation through BDNF. *Cell, 155*(7), 1596-1609. doi:10.1016/j.cell.2013.11.030
Patnala, R., Arumugam, T. V., Gupta, N., & Dheen, S. T. (2016). HDAC Inhibitor Sodium Butyrate-Mediated Epigenetic Regulation Enhances Neuroprotective Function of Microglia During Ischemic Stroke. *Mol Neurobiol*, 1-21. doi:10.1007/s12035-016-0149-z
Perry, V. H., Matyszak, M. K., & Fearn, S. (1993). Altered antigen expression of microglia in the aged rodent CNS. *Glia, 7*(1), 60-67. doi:10.1002/glia.440070111
Peters, R. (2006). Ageing and the brain. *Postgraduate Medical Journal, 82*(964), 84-88. doi:10.1136/pgmj.2005.036665
Peterson, L. W., & Artis, D. (2014). Intestinal epithelial cells: regulators of barrier function and immune homeostasis. *Nat Rev Immunol, 14*(3), 141-153. doi:10.1038/nri3608
Pizza, V., Agresta, A., D'Acunto, C. W., Festa, M., & Capasso, A. (2011). Neuroinflamm-aging and neurodegenerative diseases: an overview. *CNS Neurol Disord Drug Targets, 10*(5), 621-634.
Pogribny, I. P., & Vanyushin, B. F. (2010a). Age-Related Genomic Hypomethylation. 11-27. doi:10.1007/978-1-4419-0639-7_2
Pogribny, I. P., & Vanyushin, B. F. (2010b). Age-Related Genomic Hypomethylation. In O. T. Tollefsbol (Ed.), *Epigenetics of Aging* (pp. 11-27). New York, NY: Springer New York.
Quan, N., & Banks, W. A. (2007). Brain-immune communication pathways. *Brain Behav Immun, 21*(6), 727-735. doi:10.1016/j.bbi.2007.05.005
Ransohoff, R. M. (2016). A polarizing question: do M1 and M2 microglia exist? *Nat Neurosci, 19*(8), 987-991. doi:10.1038/nn.4338
Ransohoff, R. M., & Perry, V. H. (2009). Microglial physiology: unique stimuli, specialized responses. *Annu Rev Immunol, 27*, 119-145. doi:10.1146/annurev.immunol.021908.132528
Roberfroid, M. (2007). Prebiotics: the concept revisited. *J Nutr, 137*(3 Suppl 2), 830s-837s.
Roth, T. L., Lubin, F. D., Funk, A. J., & Sweatt, J. D. (2009). Lasting epigenetic influence of early-life adversity on the BDNF gene. *Biol Psychiatry, 65*(9), 760-769. doi:10.1016/j.biopsych.2008.11.028
Sarkar, S., Abujamra, A. L., Loew, J. E., Forman, L. W., Perrine, S. P., & Faller, D. V. (2011). Histone deacetylase inhibitors reverse CpG methylation by regulating DNMT1 through ERK signaling. *Anticancer Res, 31*(9), 2723-2732.
Satoh, A., Brace, C. S., Rensing, N., Cliften, P., Wozniak, D. F., Herzog, E. D., . . . Imai, S. (2013). Sirt1 extends life span and delays aging in mice through the regulation of Nk2

homeobox 1 in the DMH and LH. *Cell Metab, 18*(3), 416-430. doi:10.1016/j.cmet.2013.07.013
Schaafsma, G., & Slavin, J. L. (2015). Significance of Inulin Fructans in the Human Diet. *Comprehensive Reviews in Food Science and Food Safety, 14*(1), 37-47. doi:10.1111/1541-4337.12119
Schaafsma, W., Zhang, X., van Zomeren, K. C., Jacobs, S., Georgieva, P. B., Wolf, S. A., . . . Eggen, B. J. (2015). Long-lasting pro-inflammatory suppression of microglia by LPS-preconditioning is mediated by RelB-dependent epigenetic silencing. *Brain Behav Immun, 48*, 205-221. doi:10.1016/j.bbi.2015.03.013
Schwarz, J. M., & Bilbo, S. D. (2013). Adolescent morphine exposure affects long-term microglial function and later-life relapse liability in a model of addiction. *J Neurosci, 33*(3), 961-971. doi:10.1523/jneurosci.2516-12.2013
Sewal, A. S., Patzke, H., Perez, E. J., Park, P., Lehrmann, E., Zhang, Y., . . . Rapp, P. R. (2015). Experience Modulates the Effects of Histone Deacetylase Inhibitors on Gene and Protein Expression in the Hippocampus: Impaired Plasticity in Aging. *J Neurosci, 35*(33), 11729-11742. doi:10.1523/jneurosci.4339-14.2015
Sharma, S., & Taliyan, R. (2015). Targeting Histone Deacetylases: A Novel Approach in Parkinson's Disease. *Parkinson's Disease, 2015*, 303294. doi:10.1155/2015/303294
Sheffield, L. G., & Berman, N. E. (1998). Microglial expression of MHC class II increases in normal aging of nonhuman primates. *Neurobiol Aging, 19*(1), 47-55.
Sherry, C. L., Kim, S. S., Dilger, R. N., Bauer, L. L., Moon, M. L., Tapping, R. I., . . . Freund, G. G. (2010). Sickness behavior induced by endotoxin can be mitigated by the dietary soluble fiber, pectin, through up-regulation of IL-4 and Th2 polarization. *Brain Behav Immun, 24*(4), 631-640. doi:10.1016/j.bbi.2010.01.015
Sherwin, E., Sandhu, K. V., Dinan, T. G., & Cryan, J. F. (2016). May the Force Be With You: The Light and Dark Sides of the Microbiota–Gut–Brain Axis in Neuropsychiatry. *CNS Drugs, 30*(11), 1019-1041. doi:10.1007/s40263-016-0370-3
Shin, H., Kim, J. H., Lee, Y. S., & Lee, Y. C. (2012). Change in gene expression profiles of secreted frizzled-related proteins (SFRPs) by sodium butyrate in gastric cancers: induction of promoter demethylation and histone modification causing inhibition of Wnt signaling. *Int J Oncol, 40*(5), 1533-1542. doi:10.3892/ijo.2012.1327
Sierra, A., Gottfried-Blackmore, A. C., McEwen, B. S., & Bulloch, K. (2007). Microglia derived from aging mice exhibit an altered inflammatory profile. *Glia, 55*(4), 412-424. doi:10.1002/glia.20468
Simen, A. A., Bordner, K. A., Martin, M. P., Moy, L. A., & Barry, L. C. (2011). Cognitive Dysfunction with Aging and the Role of Inflammation. *Therapeutic Advances in Chronic Disease, 2*(3), 175-195. doi:10.1177/2040622311399145
Slavin, J. (2013). Fiber and Prebiotics: Mechanisms and Health Benefits. *Nutrients, 5*(4), 1417-1435. doi:10.3390/nu5041417
Sobel, R. A., & Ames, M. B. (1988). Major histocompatibility complex molecule expression in the human central nervous system: immunohistochemical analysis of 40 patients. *J Neuropathol Exp Neurol, 47*(1), 19-28.
Song, S. H., Han, S. W., & Bang, Y. J. (2011). Epigenetic-based therapies in cancer: progress to date. *Drugs, 71*(18), 2391-2403. doi:10.2165/11596690-000000000-00000

Sparkman, N. L., & Johnson, R. W. (2008). Neuroinflammation associated with aging sensitizes the brain to the effects of infection or stress. *Neuroimmunomodulation, 15*(4-6), 323-330. doi:10.1159/000156474

Spulber, S., Bartfai, T., & Schultzberg, M. (2009). IL-1/IL-1ra balance in the brain revisited - evidence from transgenic mouse models. *Brain Behav Immun, 23*(5), 573-579. doi:10.1016/j.bbi.2009.02.015

Strahl, B. D., & Allis, C. D. (2000). The language of covalent histone modifications. *Nature, 403*(6765), 41-45. doi:10.1038/47412

Streit, W. J., Sammons, N. W., Kuhns, A. J., & Sparks, D. L. (2004). Dystrophic microglia in the aging human brain. *Glia, 45*(2), 208-212. doi:10.1002/glia.10319

Sui, L., Wang, Y., Ju, L. H., & Chen, M. (2012). Epigenetic regulation of reelin and brain-derived neurotrophic factor genes in long-term potentiation in rat medial prefrontal cortex. *Neurobiol Learn Mem, 97*(4), 425-440. doi:10.1016/j.nlm.2012.03.007

Sullivan, K. E., Reddy, A. B. M., Dietzmann, K., Suriano, A. R., Kocieda, V. P., Stewart, M., & Bhatia, M. (2007). Epigenetic Regulation of Tumor Necrosis Factor Alpha. *Molecular and Cellular Biology, 27*(14), 5147-5160. doi:10.1128/MCB.02429-06

Szyf, M. (2009). Epigenetics, DNA methylation, and chromatin modifying drugs. *Annu Rev Pharmacol Toxicol, 49*, 243-263. doi:10.1146/annurev-pharmtox-061008-103102

Szyf, M. (2017). Prospects for Medications to Reverse Causative Epigenetic Processes in Neuropsychiatry Disorders. *Neuropsychopharmacology, 42*(1), 367-368. doi:10.1038/npp.2016.219

Szyf, M., McGowan, P., & Meaney, M. J. (2008). The social environment and the epigenome. *Environ Mol Mutagen, 49*(1), 46-60. doi:10.1002/em.20357

Tang, Y., Li, T., Li, J., Yang, J., Liu, H., Zhang, X. J., & Le, W. (2014). Jmjd3 is essential for the epigenetic modulation of microglia phenotypes in the immune pathogenesis of Parkinson/'s disease. *Cell Death Differ, 21*(3), 369-380. doi:10.1038/cdd.2013.159

Tay, T. L., Mai, D., Dautzenberg, J., Fernandez-Klett, F., Lin, G., Sagar, . . . Prinz, M. (2017). A new fate mapping system reveals context-dependent random or clonal expansion of microglia. *Nat Neurosci, 20*(6), 793-803. doi:10.1038/nn.4547

Thevaranjan, N., Puchta, A., Schulz, C., Naidoo, A., Szamosi, J. C., Verschoor, C. P., . . . Bowdish, D. M. E. (2017). Age-Associated Microbial Dysbiosis Promotes Intestinal Permeability, Systemic Inflammation, and Macrophage Dysfunction. *Cell Host Microbe, 21*(4), 455-466.e454. doi:10.1016/j.chom.2017.03.002

Thion, M. S., Low, D., Silvin, A., Chen, J., Grisel, P., Schulte-Schrepping, J., . . . Garel, S. (2018). Microbiome Influences Prenatal and Adult Microglia in a Sex-Specific Manner. *Cell, 172*(3), 500-516.e516. doi:https://doi.org/10.1016/j.cell.2017.11.042

Thome, A. D., Harms, A. S., Volpicelli-Daley, L. A., & Standaert, D. G. (2016). microRNA-155 Regulates Alpha-Synuclein-Induced Inflammatory Responses in Models of Parkinson Disease. *J Neurosci, 36*(8), 2383-2390. doi:10.1523/jneurosci.3900-15.2016

Tough, D. F., Lewis, H. D., Rioja, I., Lindon, M. J., & Prinjha, R. K. (2014). Epigenetic pathway targets for the treatment of disease: accelerating progress in the development of pharmacological tools: IUPHAR Review 11. *Br J Pharmacol, 171*(22), 4981-5010. doi:10.1111/bph.12848

Tough, D. F., Tak, P. P., Tarakhovsky, A., & Prinjha, R. K. (2016). Epigenetic drug discovery: breaking through the immune barrier. *Nat Rev Drug Discov, 15*(12), 835-853. doi:10.1038/nrd.2016.185

Tremblay, M. E., Zettel, M. L., Ison, J. R., Allen, P. D., & Majewska, A. K. (2012). Effects of aging and sensory loss on glial cells in mouse visual and auditory cortices. *Glia, 60*(4), 541-558. doi:10.1002/glia.22287

van Tongeren, S. P., Slaets, J. P., Harmsen, H. J., & Welling, G. W. (2005). Fecal microbiota composition and frailty. *Appl Environ Microbiol, 71*(10), 6438-6442. doi:10.1128/aem.71.10.6438-6442.2005

vel Szic, K. S., Declerck, K., Vidaković, M., & Vanden Berghe, W. (2015). From inflammaging to healthy aging by dietary lifestyle choices: is epigenetics the key to personalized nutrition? *Clinical Epigenetics, 7*(1), 1-18. doi:10.1186/s13148-015-0068-2

Villacampa, N., Almolda, B., Vilella, A., Campbell, I. L., González, B., & Castellano, B. (2015). Astrocyte-targeted production of IL-10 induces changes in microglial reactivity and reduces motor neuron death after facial nerve axotomy. *Glia, 63*(7), 1166-1184. doi:10.1002/glia.22807

von Bernhardi, R., Eugenín-von Bernhardi, L., & Eugenín, J. (2015). Microglial cell dysregulation in brain aging and neurodegeneration. *Frontiers in Aging Neuroscience, 7*, 124. doi:10.3389/fnagi.2015.00124

Wagner, J. R., Busche, S., Ge, B., Kwan, T., Pastinen, T., & Blanchette, M. (2014). The relationship between DNA methylation, genetic and expression inter-individual variation in untransformed human fibroblasts. *Genome Biology, 15*(2), R37-R37. doi:10.1186/gb-2014-15-2-r37

Wake, H., Moorhouse, A. J., Jinno, S., Kohsaka, S., & Nabekura, J. (2009). Resting microglia directly monitor the functional state of synapses in vivo and determine the fate of ischemic terminals. *J Neurosci, 29*(13), 3974-3980. doi:10.1523/jneurosci.4363-08.2009

Wang, P., Zhang, Y., Gong, Y., Yang, R., Chen, Z., Hu, W., . . . Huang, C. (2018). Sodium butyrate triggers a functional elongation of microglial process via Akt-small RhoGTPase activation and HDACs inhibition. *Neurobiology of Disease, 111*, 12-25. doi:https://doi.org/10.1016/j.nbd.2017.12.006

Wang, W.-Y., Tan, M.-S., Yu, J.-T., & Tan, L. (2015). Role of pro-inflammatory cytokines released from microglia in Alzheimer's disease. *Annals of Translational Medicine, 3*(10), 136. doi:10.3978/j.issn.2305-5839.2015.03.49

Wei, Y. B., Melas, P. A., Wegener, G., Mathé, A. A., & Lavebratt, C. (2015). Antidepressant-Like Effect of Sodium Butyrate is Associated with an Increase in TET1 and in 5-Hydroxymethylation Levels in the Bdnf Gene. *International Journal of Neuropsychopharmacology, 18*(2), pyu032. doi:10.1093/ijnp/pyu032

Wes, P. D., Holtman, I. R., Boddeke, E. W. G. M., Möller, T., & Eggen, B. J. L. (2016). Next generation transcriptomics and genomics elucidate biological complexity of microglia in health and disease. *Glia, 64*(2), 197-213. doi:10.1002/glia.22866

Wessels, I., Fleischer, D., Rink, L., & Uciechowski, P. (2010). Changes in chromatin structure and methylation of the human interleukin-1beta gene during monopoiesis. *Immunology, 130*(3), 410-417. doi:10.1111/j.1365-2567.2009.03243.x

Wilson, V. L., & Jones, P. A. (1983). DNA methylation decreases in aging but not in immortal cells. *Science, 220*(4601), 1055-1057.

Yamawaki, Y., Yoshioka, N., Nozaki, K., Ito, H., Oda, K., Harada, K., . . . Akagi, H. (2018). Sodium butyrate abolishes lipopolysaccharide-induced depression-like behaviors and hippocampal microglial activation in mice. *Brain Research, 1680*, 13-38. doi:https://doi.org/10.1016/j.brainres.2017.12.004

Yang, X., Wang, X., Liu, D., Yu, L., Xue, B., & Shi, H. (2014). Epigenetic regulation of macrophage polarization by DNA methyltransferase 3b. *Mol Endocrinol, 28*.

Yona, S., Kim, K. W., Wolf, Y., Mildner, A., Varol, D., Breker, M., . . . Jung, S. (2013). Fate mapping reveals origins and dynamics of monocytes and tissue macrophages under homeostasis. *Immunity, 38*(1), 79-91. doi:10.1016/j.immuni.2012.12.001

Zampieri, M., Ciccarone, F., Calabrese, R., Franceschi, C., Bürkle, A., & Caiafa, P. (2015). Reconfiguration of DNA methylation in aging. *Mechanisms of Ageing and Development, 151*, 60-70. doi:http://dx.doi.org/10.1016/j.mad.2015.02.002

Ze, X., Duncan, S. H., Louis, P., & Flint, H. J. (2012). Ruminococcus bromii is a keystone species for the degradation of resistant starch in the human colon. *The ISME Journal, 6*(8), 1535-1543. doi:10.1038/ismej.2012.4

Zhang, G., Li, J., Purkayastha, S., Tang, Y., Zhang, H., Yin, Y., . . . Cai, D. (2013). Hypothalamic programming of systemic ageing involving IKK-beta, NF-kappaB and GnRH. *Nature, 497*(7448), 211-216. doi:10.1038/nature12143

Zhang, Q., Zhao, K., Shen, Q., Han, Y., Gu, Y., Li, X., . . . Cao, X. (2015). Tet2 is required to resolve inflammation by recruiting Hdac2 to specifically repress IL-6. *Nature, 525*(7569), 389-393. doi:10.1038/nature15252

Zhang, Z., Deng, C., Lu, Q., & Richardson, B. (2002). Age-dependent DNA methylation changes in the ITGAL (CD11a) promoter. *Mech Ageing Dev, 123*(9), 1257-1268.

Zhu, X., Wang, S., Yu, L., Jin, J., Ye, X., Liu, Y., & Xu, Y. (2017). HDAC3 negatively regulates spatial memory in a mouse model of Alzheimer's disease. *Aging Cell, 16*(5), 1073-1082. doi:10.1111/acel.12642